Title

The role of the genes dpy-19, unc-40, unc-73, and mig-14 in generating the left/right asymmetric Q neuroblast migrations in C. elegans

Author

Honigberg, Lee A.

Publication Date

1998

Peer reviewed|Thesis/dissertation

The role of the genes dpy-19, unc-40, unc-73, and mig-14

in generating the left/right asymmetric Q neuroblast migrations in *C. elegans*

by

Lee A. Honigberg

DISSERTATION

Submitted in partial satisfaction of the requirements for the degree of

DOCTOR OF PHILOSOPHY

in

Neuroscience

in the

GRADUATE DIVISION

of the

UNIVERSITY OF CALIFORNIA

San Francisco

Date **University Librarian**

Degree Conferred: . . . . . .

To my parents.

PREFACE

I am indebted to Cynthia Kenyon for her enthusiasm, optimism, and inspiring creativity. I am also grateful to the members of my thesis committee. Cori Bargmann has always taken time to think about my work as if it were her own and her advice through the years has been invaluable. Marc Tessier-Lavigne always focused rapidly on the crux of any issue and his rational approach to experimental design has set a standard to which I aspire. Gian Garriga graciously agreed to read my thesis on short notice, has given his time freely, and has provided many useful suggestions.

Kenyon Lab members, past and present, have always been happy to talk about science at all levels at all times and I am thankful to them all. I am especially grateful to Craig Hunter, Jeanne Harris, and Julin Maloof who patiently helped me during the early, clueless years. In particular, I thank Julin for spending time to talk about almost every experiment that I have done. discussing almost every experiment I have done. His wisdom, whether scientific, technical, philosophical, or culinary, will be sorely missed. I am particularly grateful to Bela Albinder for keeping our lab running with kindness and humor.

The work in this thesis would not have been possible without the earlier work of former Kenyon Lab member Judith Austin. She first characterized the unusual shapes of the Q neuroblasts, described the phenotype of *unc-40* mutants, and generously bestowed upon me the Q migration mutant that turned out to be *dpy-19*.

I am extremely glad that my Ph.D. program came with an added bonus: great friends. Among the many friendly people at UCSF, I owe special thanks to Josh Gordan, Adrian Erlebacher, Noelle Dwyer, and Julia Mossbridge for be both entertaining and sympathetic over the years. Erin Peckol has brought much joy into my last year at UCSF and deserves more thanks than I could possibly convey. Finally, thanks to my family for supporting me from the very beginning.

Chapter 3 originally appeared in Development.

ABSTRACT **Lee Honigberg**

The role of the genes *dpy-19, unc-40, unc-73,* and *mig-14* in generating the left/right asymmetric Q neuroblast migrations in *C. elegans*

Migrating cells and axons follow complex trajectories as they move through the cellular environment of a developing animal. How do cells orient toward the direction they will migrate and how are cells programmed to choose different directions as they migrate? I have addressed these questions by studying the migration of the bilateral Q neuroblasts in *C. elegans*. QL and QR are born in the same anterior/posterior position on the left and right sides of the animal, but they polarize and then migrate in opposite directions: QL toward the posterior and QR toward the anterior. After these migrations, QL, but not QR, starts expressing the Hox gene *mab-5*. *mab-5* then acts as a switch to direct the migration of the Q descendants, sending the QL descendants further posterior, and, through its absence, allowing the QR descendants to migrate anteriorly. I have found that mutations in the genes *unc-40* and *dpy-19* prevent the Q cells from migrating as well as causing them to polarize randomly, pointing in different directions over time. Mutations in *unc-73* also prevent the Q cells from migrating, but do not cause them to polarize incorrectly. All three mutations also cause the Q descendants to misexpress *mab-5*. I have determined that *dpy-19* encodes a novel, putative transmembrane protein. These results suggest that DPY-19, the UNC-40/Netrin-receptor, and the UNC-73/Trio-like protein act to orient the Q cells in the first step of their left/right asymmetry. I have also characterized the role of a gene, *mig-14*, and found that it functions, later, after QL and QR have migrated. *mig-14* is required for *mab-5* expression in the QL descendants and full anterior migration of the QR descendants. *mig-14* mutants

have a similar phenotype to *egl-20/Wnt* mutants, suggesting that *mig-14* may be part of a Wnt signaling pathway that activates *mab-5* in QL. Taken together, these results define several new components in the pathway that generates the left/right asymmetric pattern of polarization, migration, and Hox expression in the Q neuroblasts.

TABLE OF CONTENTS

LIST OF TABLES

LIST OF FIGURES

CHAPTER 1:Introduction

> The phenomena of developmental kinetics thus present us with the following questions. Why do particles, cells, and cell layers shift during development? Why do they cease to move once they have reached certain localities or have combined with certain other groups coming from other directions? What determines their course and how do they get to their proper destinations?
>
> (Weiss, 1947)

INTRODUCTION

Generations of biologists have been struck by the mysteries of cell migration. To watch a cell or growth cone move toward its target in a developing animal is to wonder, how does the cell know which way to go? Although hundreds of different proteins have been implicated in cell motility, there is no case in which the molecules involved can be linked together in a step by step pathway from environmental cue to signal transduction to cytoskeletal reorganization to directed migration. In addition, the more we learn about how cells and axons are guided, the more often we find that they do not just home in on a single target, but instead proceed through complex, multi-step choices as they migrate (e.g. O'Connor, et al., 1990, Kidd, et al., 1998). With the goal of using genetics to learn how the intricate choreography of cell migration is regulated *in vivo*, I have focused on the migration of the Q neuroblasts in *C. elegans*.

There are several reasons to study cell migration in *C. elegans*. First, the worm is transparent, making it easy to view cells as they migrate. Second, the *C. elegans* cell lineage is completely known, so migratory cells are precisely defined and invariant from animal to animal. Third, with an almost fully sequenced genome and fast generation time, *C. elegans* is an

ideal organism in which to take a genetic approach to the study of complex multicellular processes.

Among the various migratory cells in *C. elegans*, the two Q neuroblasts have several unique features that make them especially worthy of thorough analysis. Unlike most bilateral cells, QL and QR migrate in opposite directions. Thus, there may be simple differences between them that can then give us insight into how the direction of migration is controlled. In addition, the three neurons that are derived from each Q cell migrate to precise stopping points that span the entire A/P axis of the worm. Studying how the final location of the Q descendants is determined may reveal how cells measure position as they migrate. The Q cells also provide access to a remarkable range of fundamental issues in developmental biology: left/right asymmetry, control of Hox gene expression, and the encoding of anterior/posterior positional information. Finally, the first step in the Q cell migrations is the polarization of QL and QR in opposite directions. Thus these cells also present a unique opportunity to study how cells detect and respond to polarizing signals as they occur *in vivo*.

The Q cell migrations are shown in more detail in Figure 1.1. QL and QR are born in similar A/P positions on opposite sides of the animal. Soon after hatching, QL sends a cytoplasmic projection toward the posterior while QR sends a projection toward the anterior. (In this work, the term "Q cell polarization" refers to these asymmetric leading protrusions.) QL and QR then migrate toward the direction of their polarizations, and in the next step of the Q cell migrations, QL, but not QR, expresses the Hox gene *mab-5*. Both Q cells then divide, and the QL descendants continue to migrate posteriorly. Expression of *mab-5* is

necessary and sufficient for the posterior pattern of migration in the Q descendants. The QR descendants, which do not express *mab-5*, migrate anteriorly.

The starting point for my work on the Q cell migrations was the analysis of two mutants that disrupted Q cell migration: *dpy-19* and *mig-14*. I found that *dpy-19(+)* was required for the first step in the Q migrations, when QL and QR migrate in opposite directions. This led me to study this first step in more detail and develop techniques that would allow me to watch the shape of the Q cells as they migrated. I used these techniques to characterize the function of *dpy-19*, as well as the function of *unc-40* and *unc-73*, two genes also found to be required for the migrations of QL and QR (J. Austin, M. Sym, and C. Kenyon, unpublished). In another project, I identified the *mig-14* gene in a screen for Q cell migration mutants. I found that *mig-14(+)* was required to initiate expression of *mab-5* in QL and then collaborated with Jeanne Harris, who was characterizing several other genes with similar roles in the Q cell migrations. What follows is a more detailed description my work and a brief review of research relevant to this work.

OVERVIEW

In Chapter 2, I address the question of what makes QL and QR migrate in opposite directions and how this migration relates to the subsequent expression of *mab-5* in QL but not QR. I characterized the earliest visible left/right difference between the two Q neuroblasts by looking closely at the shape of the Q cell bodies during their migration. I found that prior to migrating, QL polarizes toward the posterior and QR polarizes toward the anterior. To understand how the left/right

asymmetry of the polarization and migration of the Q cells is generated, I examined the role of three genes that are required for their migration: *unc-40*, *dpy-19*, and *unc-73*.

I found that mutations in *unc-40* or *dpy-19* prevented QL and QR from migrating and caused the cells to polarize randomly. *unc-40* encodes a transmembrane receptor with an evolutionarily conserved role in dorsal/ventral guidance (Chan, et al., 1996). Surprisingly, I found that *unc-6*/Netrin, the known *unc-40* ligand, is not required for the migrations of QL and QR, suggesting the existence of an additional, yet undiscovered, ligand that functions with *unc-40* in guiding the Q cells.

Chapter 2 also describes the cloning of *dpy-19*, which I found encodes a novel, putative transmembrane protein. Because the Q phenotype of *dpy-19* mutants is so similar to that of *unc-40* mutants, this novel protein may define a new component of the *unc-40* guidance pathway. I also characterized the effects of mutations in the gene *unc-73*, which encodes a multi-domain protein similar to the vertebrate Trio protein (Steven, et al., 1998). *unc-73* mutations prevented the Q cells from migrating, but did not cause them to polarize in the wrong directions. Thus, *unc-73* is likely to be involved in effecting the polarization and migration of Q, but not in orienting the direction of these processes. The phenotypes of these mutants suggest a model in which *unc-40*, *dpy-19*, and *unc-73* are elements in a signaling pathway that links L/R asymmetry in the Q cells to the generation of opposing cell polarizations relative to the A/P axis.

I also found that mutations in *unc-40*, *dpy-19*, and *unc-73* cause the Q cells to misexpress *mab-5*. In all three mutants, the frequency with which the Q cells polarize toward the posterior correlates with the

frequency of subsequent *mab-5* expression. As described in further detail later, this correlation is consistent with a model for *mab-5* activation that depends on an A/P localized signal.

Chapter 3 focuses on the steps that occur after QL and QR migrate, i.e. the initiation of *mab-5* expression, the control of migration direction by the *mab-5* switch, and the precise final positioning of the Q descendants along the A/P axis. I describe a gene, *mig-14*, which I found had two roles in the Q cell migrations. First, *mig-14* is required for *mab-5* to be expressed in QL after it migrates toward the posterior. Second, *mig-14* is required for anteriorly migrating Q descendants to reach their normal final positions. The defect in final positioning seen in *mig-14* mutants does not involve *mab-5* and does not seem to reflect a simple decrease in motility of the Q descendants. Thus, *mig-14* may be part of the system that the Q descendants use to measure their A/P location. The Q phenotype in *mig-14* mutants is very similar to the phenotype of *egl-20* mutants. Because *egl-20* is now known to encode a Wnt homolog (J. Whangbo and C. Kenyon, unpublished), *mig-14* is likely to function in the Wnt pathway, an evolutionarily conserved intercellular signaling system (reviewed in Cadigan and Nusse, 1997). There are many example of downstream targets whose transcription is regulated by Wnt signaling (e.g. Siegfried, et al., 1992), and some evidence that Wnt can act as a morphogen, with different levels of signaling generating qualitatively different cell fates (Zecca, et al., 1996, Neumann and Cohen, 1997). However, the requirement for *egl-20*/Wnt and *mig-14* in the precise positioning of the Q descendants suggests the intriguing possibility that Wnt signals may act over a long

range to set up the coordinates that migrating cells use to determine their stopping points.

Chapter 3 also describes experiments testing the autonomy of *mab-5* in determining the direction of migration in the Q descendants. In transgenic worms that expressed *mab-5* only under the control of a heat-shock promoter, I used a laser to activate *mab-5* in an anteriorly migrating Q descendant. I found that autonomous expression of *mab-5* was sufficient to cause that cell to reverse directions and migrate posteriorly. This result builds on earlier work (Kenyon, 1986) suggesting that *mab-5* acts cell autonomously to control the direction of Q descendant migration. *mab-5*, as a homeobox containing gene (Costa, et al., 1988), is expected to act as a transcriptional regulator. Since *mab-5* functions within a migrating cell, its downstream targets must be connected, directly or indirectly, with the machinery that determines the direction of cell migration.

BACKGROUND

Because my work has focused primarily on the early steps in the Q lineages (the migrations of QL and QR themselves and the activation of *mab-5*), I will review literature from other fields that relates primarily to these steps. The Q migrations are most fundamentally a problem of generating left/right asymmetry but they can also be considered as examples of polarizing cells responding to their environment. Lastly, the question of how *mab-5* expression is initiated in QL is most related to the study of Hox gene regulation.

Left/Right Asymmetry

L/R axis formation is an intriguing problem because the L/R axis has to be established relative to the other two axes (Wood, 1997) and because L/R asymmetry involves differentially placing and orienting cells relative to the midline within a background of many cells that are bilaterally symmetric. It is helpful to divide the process of L/R asymmetry into three phases: 1) A mechanism for determining left-ness or right-ness relative to the other two axes. 2) A set of genes that is then expressed in a L/R asymmetric pattern. These serve to propagate the initial L/R determination as the embryo develops and act as signals to induce differences in tissues that develop asymmetrically. 3) A mechanism for individual tissues to interpret these asymmetrically expressed signals and use them to control proliferation or bias morphogenesis in a given orientation (Levin, 1997).

In vertebrate development, the molecular details of the first two phases are starting to emerge. Much thought on the initial determination of L/R asymmetry is based on the phenotype of the mouse mutant *inversus viscerum (iv)*. In these mice, L/R asymmetry is randomized, i.e. half the animals show normal L/R asymmetries and half the animals show reversed asymmetries. The *iv* mutation was recently shown to be associated with a point mutation in one of the dyneins, a family of minus-end directed microtubule motor proteins (Supp, et al., 1997). An early hypothesis for how the L/R axis might be reproducibly aligned with the other two axes suggested a molecular basis for the solution: a chiral molecule, which can assume only one orientation relative to the A/P and D/V axis, might generate a defined asymmetry within certain cells allowing them to signal neighboring cells and specify the L/R axis (Brown

and Wolpert, 1990). Given the identity of *iv*, it is tempting to propose a more specific model: perhaps this unidirectional motor protein travels along microtubules that have been organized relative to, for example, the apical/basal and early/late axes of an involuting epithelium, and transports a determinant to one side of the cells to mark the third (L/R) axis of the epithelium. In the absence of this motor, the determinant is evenly distributed, resulting in animals with randomized L/R asymmetries (Levin and Mercola, 1998).

A wide variety of genes have recently been found that are likely to be involved in the second phase of L/R axis formation (reviewed in Varlet and Robertson, 1997, Wood, 1997, Levin and Mercola, 1998). These genes are expressed in L/R asymmetric patterns after gastrulation, but prior to the appearance of morphological asymmetries such as the orientation of the heart and gut. Signaling cascades for many of these genes have been established, and thus far, the only common asymmetrically expressed gene across chick, mouse, and frog is *nodal*, a TGFβ family member that is expressed on the left side (Levin, et al., 1995, Collignon, et al., 1996, Hyatt, et al., 1996, Lowe, et al., 1996). The different vertebrate species appear to use different mechanisms to generate asymmetric *nodal* (e.g., asymmetric *Sonic hedgehog* is asymmetrically expressed and upstream of *nodal* in chick (Levin, et al., 1995), but not in mouse (Chiang, et al., 1996). In contrast, *nodal*'s role in specifying handedness seems essential and conserved. First, in several different types of mutant or manipulated embryos, *nodal* expression is well-correlated with orientation: left-sided *nodal* expression occurs in normal embryos, right-sided *nodal* expression occurs in reversed embryos and equalized *nodal* expression occurs in randomized embryos (e.g. the *iv* mice described above) (Collignon, et al.,

1996, Lowe, et al., 1996, Levin, et al., 1997). Second, bilateral *nodal* expression, induced by injecting *nodal* mRNA into early *xenopus* embryos, is sufficient to cause randomization of embryo handedness (Sampath, et al., 1997). A key observation is that manipulations that cause symmetric expression of *nodal* result in randomized embryos, not symmetric embryos. Thus an underlying system must generate asymmetry, and *nodal* acts only to bias the direction of the asymmetry.

Less is known about what is downstream of *nodal*, and how *nodal* is linked to the third phase, the generation of left/right tissue differences such as the direction of looping of the heart. In the mouse, two bHLH proteins, eHAND and dHAND, are expressed on the left and right sides of the cardiac precursor field, are required for correct looping, and are reversed in *inv* mutant mice (Biben and Harvey, 1997, Srivastava, et al., 1997). At this time, however, no direct link to *nodal* is known.

In *C. elegans*, the equivalent of the first phase of L/R asymmetry occurs at the six-cell stage, when the arrangement of cells in the egg shell places the AB.al and AB.pl cells slightly anterior to the AB.ar and AB.pr cells. If micromanipulation is used to push the AB.al and AB.pl cells toward the posterior at the six-cell stage, animals hatch normally, but with their L/R differences reversed (Wood, 1991). Thus the left and right AB descendants have equivalent potential and handedness is imposed very early in *C. elegans*. It is still not known what molecular differences are induced by these interactions. As in vertebrate handedness, the connection between the early L/R specification and the later interpretation of asymmetry is still unclear.

What does knowing the entire lineage tell us about asymmetry in *C. elegans*? As expected, there are bilateral precursor cells that generate many

of the bilateral cells in the animal through exactly analogous lineage patterns (e.g. AB.pl and AB.pr give rise to QL and QR, respectively, via the same pattern of divisions: apapaaa). However, many bilateral pairs in the animal do not share analogous ancestries (e.g. the neuron SAADL=AB.alppapapa, while SAADR=AB.arapppapa). Thus, left/right symmetry in the worm is non-trivially imposed on the lineage, implying that asymmetries may either break the rules of that system or as be layered on top of it.

Interestingly, in several bilateral cell pairs, there seems to be a posteriorward bias of the cell on the left side. The left distal tip cell (DTC) initially migrates posteriorly while the right DTC migrates anteriorly, the left juvenile coelomocytes migrate farther posteriorly than their right side counterparts, the position of body wall muscles on the left is shifted toward the posterior, and of course, the left Q cell migrates posteriorly. (Sulston and Horvitz, 1977). The only common ancestor of all these posteriorly biased cells on the left side is P0, i.e. the one cell embryo. Since the L/R axis is not yet specified in P0, we can rule out the simple model in which a common precursor cell segregates a "posterior-bias inducing" factor to all the cells that end up on the left side. Instead, it seems more likely that the left=posterior bias is generated non-cell autonomously.

What can we hope to learn about L/R axis formation by focusing particularly on the left/right asymmetry of the Q neuroblasts? There is currently no evidence that the genes involved in generating the first two phases of L/R specification are conserved between vertebrates and nematodes. However, there is very little known in any species about the mechanisms used in the third phase, when particular tissues respond to asymmetric information to organize their differentiation. In comparison

to vertebrate organogenesis, the behavior of the Q cells is simple. The mutants described in Chapter 2 are prime candidates for being involved in the last phase of asymmetry generation because they disrupt Q cell asymmetry without causing whole animal reversals.

Cell polarization

Another way to view the asymmetry of QL and QR is to consider the first visible difference between these cells - their cytoplasmic polarization. A wide range of cells organize their shape and contents to point in a particular direction. Mating and budding yeast cells, transporting epithelial cells, and essentially all motile cells must choose and maintain a direction of polarization (Drubin and Nelson, 1996). The chosen site can be determined intrinsically or in response to extrinsic signals. The unifying themes of work studying cell polarity are the search for localized proteins or signals that serve to mark the site of polarization and the search for the proteins that connect such a mark to the organization of the cytoskeleton. The process of intrinsic polarization has been most thoroughly dissected in *S. cerevisiae* cells, which produce daughter cells via budding (Herskowitz, et al., 1995, Pringle, et al., 1995, Chant, 1996). The bud site is chosen in a defined position relative to the site of the previous bud. The analysis of mutants that disrupt the normal budding pattern has placed the genes involved into three broad classes: site selection, polarity establishment, and cytoskeletal/structural elements. Site selection genes determine the site at which budding will occur. Their unifying characteristic is that in their absence, polarization still occurs, but its direction is randomized (Chant and Herskowitz, 1991). Because haploid and diploid cells follow different rules for where, relative to the previous

bud site, the next bud will form, the regulation of bud site selection is quite complex. Nonetheless, there are some simple examples that serve to illustrate some of the mechanisms used in site selection. Some proteins, such as Bud3 and Bud4, (Chant, et al., 1995, Sanders and Herskowitz, 1996) are themselves localized. Other proteins, such as the Bud1 GTPase, are not localized, but their activity is presumed to be regulated by other localized proteins. Bud1 also serves to illustrate the frequent involvement of small GTPases in determining polarity (Chant and Stowers, 1995). As for many of the GTPases involved in cell polarity, cycling between the GTP and GDP bound forms is essential for Rsr1p/Bud1p function.

In contrast to the bud site selection genes, polarity establishment genes are required for polarized growth to occur at all. In their absence, instead of budding, yeast cells remain round and grow larger and larger until they eventually burst, as if their cytoskeleton and secretion machinery were driving growth in the absence of polarity. The Cdc42 GTPase and its exchange factor Cdc24 are both polarity establishment genes. Cdc24 is regulated by Bud1, thus making the connection between site selection and polarity establishment. Remarkably, activation of the mammalian Cdc42 homolog promotes the outgrowth of filopodia. Cdc42 and other small GTPases are also involved in the formation of lamellopodia, focal adhesions, and stress fibers, all hallmarks of migrating cells (Nobes and Hall, 1995).

How are polarity establishment signals then passed on to orient the actin cytoskeleton and organize the structural proteins at the site of budding? This process remains largely unexplained. Although several Cdc42 binding proteins have been identified in yeast and mammalian cells (Lim, et al., 1996, Keely, et al., 1997, Miki, et al., 1998), their precise effects

on actin organization, especially *in vivo*, is unclear (Simon, et al., 1995). Recent work has shown that Cdc42 can promote actin polymerization in cell extracts (Zigmond, et al., 1997, Ma, et al., 1998).

S. cerevisiae also serves as a model system for polarization to extrinsic signals (Chenevert, 1994). During mating, yeast cells send a projection (or "shmoo") toward their mating partner. The shmoo is oriented by a gradient of mating pheromone, normally produced by the mating partner. Ste2, a G-protein coupled transmembrane protein, acts as the pheromone receptor. No "shmoo" site selection genes equivalent to the budding site selection genes have been identified, i.e. no mutants have been found that cause yeast cells to polarize randomly in response to a gradient of pheromone. Some alleles of *far-1* cause yeast cells to shmoo toward the last bud site rather than toward pheromone (Valtz, et al., 1995), suggesting that polarization during mating may involve overriding the bud site selection system. Interestingly, wild-type cells polarize randomly when they are placed in a uniform concentration of pheromone (Segall, 1993). Thus, in shmooing, as in budding, it seems that yeast cells have one set of proteins that allow polarized growth, and another set that establish a bias for where this polarization will occur.

What questions does this lead us to ask about polarization in the Q cells? First, we should consider whether polarity in QL and QR is determined intrinsically or in response to extracellular signals. Because *unc-40*, a transmembrane receptor, is required for the Q cells to polarize correctly, it is likely that they are orienting toward extracellular cues. Second, what is the underlying cause of the irregular and incorrectly polarized Q cell shapes seen in *unc-40* and *dpy-19* mutants? Perhaps the Q cells in these mutants are analogous to yeast mutants in which the cells

are primed to polarize, but lack the marker telling them where to direct growth. Such a situation also occurs in wild-type yeast cells placed in a high uniform concentration of pheromone, where it was found that "...sustained growth from a single site did not occur. Rather a series of protrusions grew sequentially from different sides of the cells." (Segall, 1993). This description sounds remarkably similar to my observations of Q cell morphology in *unc-40* and *dpy-19* mutants. Thus, these mutants may be primarily defective in guidance in the Q cells, and only secondarily defective in motility. Finally, is the mechanism controlling polarity in yeast cells and in the Q cells evolutionarily conserved? My work has shown that *unc-73* (which contains two guanine-nucleotide-exchange factor domains (Steven, et al., 1998) is required for QL and QR to polarize. Furthermore, the MIG-2 rho-family GTPase is required for QL and QR to migrate (Zipkin, et al., 1997), and thus may also be required for these cells to polarize. These hints of conserved molecular mechanism suggest that learning more about the polarization of the Q cells may shed light on the process of polarization in general and in particular how polarization occurs in a multicellular environment.

Control of Hox Expression

Hox genes were first characterized in *Drosophila* because mutations in these genes caused dramatic transformation of one body segment into another (Lewis, 1978). The defining characteristics of Hox proteins are that they contain the homeobox DNA binding motif, that they are expressed in stripes along the A/P axis, that they are encoded by genes that are arranged in clusters, and that the order of genes in these clusters corresponds to the order of their stripes of expression (Krumlauf, 1994, Lawrence and Morata,

1994). The ordering of the Hox genes and their function in specifying A/P pattern is essentially conserved in all metazoans: for example, the *Deformed* Hox homolog is expressed in a limited A/P domain that is more anterior than the *Abdominal-B* domain in mice, frogs, worms, and flies (Slack, et al., 1993, Manak and Scott, 1994). This is truly amazing, given the significant differences in the patterns of early embryogenesis across different animal phyla.

How might the regional patterns of Hox expression be established? There are three possible mechanisms: spatially localized cues, temporal cues (timing of cell birth), and lineage. In the cases of temporal or lineage controls, the A/P localized domains of expression would then arise as a byproduct. In *Drosophila*, it is clear that the Hox genes are positionally regulated. Localized Hox expression depends on the gap genes, which in turn are positionally regulated by the maternally supplied (and localized) *bicoid* and *nanos* proteins (reviewed in Lawrence, 1992). Manipulations that change gap gene expression domains cause subsequent changes in Hox expression domains (Harding and Levine, 1988). This cascade of positional information is facilitated in *Drosophila* because the early embryo is syncytial, allowing easy access for diffusible transcription factors to pattern neighboring cells. Nonetheless, the regulatory interactions that lead to sharp stripes of Hox expression are extremely complex (reviewed in Lawrence, 1992).

In vertebrates, transplant experiments also suggest that Hox expression is positionally controlled. The developing hindbrain is segmented into rhombomeres along the A/P axis with different Hox genes expressed in different rhombomeres (Krumlauf, 1994). If presumptive rhombomere tissue is transplanted to a different A/P position, it can adopt

the Hox gene fate of the target tissue (Grapin-Botton, et al., 1995). However, in *C. elegans* at least, position-independent mechanisms can also be responsible for the pattern of Hox expression. In the *C. elegans* embryo, the mesodermal cell M normally migrates toward the posterior and then starts expressing the Hox gene *mab-5*. Surprisingly, if this migration is blocked, M still expresses *mab-5* even though it remains in the anterior (Cowing and Kenyon, 1996). In order to argue that *mab-5* is positionally controlled in the M cell, one would have to claim that the positional signals can reach far enough to contact an anterior M cell. At some point, such broad signals can no longer be considered positional cues. A simpler explanation is that non-positional controls lead to *mab-5* expression in M.

An example of Hox regulation by timing is provided by the leech *Helobdella*. In this organism, parallel lines of cells stretching along the A/P axis are produced by budding blast cells at one end. Hox genes are normally expressed in coordinated stripes that span multiple lines of cells, but if division in one blast cell is blocked, it generates Hox patterns appropriate for its adjusted timing, no longer in register with the neighboring lines of cells (Nardelli-Haefliger, et al., 1994).

What can the Q cells add to our understanding of the control of Hox expression? *mab-5* normally comes on in QL after it migrates toward the posterior. Meanwhile, QR, which migrates toward the anterior, does not express *mab-5*. Is this difference in *mab-5* expression the result of an A/P localized signal? Or is the example of the M cell described above more typical in *C. elegans*, with Hox expression under non-positional controls? Formally, there are two possible ways in which a signal could produce differential *mab-5* expression in the Q cells. A posterior signal could

activate *mab-5* in QL or *mab-5* expression could be the default, with an anteriorly localized signal repressing *mab-5* in QR. It has proved difficult to surgically or pharmacologically alter the location of the Q cells to test these positional models directly, but some previous work and the experiments described in Chapter 2 indirectly address the issue of QL specific *mab-5* expression.

The *mab-5* missense allele, *bx54*, produces MAB-5 protein that is non-functional but is still recognized by anti-MAB-5 antibodies. This mutant MAB-5 protein is detectable in QL immediately following its migration to the posterior, but as the QL descendants migrate anteriorly, they stop expressing MAB-5 (S. Salser and C. Kenyon, unpublished). Although this is what one would expect if an extracellular signal controlled MAB-5 expression in QL, the result does not prove the positional model. The more accurate interpretation is that it demonstrates that *mab-5* is required for maintenance of its own expression in QL. This maintenance could be by a positional signal or simply by a cell-autonomous, auto-regulatory loop.

The mutants described in Chapter 2, *unc-73(-)*, *unc-40(-)*, and *dpy-19(-)*, all prevent QL and QR from migrating in opposite directions. These mutations also sometimes prevent the expression of *mab-5* in QL. In addition, in *unc-40* and *dpy-19* mutants, QR sometimes inappropriately expresses *mab-5*. I also found that the Q cells normally send leading projections in the direction they will migrate, and that these projections are misdirected in *unc-40* and *dpy-19* mutants. Interestingly, the frequency with which the projections point toward the posterior correlates with the frequency of *mab-5* expression. This correlation, like the *bx54* experiment

described above, lends support to the positional model only because it fails to rule it out.

At this point, then, it remains unclear whether positional signals control *mab-5* expression in the Q cells. The resolution of this question will most likely come by discovering the molecular identity of the genes required to activate *mab-5* in QL and learning where these genes are expressed and where they function. Whatever the answer is for the Q cells, the larger positional vs. non-positional debate is likely to fade as more and more details of Hox regulation are revealed. For example, in the lineage of the V5 epidermal cell in *C. elegans*, the pattern of *mab-5* expression switches on and off repeatedly and this complex expression pattern is required to specify many different cell fates (Salser and Kenyon, 1996). Similar dynamic patterns of Hox expression are seen in *Drosophila* and vertebrates (Carroll, et al., 1986, Nelson, et al., 1996). Moreover, the *Polycomb group* and *trithorax group* genes, which are involved in the formation of chromatin complexes, are required for maintenance of Hox expression. These genes add another layer of complexity to Hox regulation (reviewed in Kennison, 1995, Simon, 1995, Pirrotta, 1997). Thus, the control of which cells express which Hox genes is, like any cell fate, best viewed as reflection of the interaction of cell autonomous and non-autonomous mechanisms.

CONCLUSION

The study of the migration of the Q neuroblasts captures a number of significant mysteries in developmental biology. In addition to telling us about left/right asymmetry, cell polarization, and regulation of Hox genes,

the Q cells also have the potential to tell us how these processes are integrated to carry out pattern formation during development.

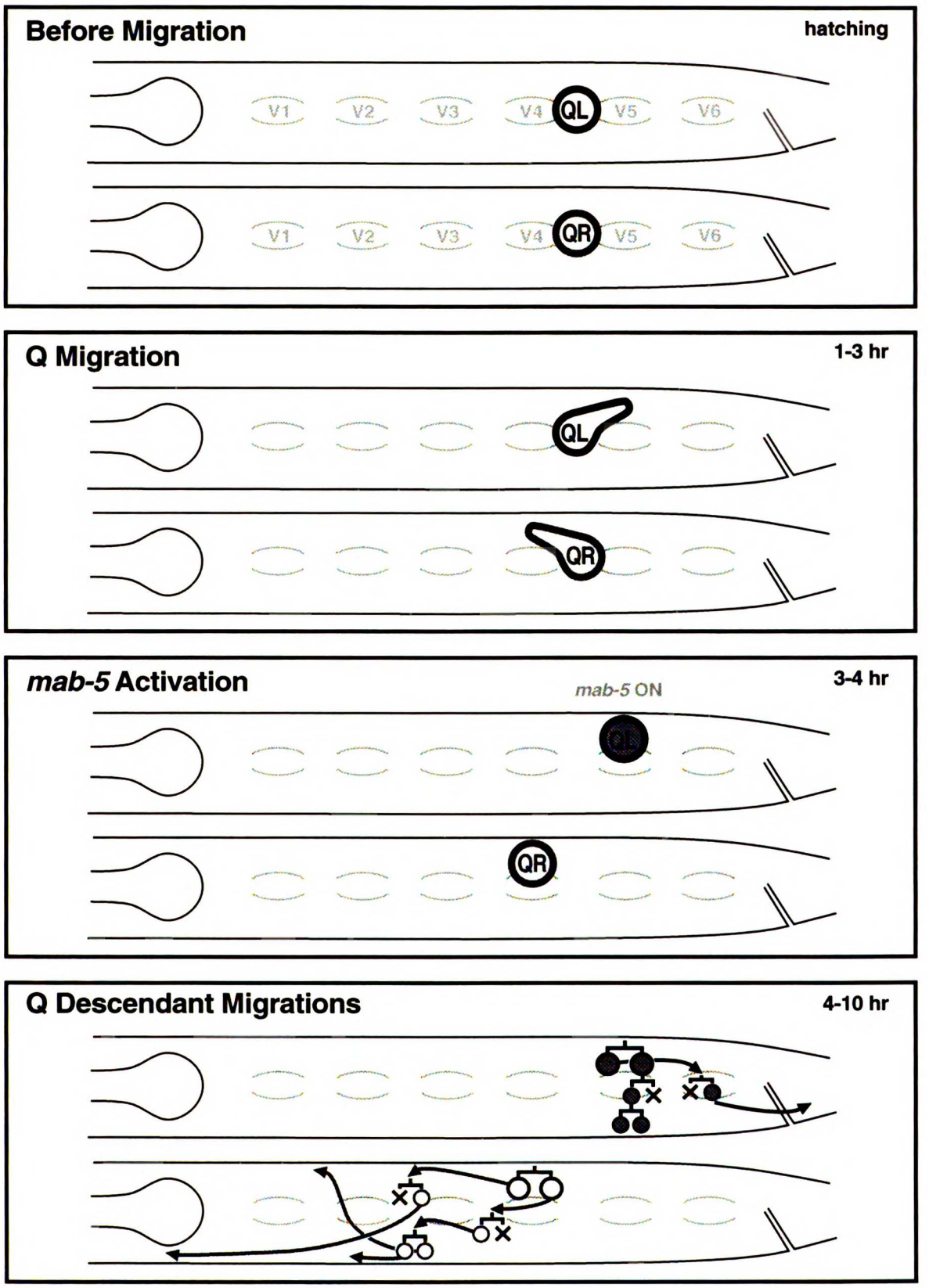
Before Migration
hatching
V1
V2
V3
V4
QL
V5
V6
V1
V2
V3
V4
QR
V5
V6
Q Migration
1-3 hr
QL
QR
mab-5 Activation
mab-5 ON
3-4 hr
QL
QR
Q Descendant Migrations
4-10 hr

Figure 1.1

REFERENCES

Biben, C. and R. P. Harvey (1997). Homeodomain factor Nkx2-5 controls left/right asymmetric expression of bHLH gene eHand during murine heart development. *Genes and Development* **11**, 1357-69.

Brown, N. A. and L. Wolpert (1990). The development of handedness in left/right asymmetry. *Development* **109**, 1-9.

Cadigan, K. M. and R. Nusse (1997). Wnt signaling: a common theme in animal development. *Genes Dev* **11**, 3286-305.

Carroll, S. B., R. A. Laymon, M. A. McCutcheon, P. D. Riley and M. P. Scott (1986). The localization and regulation of Antennapedia protein expression in Drosophila embryos. *Cell* **47**, 113-22.

Chan, S. S., H. Zheng, M. W. Su, R. Wilk, M. T. Killeen, et al. (1996). UNC-40, a C. elegans homolog of DCC (Deleted in Colorectal Cancer), is required in motile cells responding to UNC-6 netrin cues. *Cell* **87**, 187-95.

Chant, J. (1996). Generation of cell polarity in yeast. *Curr Opin Cell Biol* **8**, 557-65.

Chant, J. and I. Herskowitz (1991). Genetic control of bud site selection in yeast by a set of gene products that constitute a morphogenetic pathway. *Cell* **65**, 1203-12.

Chant, J., M. Mischke, E. Mitchell, I. Herskowitz and J. R. Pringle (1995). Role of Bud3p in producing the axial budding pattern of yeast. *J Cell Biol* **129**, 767-78.

Chant, J. and L. Stowers (1995). GTPase cascades choreographing cellular behavior: movement, morphogenesis, and more. *Cell* **81**, 1-4.

Chenevert, J. (1994). Cell polarization directed by extracellular cues in yeast. *Mol Biol Cell* **5**, 1169-75.

Chiang, C., Y. Litingtung, E. Lee, K. E. Young, J. L. Corden, et al. (1996). Cyclopia and defective axial patterning in mice lacking Sonic hedgehog gene function. *Nature* **383**, 407-13.

Collignon, J., I. Varlet and E. J. Robertson (1996). Relationship between asymmetric nodal expression and the direction of embryonic turning. *Nature* **381**, 155-8.

Costa, M., M. Weir, A. Coulson, J. Sulston and C. Kenyon (1988). Posterior pattern formation in C. elegans involves position-specific expression of a gene containing a homeobox. *Cell* **55**, 747-56.

Cowing, D. and C. Kenyon (1996). Correct Hox gene expression established independently of position in Caenorhabditis elegans. *Nature* **382**, 353-6.

Drubin, D. G. and W. J. Nelson (1996). Origins of cell polarity. *Cell* **84**, 335-44.

Grapin-Botton, A., M. A. Bonnin, L. A. McNaughton, R. Krumlauf and N. M. Le Douarin (1995). Plasticity of transposed rhombomeres: Hox gene induction is correlated with phenotypic modifications. *Development* **121**, 2707-21.

Harding, K. and M. Levine (1988). Gap genes define the limits of antennapedia and bithorax gene expression during early development in Drosophila. *Embo J* **7**, 205-14.

Herskowitz, I., H. O. Park, S. Sanders, N. Valtz and M. Peter (1995). Programming of cell polarity in budding yeast by endogenous and exogenous signals. *Cold Spring Harb Symp Quant Biol* **60**, 717-27.

Hyatt, B. A., J. L. Lohr and H. J. Yost (1996). Initiation of vertebrate left-right axis formation by maternal Vg1. *Nature* **384**, 62-5.

Keely, P. J., J. K. Westwick, I. P. Whitehead, C. J. Der and L. V. Parise (1997). Cdc42 and Rac1 induce integrin-mediated cell motility and invasiveness through PI(3)K. *Nature* **390**, 632-6.

Kennison, J. A. (1995). The Polycomb and trithorax group proteins of Drosophila: trans-regulators of homeotic gene function. *Annual Review of Genetics* **29**, 289-303.

Kenyon, C. (1986). A gene involved in the development of the posterior body region of *C. elegans*. *Cell* **46**, 477-487.

Kidd, T., K. Brose, K. J. Mitchell, R. D. Fetter, M. Tessier-Lavigne, et al. (1998). Roundabout controls axon crossing of the CNS midline and defines a novel subfamily of evolutionarily conserved guidance receptors. *Cell* **92**, 205-15.

Krumlauf, R. (1994). Hox genes in vertebrate development. *Cell* **78**, 191-201.

Lawrence, P. A. (1992). The making of a fly : the genetics of animal design. (Cambridge, Mass., USA: Blackwell Science).

Lawrence, P. A. and G. Morata (1994). Homeobox genes: their function in Drosophila segmentation and pattern formation. *Cell* **78**, 181-9.

Levin, M. (1997). Left-right asymmetry in vertebrate embryogenesis. *Bioessays* **19**, 287-96.

Levin, M., R. L. Johnson, C. D. Stern, M. Kuehn and C. Tabin (1995). A molecular pathway determining left-right asymmetry in chick embryogenesis. *Cell* **82**, 803-14.

Levin, M. and M. Mercola (1998). The compulsion of chirality: toward an understanding of left-right asymmetry. *Genes and Development* **12**, 763-9.

Levin, M., S. Pagan, D. J. Roberts, J. Cooke, M. R. Kuehn, et al. (1997). Left/right patterning signals and the independent regulation of different aspects of situs in the chick embryo. *Dev Biol* **189**, 57-67.

Lewis, E. B. (1978). A gene complex controlling segmentation in Drosophila. *Nature* **276**, 565-70.

Lim, L., E. Manser, T. Leung and C. Hall (1996). Regulation of phosphorylation pathways by p21 GTPases. The p21 Ras-related Rho subfamily and its role in phosphorylation signalling pathways. *Eur J Biochem* **242**, 171-85.

Lowe, L. A., D. M. Supp, K. Sampath, T. Yokoyama, C. V. Wright, et al. (1996). Conserved left-right asymmetry of nodal expression and alterations in murine situs inversus. *Nature* **381**, 158-61.

Ma, L., L. C. Cantley, P. A. Janmey and M. W. Kirschner (1998). Corequirement of specific phosphoinositides and small GTP-binding protein Cdc42 in inducing actin assembly in Xenopus egg extracts. *Journal of Cell Biology* **140**, 1125-36.

Manak, J. R. and M. P. Scott (1994). A class act: conservation of homeodomain protein functions. *Dev Suppl* **1994**, 61-77.

Miki, H., T. Sasaki, Y. Takai and T. Takenawa (1998). Induction of filopodium formation by a WASP-related actin-depolymerizing protein N-WASP. *Nature* **391**, 93-6.

Nardelli-Haefliger, D., A. E. Bruce and M. Shankland (1994). An axial domain of HOM/Hox gene expression is formed by morphogenetic alignment of independently specified cell lineages in the leech Helobdella. *Development* **120**, 1839-49.

Nelson, C. E., B. A. Morgan, A. C. Burke, E. Laufer, E. DiMambro, et al. (1996). Analysis of Hox gene expression in the chick limb bud. *Development* **122**, 1449-66.

Neumann, C. J. and S. M. Cohen (1997). Long-range action of Wingless organizes the dorsal-ventral axis of the Drosophila wing. *Development* **124**, 871-80.

Nobes, C. D. and A. Hall (1995). Rho, rac, and cdc42 GTPases regulate the assembly of multimolecular focal complexes associated with actin stress fibers, lamellipodia, and filopodia. *Cell* **81**, 53-62.

O'Connor, T. P., J. S. Duerr and D. Bentley (1990). Pioneer growth cone steering decisions mediated by single filopodial contacts in situ. *J Neurosci* **10**, 3935-46.

Pirrotta, V. (1997). Chromatin-silencing mechanisms in Drosophila maintain patterns of gene expression. *Trends in Genetics* **13**, 314-8.

Pringle, J. R., E. Bi, H. A. Harkins, J. E. Zahner, V. C. De, et al. (1995). Establishment of cell polarity in yeast. *Cold Spring Harb Symp Quant Biol* **60**, 729-44.

Salser, S. J. and C. Kenyon (1996). A C. elegans Hox gene switches on, off, on and off again to regulate proliferation, differentiation and morphogenesis. *Development* **122**, 1651-61.

Sampath, K., A. M. Cheng, A. Frisch and C. V. Wright (1997). Functional differences among Xenopus nodal-related genes in left-right axis determination. *Development* **124**, 3293-302.

Sanders, S. L. and I. Herskowitz (1996). The BUD4 protein of yeast, required for axial budding, is localized to the mother/BUD neck in a cell cycle-dependent manner. *J Cell Biol* **134**, 413-27.

Segall, J. E. (1993). Polarization of yeast cells in spatial gradients of alpha mating factor. *Proc Natl Acad Sci U S A* **90**, 8332-6.

Siegfried, E., T. B. Chou and N. Perrimon (1992). wingless signaling acts through zeste-white 3, the Drosophila homolog of glycogen synthase kinase-3, to regulate engrailed and establish cell fate. *Cell* **71**, 1167-79.

Simon, J. (1995). Locking in stable states of gene expression: transcriptional control during Drosophila development. *Current Opinion in Cell Biology* **7**, 376-85.

Simon, M. N., V. C. De, B. Souza, J. R. Pringle, A. Abo, et al. (1995). Role for the Rho-family GTPase Cdc42 in yeast mating-pheromone signal pathway. *Nature* **376**, 702-5.

Slack, J. M., P. W. Holland and C. F. Graham (1993). The zootype and the phylotypic stage. *Nature* **361**, 490-2.

Srivastava, D., T. Thomas, Q. Lin, M. L. Kirby, D. Brown, et al. (1997). Regulation of cardiac mesodermal and neural crest development by the bHLH transcription factor, dHAND. *Nature Genetics* **16**, 154-60.

Steven, R., T. J. Kubiseski, H. Zheng, S. Kulkarni, J. Mancillas, et al. (1998). UNC-73 activates the Rac GTPase and is required for cell and growth cone migrations in C. elegans. *Cell* **92**, 785-95.

Sulston, J. and H. Horvitz (1977). Post-embryonic cell lineages of the nematode, *C elegans*. *Developmental Biology* **56**, 110-156.

Supp, D. M., D. P. Witte, S. S. Potter and M. Brueckner (1997). Mutation of an axonemal dynein affects left-right asymmetry in inversus viscerum mice. *Nature* **389**, 963-6.

Valtz, N., M. Peter and I. Herskowitz (1995). FAR1 is required for oriented polarization of yeast cells in response to mating pheromones. *J Cell Biol* **131**, 863-73.

Varlet, I. and E. J. Robertson (1997). Left-right asymmetry in vertebrates. *Curr Opin Genet Dev* **7**, 519-23.

Weiss, P. (1947). The Problem of Specificity in Growth and Development. *Yale Journal of Biology and Medicine* **19**, 235-278.

Wood, W. B. (1991). Evidence from reversal of handedness in C. elegans embryos for early cell interactions determining cell fates. *Nature* **349**, 536-8.

Wood, W. B. (1997). Left-right asymmetry in animal development. *Annual Review of Cell and Developmental Biology* **13**, 53-82.

Zecca, M., K. Basler and G. Struhl (1996). Direct and long-range action of a wingless morphogen gradient. *Cell* **87**, 833-44.

Zigmond, S. H., M. Joyce, J. Borleis, G. M. Bokoch and P. N. Devreotes (1997). Regulation of actin polymerization in cell-free systems by GTPgammaS and Cdc42. *Journal of Cell Biology* **138**, 363-74.

Zipkin, I. D., R. M. Kindt and C. J. Kenyon (1997). Role of a new Rho family member in cell migration and axon guidance in C. elegans. *Cell* **90**, 883-894.

CHAPTER 2: Genes required to orient left/right asymmetric cell migration in *C. elegans*.

This work relied on data provided by other Kenyon Lab members. Judith Austin originally characterized the Q migration defect in *unc-40* mutants, and isolated the *dpy-19* alleles, *mu78* and *mu79*. Jeanne Harris did the MAB-5 antibody staining in *unc-40*. mutants. Naomi Robinson constructed the *unc-40;mab-5* double mutant and scored the final position of the Q descendants in that strain. Mary Sym originally noticed the Q migration defect in *unc-73* mutants, constructed the *unc-73;mab-5* double, and scored the final position of the Q descendants in that strain. Everything else, including the writing, was done by me.

SUMMARY

The bilateral *C. elegans* neuroblasts QL and QR are born in the same anterior/posterior (A/P) position, but polarize and migrate left/right asymmetrically: QL toward the posterior and QR toward the anterior. After their migrations, QL but not QR switches on the Hox gene *mab-5*. We find that in animals lacking either the UNC-40/Netrin receptor or a novel transmembrane protein DPY-19, the Q cells polarize randomly; in fact, an individual Q cell polarizes in multiple directions over time. In addition, either cell can express *mab-5*. Both UNC-40 and DPY-19, as well as the Trio/GTPase exchange factor homolog UNC-73, are also required for full polarization and migration. These proteins may participate in a signaling system that orients and polarizes these migrating cells in a left/right asymmetrical fashion during development.

INTRODUCTION

The left/right asymmetry of *C. elegans* is established at the 6 cell stage by cell-cell interactions and is manifest as subsequent left/right differences in many tissues in the developing animal (Hutter and Schnabel, 1995). One particularly intricate asymmetry involves the behavior of the Q neuroblasts. QL, on the left side of the animal, migrates toward the posterior whereas QR, on the right side, migrates toward the anterior (Figure 2.1A). After its migration, QL starts expressing the Hox gene *mab-5* (Salser and Kenyon, 1991). *mab-5*, which is presumed to act as a transcriptional regulator, directs the QL descendants to remain in the posterior: the QL.p branch of the lineage remains stationary and the QL.a branch of the lineage migrates further posteriorly. QR does not express *mab-5*, and this allows both branches of the QR lineage to migrate anteriorly (Figure 2.1B). *mab-5*, which specifies many

cell fates in the posterior body region (Kenyon, 1986), is required for the posterior pattern of migration in the QL descendants. In *mab-5(-)* animals, QL itself migrates normally toward the posterior, but the QL descendants then migrate anteriorly (Chalfie, et al., 1983). *mab-5* expression is not only necessary, but also sufficient for the posterior pattern of migration in the Q descendants. Ectopic expression of *mab-5(+)* in the QR descendants can cause them to migrate posteriorly. (Salser and Kenyon, 1991). Mosaic analysis and laser induced single-cell delivery of heat-shock-*mab-5* have shown that *mab-5* acts in the Q descendants to determine their direction of migration (Kenyon, 1986, Harris, et al., 1996).

(Some researchers have used the term "Q migration" to refer to the migrations of the Q cells and their descendants. In this paper, "Q migration" refers strictly to the migrations of QL and QR. The subsequent *mab-5* dependent migrations that occur after QL and QR divide are referred to as the "Q descendant migrations.")

The observation that QL normally migrates toward the posterior before expressing *mab-5* has led to a "positional model" for *mab-5* activation in the Q cell (Salser and Kenyon, 1991). In this model, QL's migration would bring it in contact with a hypothetical A/P localized signal to turn on *mab-5*. QR, by migrating anteriorly, would avoid this signal and therefore not express *mab-5*. One candidate for such a signal is the *C. elegans* Wnt homolog *egl-20*. Recent work has demonstrated that several of the genes required to activate *mab-5* in QL (Harris, et al., 1996) (J. Maloof and C. K., unpublished) are components of a Wnt signaling pathway. *egl-20* is a Wnt homolog (J. Whangbo & C. Kenyon, unpublished), *lin-17* is a frizzled homologs (Sawa, et al., 1996), and *bar-1* is a beta-catenin/armadillo homolog (D. Eisenmann and S. Kim, personal communication and J. Maloof and C. Kenyon, unpublished).

However, these Wnt pathway genes are not required for the migration of QL and QR in opposite directions. Thus, some other system must generate the initial asymmetry in the Q neuroblasts.

To understand this initial asymmetry and how it is linked to the subsequent Wnt-dependent system that establishes *mab-5* asymmetry, we have characterized three genes that are required for the migration of QL and QR: *unc-40*, *dpy-19* and *unc-73*.

unc-40 encodes an Ig-superfamily member that functions as a receptor and responds to UNC-6/Netrin in an evolutionarily conserved system for guiding dorsal-ventral (D/V) cell migration and axon pathfinding (Chan, et al., 1996, Keino, et al., 1996, Kolodziej, et al., 1996, Guthrie, 1997). In *C. elegans*, mutations in *unc-40* cause many defects in ventrally directed axon guidance and cell migration as well as defects in the migration of the Q descendants (Hedgecock, et al., 1990). We found that *unc-40* mutations prevent the migration of the Q neuroblasts and cause them to polarize in random directions. Finally, in *unc-40* mutants, the Q descendants misexpress *mab-5*, which then causes them to migrate incorrectly.

dpy-19 was originally identified as one of a large set of mutants that cause animals to be short (DumPY) (Brenner, 1974). We found that mutations in the gene *dpy-19* cause the same defects in the Q cells as seen in *unc-40* mutants: the Q cells polarize incorrectly and their descendants misexpress *mab-5*. We show here that *dpy-19* encodes a novel transmembrane protein that may define a new component in the conserved Netrin guidance system.

Previous work has shown that *unc-73* is required for directed growth and guidance of many cells and axons along A/P and D/V trajectories (Hedgecock, et al., 1987, McIntire, et al., 1992, Way, et al., 1992, Forrester and

Garriga, 1997). The sequence of *unc-73* is similar to the vertebrate Trio protein and contains multiple domains including spectrin and pleckstrin homologies, two dbl-type guanine-exchange-factor (GEF) domains, a transmembrane domain and Ig and Fibronectin repeats (Steven, et al., 1998). We found that mutations in *unc-73* prevent the migrations of QL and QR, but, in contrast to *dpy-19* and *unc-40*, only mildly disrupt the direction of Q polarizations and the expression of *mab-5* in the Q descendants.

RESULTS

Overview of the Q neuroblast migrations in wild type.

Shortly before the worm hatches, QL and QR are born as the anterior daughters of the Q/V5 precursor cells found on either side of the animal. This places the Q cells neatly in a line with the epidermal cells V1-V6 found on each side, with QL and QR just anterior of V5L and V5R, respectively. From 1 to 3 hours after hatching, QL and QR undergo their migrations: QL toward the posterior and QR toward the anterior (Figure 2.1A). Using Nomarksi optics, only cell nuclei are visible in C. elegans. In order to see cell outlines, we first *clr-1(e1745ts)* mutants (Hedgecock, et al., 1990) and observed that the first step of the Q cell migrations is the growth of a distinct cytoplasmic protrusion in the direction that the whole cell will migrate (Figure 2.1C,D and J. Austin and C. K. unpublished). Because *clr-1* mutations can arrest development, and because *clr-1* interacts genetically with *egl-15*, a gene involved in sex myoblast migration in C. elegans (DeVore, et al., 1995), we have sought a better approach to revealing the shape of the Q cells. *mig-2::GFP* is a membrane localized reporter construct that is expressed in the Q and V cells (Zipkin, et al., 1997), and it has enabled us to observe the shape of the Q cells during their migration. QL and QR at hatching appear identical to

one another and similar in shape to the V cells (Figure 2.1E-H). By one hour after hatching, QL has clearly sent a protrusion toward the posterior whereas QR has an anterior protrusion (Figure 2.1I,J). We will refer to this first asymmetric difference as posterior and anterior polarization of the Q cells. At 2 hours, the Q cells have begun to migrate, moving slightly dorsally past the neighboring V cells. The cells continue to migrate, sometimes leaving behind a process attached to their starting point (Figure 2.1K,L). At 3.5 hours after hatching the Q cells divide (Figure 2.1M,N).

Mutations in *unc-40*, *unc-73*, and *dpy-19* block the nuclear migration of QL and QR.

To learn more about the mechanisms that generate the asymmetry of the Q cell migrations, we have focused on genes that are required for this first step. We found that in *unc-40*, *dpy-19* and *unc-73* mutants, the Q cells do not complete their migrations. We quantified the extent of their migrations by measuring the separation of the Q cell nuclei along the A/P axis at 2.5-3.5 hours. At this time in wild-type animals, the Q cells have moved approximately 25 μm apart from one another. In contrast, in *unc-40*, *dpy-19* and *unc-73* mutants, QL and QR are still in similar A/P positions (Figure 2.2). Based on nuclear migration, these three mutants had similar phenotypes, but we looked in more detail to understand their effects on the polarization of the Q cells. We will describe how each of these mutants affects the shape of the Q cells and then describe their effects on *mab-5* expression in the Q descendants.

Mutations in *unc-40* randomize the direction of Q cell polarization

At 2-3 hours after hatching, wild-type animals always displayed strong polarization of QL toward the posterior and QR toward the anterior (Figure

2.1K,L). In *unc-40* mutants at this time, both QL and QR had shortened projections and these projections sometimes pointed in the wrong direction. We saw QL cells that were polarized weakly toward the posterior (Figure 2.3A) or toward the anterior (Figure 2.3B), or were irregularly shaped (Figure 2.3C). QR had similar polarization defects. Figure 2.3D shows an animal in which QR points toward the posterior. Although the shape of the Q cells varied from animal to animal, we roughly quantitated their phenotypes according to how far toward the anterior or posterior the Q cell extended (Figure 2.3L,M). In *unc-40(e1430)*, 29% of QL cells showed no clear direction of polarization and 4% were misdirected toward the anterior. Similarly, 38% of QR cells were unpolarized, and 14% of QR cells were incorrectly polarized toward the posterior. There was no correlation between the shape of the QL and QR cells in an individual animal (data not shown).

Single Q cells can polarize in different directions over time in *unc-40* mutants

The wide range of Q cell shapes that we saw in *unc-40(-)* animals could have reflected either of two different kinds of underlying phenotypes. One possibility was that in any individual, the Q cell polarized in one direction, with the variability arising across different individuals. The other possibility was that each Q cell in each animal was able to polarize in multiple directions. In this case, the observed variation in Q cell shape would reflect the fact that we observed snapshots of different animals that were each varying over time. To distinguish between these two possibilities we followed the shape of the Q cells in single animals from 0 to 3 hours after hatching. Although time-lapse imaging of GFP in living animals limited our resolution, we found that the Q cells can point in multiple directions in a single animal (compare Figure 2.4C and 2.4I). The most common Q cell shape

in these time-lapse experiments was irregular or unpolarized, but in *unc-40(e1430)* mutants, we saw polarization of QL toward both the anterior and posterior at different times in 3/11 animals.

***unc-40* is expressed in the Q cells**

The UNC-40/DCC receptor is required for many cell and axon migrations in *C. elegans*. It has been shown that *unc-40* can act cell autonomously to orient axon outgrowth and that an *unc-40::GFP* construct is expressed in many of the cells that require *unc-40* for D/V guidance (Chan, et al., 1996). We found that *unc-40::GFP* is also expressed in the Q cells at the time of their migration (Figure 2.10A,B and Chan, et al., 1996), suggesting that it may act as the receptor or part of the receptor that orients the QL and QR migrations toward opposite directions along the A/P axis.

The Q cell migrations do not require UNC-6, the known UNC-40 ligand.

UNC-6/Netrin is expressed at the ventral midline and is likely to function as a ligand for *unc-40* in guiding D/V migrations (Wadsworth, et al., 1996). We tested whether *unc-6* was also required for the A/P migrations of the Q neuroblasts. We found that in the null allele *unc-6 (ev400)*(Ishii, et al., 1992), the Q cells still migrated in opposite directions (Figure 2.5). Using *mig-2::GFP*, we confirmed that Q cell polarization in *unc-6* was also normal (data not shown). We also tested whether *unc-5*, another gene involved in D/V guidance was required for the Q cell migrations. *unc-5* encodes a transmembrane protein that directs dorsal axon migrations away from *unc-6* (Leung, et al., 1992). Because *unc-5*-dependent UNC-6 avoidance requires *unc-40* (Chan, et al., 1996), it has been suggested that UNC-5 and UNC-40 may act as a complex to guide migration away from UNC-6 (Leonardo, et al., 1997).

We found that *unc-5* was not required for the Q cell migrations (Figure 2.5) and thus is unlikely to be a part of the *unc-40* guidance system in Q. Finally, given *unc-40*'s proposed role in Netrin avoidance, the Q cell migration defect seen in an *unc-40* mutant might be the result of these cells inappropriately responding to an UNC-6 signal that they would normally ignore. To test this, we asked whether QL and QR could migrate in opposite directions in an *unc-40; unc-6* double mutant. The Q migrations were still blocked (Figure 2.5), implying that *unc-40*'s role in the Q migrations is completely independent of *unc-6*. Thus, of the known genes involved in the *C. elegans* Netrin guidance system, only *unc-40* is also required for the polarization and migration of the Q cells.

Mutations in *dpy-19* also randomize the direction of Q cell polarization

As observed in *unc-40* mutants, the Q cells in *dpy-19* mutants did not extend projections as far as in wild type, and these projections were sometimes misdirected (Figure 2.3L,M). QL polarized weakly toward the posterior (Figure 2.3E), weakly toward the anterior (Figure 2.3F), or was irregularly shaped (Figure 2.3G). QR was affected similarly (Figure 2.3H). In the null *dpy-19* allele, *n13471348* (see below), QL showed no clear direction of polarization in 72% of animals and projected anteriorly in 8% of animals. Similarly, QR lacked clear polarization in 70% of animals and projected incorrectly toward the posterior in 8% of animals. Like mutations in *unc-40*, mutations in *dpy-19* can cause the Q cells in a single animal to point in different directions over time. In time-lapse video experiments similar to those described for *unc-40*, we saw polarization toward both the anterior and posterior at different times in QL in 4/11 animals and in QR in 3/11 animals.

***dpy-19* is a novel transmembrane protein**

dpy-19 was cloned using a transposon-insertion allele to identify a predicted gene (F22B7.10) that had previously been sequenced by the *C. elegans* sequencing project (personal communication, S. Collums and R Plasterk). We isolated cDNAs corresponding to F22B7.10 and confirmed that this predicted gene was *dpy-19* by identifying mutations in all known *dpy-19* alleles (Figure 2.6A). *n1347n1348*, the allele with the most severe phenotype, contained an approximately 9 kb deletion that removed most of the *dpy-19* coding region. The *dpy-19* transcript was not detected in *n1347n1348* by Northern analysis (Figure 2.6B), confirming that this allele represents the null phenotype of *dpy-19*.

The sequence of *dpy-19* defines a novel protein with 13 putative transmembrane domains. The only significant matches identified by database searches were two regions with homology to human expressed sequence tags (ESTs) (Figure 2.6A).

In an attempt to identify proteins that might interact with DPY-19, we conducted a large screen for suppressors of *dpy-19(e1259)*. 8/8 independent suppressor mutations were tightly linked to *dpy-19* and behaved genetically as if they were intragenic revertants to near wild-type levels of *dpy-19* function. We sequenced the *dpy-19* region in the two strongest suppressors and found that they were indeed revertants (Figure 2.6A). The strongest suppressor, *e1259mu298*, contained a second mutation in the same codon that was originally mutated in *e1259*. Because all eight suppressors are likely to be intragenic and because our mutagenesis was extensive enough to find a second mutation in the originally mutated codon, we suspect that there are no extragenic targets in which a point mutation can compensate for a reduction in *dpy-19* activity.

dpy-19::GFP is expressed weakly in Q and strongly in many nearby cells

In order to learn what cells express *dpy-19*, we inserted GFP at the predicted 5' and 3' ends of the gene (see Materials and Methods). These GFP tagged constructs showed full rescuing activity and displayed similar expression patterns. At the time of the Q cell migrations, many cells faintly express GFP-tagged DPY-19 in a reticular pattern, with the brightest staining localized at the periphery of cell nuclei (Figure 2.10E). To more clearly identify the cells expressing *dpy-19*, we made a transcriptional fusion that used the same upstream region as the rescuing GFP tagged constructs, but with the *dpy-19* coding sequence replaced by a nuclear localized *GFP+lacZ* coding sequence. This construct was expressed faintly in QL and QR, more strongly in the neighboring epidermal cells (dorsal hyp7 cells, ventral P cells, and lateral V cells) and most strongly in dorsal and ventral body muscle cells (Figure 2.10F).

dpy-19 is not required for other cell migrations

To see if *dpy-19* is generally required for cell motility, we examined *dpy-19* mutants for defects in other cell and axon migrations. No defects in the embryonic migrations of HSN, CAN, M, and ALM were seen in *dpy-19(n1347n1348)* (n=35) and no defects in the postembryonic migrations of the distal tip cells (DTCs) or male linker cell were seen in *dpy-19(mu78)* (n=50). Thus, although *dpy-19* and *unc-40* have similar defects in the Q cells, *unc-40* has many other defects (Hedgecock, et al., 1990) that are not present in *dpy-19*.

Mutations in *unc-73* prevent the Q cells from fully polarizing

Mutations in *unc-73* also block the Q migrations and disrupt the polarized leading processes that normally point in the direction that Q cells will migrate (Figure 2.3I-M). In the weak *unc-73* allele, *e936*, these defects were quite mild: only 6% of QL cells were unpolarized and 9% of QR cells were unpolarized. In the stronger *unc-73* allele, *gm33*, 24% of QL cells and 26% QR cells were unpolarized. Although many cells in *dpy-19*, *unc-40*, and *unc-73* mutants were scored as having no clear polarity, the unpolarized phenotype ("-" in Figure 2.3L,M) seen in *unc-73(gm33)* mutants was qualitatively different from that seen in *dpy-19* and *unc-40* mutants: the Q cells were almost always round rather than irregularly shaped. In contrast to *unc-40* and *dpy-19* mutants, we never saw any *unc-73* mutants in which the Q cells were pointed in the wrong direction. Although relatively few cells polarize in the wrong direction in *dpy-19* and *unc-40* mutants, the complete absence of incorrectly polarized cells seen in *unc-73* mutants was significantly different from the phenotypes of *dpy-19* and *unc-40* mutants ($p<=0.007$, Fisher exact test). Finally, consistent with the hypothesis that *unc-73* acts within the Q cells to allow their outgrowth and migration, an *unc-73::GFP* fusion is expressed strongly in Q at the time of its migration (Figure 2.10C,D and Steven, et al., 1998).

***unc-40*, *dpy-19*, and *unc-73* mutants all have defects in *mab-5* expression in the Q descendants**

We next asked what affect these mutations would have on the second aspect of the Q cells' left/right asymmetry, *mab-5* expression. We stained animals with anti-MAB-5 antibodies when the Q cells had divided once. *mab-5* is normally expressed in the QL daughter cells, but not the QR

daughter cells. Interestingly, mutations in all three genes described above also partially randomize *mab-5* expression (Figure 2.7). In *unc-40* and *dpy-19* mutants, the QL descendants often failed to express *mab-5*. At a lower frequency, the QR descendants sometimes expressed *mab-5*, a phenotype never observed in wild-type. In the weak *unc-73* allele, *e936*, only a small percentage of animals failed to express *mab-5* in QL, but in the stronger *unc-73* allele, *gm33*, this defect was more pronounced: 33.3% of animals failed to express *mab-5* strongly in QL. In addition, at a very low frequency, the QR descendants in *unc-73* mutants expressed *mab-5*.

Because *mab-5* is necessary and sufficient for posterior migration in the Q descendants, the defects in *mab-5* expression described above were expected to result in defects in the migration in the Q descendants. As predicted, we found that in *unc-40* and *dpy-19* mutants, the QL descendants sometimes migrated anteriorly and the QR descendants sometimes remained in the posterior (Figure 2.8 and Hedgecock, et al., 1990). At a lower frequency, the QL and QR descendants were misplaced in *unc-73* mutants (Figure 2.8 and Way, et al., 1992). In all mutants, the frequency of animals in which the QL or QR descendants expressed *mab-5* was well correlated with the corresponding frequency of animals in which the Q descendants remained in the posterior (Figure 2.7E).

We confirmed genetically that the mispositioned Q descendants in *unc-40, dpy-19* and *unc-73* mutants were caused by the misexpression of *mab-5*. In the *unc-40;mab-5, mab-5 dpy-19,* and *unc-73;mab-5* double mutants, the QL and QR descendants always migrated anteriorly (Figure 2.8), demonstrating that the Q descendants that remained in the posterior in the single mutants were doing so because they expressed *mab-5*.

Although *dpy-19* and *unc-40* are required for QL and QR to migrate, these genes are not required for the Q descendants to migrate. In the absence of *mab-5* (in the *unc-40;mab-5* and *mab-5 dpy-19* double mutants), the QL and QR descendants go as far toward the anterior as they do in *mab-5* single mutants (Figure 2.8). By contrast, in the *unc-73;mab-5* double, the QR descendants ended their migrations at intermediate positions on the A/P axis (Figure 2.8). Therefore, *unc-73* must have two functions in the Q lineage: it is required for the migrations of QL and QR and for the full extent of the Q descendant migrations toward the anterior when*mab-5* is OFF.

Mab-5 expression in the Q cell migration mutants still requires *egl-20*/Wnt.

We also tested whether *mab-5* expression in Q in *unc-40, dpy-19,* and *unc-73* mutants was established by the same Wnt signaling pathway that is used in wild type. We stained *unc-40;egl-20, dpy-19;egl-20* and *unc-73;egl-20* mutants with MAB-5 antibodies and found that MAB-5 protein was absent in the Q descendants (*unc-40(e271);egl-20(n585)*, n=50 for QL, 42 for QR; *dpy-19(mu78);egl-20*, n=50 for QL, 54 for QR; *unc-73(e936);egl-20(n585)*, n=50 for QL, 31 for QR). Thus *unc-40, dpy-19,* and *unc-73* mutants still require *egl-20*/Wnt to express *mab-5*, implying that these mutations cause misregulation of *mab-5* by interfering with the same signaling pathway that is normally used to control *mab-5* expression.

The shape of the Q cell is correlated with the final position of the Q descendants

Because *unc-40, dpy-19* and *unc-73* mutations all caused randomization of both polarization and *mab-5* expression in the Q cells, we wondered if these two phenotypes were correlated. To investigate this, we tested multiple

alleles of all three mutants at multiple temperatures and found that, on both the left and the right, the frequency with which the Q cell polarized toward the posterior was strongly correlated with the frequency of *mab-5* expression in the Q descendants (Figure 2.9A). We tested whether the trend seen in populations of animals would hold true for individual *dpy-19(-)*or *unc-40(-)* animals, i.e. when a Q cell points the wrong way does it then misexpress *mab-5*? Because the Q cells shape in *dpy-19* and *unc-40* mutants varied over time (Figure 2.4), we considered several models for how the profile of the Q polarization might predict *mab-5* expression in the Q descendants. Our first model was that Q cells that pointed toward the posterior at any time would subsequently turn on *mab-5*. We tested this by picking individual *dpy-19(-)* animals at 2.5 hrs after hatching in which QL or QR were polarized toward the posterior. In these selected animals, the Q descendants still frequently migrated anteriorly (8/21 for QL and 6/7 for QR), thereby ruling out this model. Our second model was that the shape of the Q cell at some particular time, e.g. right before the division of Q, would correlate with the expression of *mab-5*. However, no such critical time point was apparent from the experiments in which we followed the shape of the Q cells over time (data not shown). Our third model was one of degree: those Q cells which spent the most time polarized toward the posterior would also be the most likely to express *mab-5*. When we tallied up the average polarization toward the posterior for QL cells in individual *dpy-19* and *unc-40* mutant animals, the animals with the most posterior polarization were the ones in which the Q descendants remained in the posterior (Figure 2.9B).

DISCUSSION

By studying the migration of the Q neuroblasts in *C. elegans* we can address three basic developmental questions: how are left/right asymmetries specified, how do cells orient themselves along the A/P axis in response to extracellular cues, and how is Hox gene expression regulated in migrating cells? The genes described here, *unc-40*, *dpy-19*, and *unc-73*, represent our first steps in understanding the pathway that controls the migration of QL and QR and the link between these migrations and the subsequent expression of *mab-5* in the Q descendants.

unc-40 and dpy-19 are required to orient the Q cells and to correctly express *mab-5* in the Q cell descendants

In both *unc-40* and *dpy-19* mutants the earliest detectable defect in the Q cells is their failure to form stable polarizations in opposite directions. Instead, QL and QR seem to cast about, forming short-lived, small processes that point in multiple directions. The next defect apparent in *unc-40* and *dpy-19* mutants is the failure of QL and QR to migrate in opposite directions. Finally, QL sometimes fails to express *mab-5*, and QR sometimes inappropriately expresses *mab-5*. Subsequently, as directed by their expression levels of *mab-5*, the Q descendants migrate posteriorly or anteriorly. It is interesting that the UNC-40 receptor is required for the migration of the Q descendants only indirectly, i.e. because it is required to correctly specify the pattern of *mab-5* expression. This result highlights the complexity involved in the control of cell migration and suggests that there may be other *unc-40* dependent migrations that do not use UNC-40 for guidance, but instead use it for an earlier fate-specification event that then controls subsequent migrations.

In D/V guidance, *unc-40* acts cell autonomously to orient the migration of many cells and axons. Because *unc-40::GFP* is expressed in the Q cells, *unc-40* is also likely to function as a receptor in orienting the A/P migration of QL and QR. The ligand for UNC-40 in D/V guidance is UNC-6/Netrin, but since *unc-6* is not required for the Q cell migration, we propose that a currently unidentified protein functions as a ligand for UNC-40 in the Q cells. Similarly, although the vertebrate *unc-40* homolog, DCC, is required for axon growth toward Netrin (Keino, et al., 1996, de la Torre, et al., 1997), there are other neurons that express DCC but do not respond to Netrin (Keino, et al., 1996, Fazeli, et al., 1997). Our findings are consistent with the proposal that *unc-40* may act as a co-receptor that is required for the response to multiple extracellular cues (Leonardo, et al., 1997).

dpy-19 encodes a novel protein, but the similarity of the Q phenotypes in *dpy-19* and *unc-40* mutants suggests that *dpy-19*'s function may be closely linked to the function of the UNC-40 receptor or its ligands. One surprising result is that mutations in *dpy-19*, unlike *unc-40*, do not seem to affect other cell migrations. It is possible that *dpy-19* is specifically required for only the Q cells, although the broad expression of *dpy-19::GFP* and the Dumpy phenotype suggest that *dpy-19* may be used in other tissues. One possibility is that *dpy-19* is involved in polarization or migration of many cells, but the Q cell migrations are the most sensitive to loss of *dpy-19* activity. Since all *dpy-19* alleles, including the null allele, are temperature sensitive, we suspect that the absence of *dpy-19(+)* is revealing some underlying temperature-sensitive process. Different migrating cells could have varying sensitivities to this underlying process, and, since strong *dpy-19* alleles are lethal at 25°C, it is possible that this t.s. lethality prevents us from seeing defects in other cell migrations.

***unc-73* is required for the migration of QL and QR**

Mutations in *unc-73* cause many cell and axon migration defects. The CAN, HSN, ALM, and QR descendant migrations all stop prematurely (Desai, et al., 1988, Hedgecock, et al., 1990, Forrester and Garriga, 1997) . The axons of HSN, AVL, DVB, DD, and VD are shortened, misdirected or defasciculated from their normal bundles (McIntire, et al., 1992). Because UNC-73 contains regions of homology to Cdc-24, an exchange factor for the Cdc-42 GTPase that is required for budding polarity in *S. cerevisiae*, it has been suggested that it may be involved in orienting cell polarization (Way, et al., 1994). *unc-73* has more recently been classified as a member of the Trio family of proteins (Steven, et al., 1998). The vertebrate Trio protein was identified as a protein that associates with the LAR receptor tyrosine phosphatase, which, in turn, has been found at focal adhesions. It is not yet clear whether Trio is involved in determining cell polarity or just in carrying out cell migration. We found that mutations in *unc-73* block the Q cell migrations while not strongly disrupting Q cell polarity. Although we cannot rule out the possibility that a complete elimination of *unc-73* function would cause the Q cells to polarize randomly, it seems most likely that *unc-73*'s role in the Q cell polarization is not in orienting their direction of polarization but in carrying out that polarization.

In *unc-73* mutants, as in wild-type, the QL cell at hatching is pointed slightly anteriorly (Fig.1G,H). In many *unc-73* mutant animals, QL was able to reorient and point toward the posterior without showing any signs of migration (for example, Fig.3I). This phenotype illustrates that polarization in the Q cells can occur without migration.

It is interesting to note that MIG-2, a *C. elegans* Rho-family GTPase, is also required for the migration of the Q cells (Zipkin, et al., 1997). Rho family members can regulate cytoskeletal reorganization in cultured cells (Nobes and Hall, 1995) and dominant negative or activating mutant Rho proteins in *Drosophila* are capable of blocking cell migration and axon outgrowth (Luo, et al., 1994). In *C. elegans*, *mig-2* activating and null mutations both result in shortened migrations of QL and QR, suggesting that GTP-GDP cycling of *mig-2* may be required for the Q cells to migrate. *mig-2* is therefore a good candidate to be a downstream target of the *unc-73* GEF domains in carrying out the Q cell migrations. Further experiments are needed to test this hypothesis, but the partial suppression of *unc-73(e936)* by *muIs28*, the multicopy array of GFP-tagged *mig-2(+)* (see Materials and Methods) is intriguing.

Models for Q polarization

Two simple models can explain how QL and QR might polarize and migrate in opposite directions. The first model postulates that the two Q cells are identical, in that they both seek out the same target, but that the location of the target is different on the two sides of the animal (Figure 2.11A). In the second model, the difference between the Q migrations on the left and right sides is caused by the Q cells themselves, not their surroundings. For example, QL might be attracted toward a localized signal along the A/P axis, while QR was repelled (Figure 2.11B). In both models, *unc-40* is likely to be part of a receptor in the Q cells that responds to extracellular signals. Interestingly, in the second model, *unc-40*'s role in Q would be analogous to its role in D/V migration, in which it is required for growth towards and away from *unc-6*/Netrin signals. Because *dpy-19::GFP* is seen in the Q cells as

well as in surrounding tissues, its role could be in producing, localizing or responding to the signals proposed in Figure 2.11. The *unc-73* expression pattern and mutant phenotype suggest that it could function in the Q cells to allow them to respond to these signals.

Models for activation of *mab-5*

The previously proposed "positional model" suggested that the migrations of QL and QR served to position these cells so that only one Q cell received an A/P localized signal controlling the expression of *mab-5* (Salser and Kenyon, 1991). This model was attractive for two reasons: 1) QL normally expresses *mab-5* only after it migrates toward the posterior and 2) the hallmark of Hox genes is their regional expression along the A/P axis and, for *mab-5*, this region of expression overlaps with the path of QL's migration. Thus we were surprised to find that in all the mutants described here, the Q cells do not migrate, but the Q descendants still express *mab-5*, at least some of the time. However, by visualizing the outlines of the Q cells, we found that QL and QR normally send leading projections in opposite directions prior to migrating and that the Q cells still polarize to varying degrees in all the Q cell migration mutants. In all strains examined, in both QL and QR, the degree of polarization toward the posterior correlated with the likelihood of expressing *mab-5*. This correlation is consistent with a revised positional model, in which polarization toward the posterior, in the absence of migration, is sufficient to detect an A/P localized signal directing the expression of *mab-5* (Figure 2.11C). This model would require that the signal be quite sharply defined or that the Q cells be remarkably sensitive. Such discrimination may be possible, since calculations of the sensitivity of polarizing yeast cells,

Dictyostelium, and neutrophils suggest that a cell can detect a 1% difference in receptor occupancy across its diameter (Zigmond, 1977, Segall, 1993).

We note however, that the correlation between cell shape and *mab-5* expression does not prove that these two events are causally linked. A second, non-positional model can also explain the polarization and *mab-5* expression phenotypes seen in the Q cell migration mutants. In this model, Q cell polarization and *mab-5* expression are determined in parallel by some upstream fate-specifying event (Fig.11D). Mutations in *dpy-19*, *unc-40*, and *unc-73* would all interfere with proper fate specification, leading to fates that were intermediate between QL and QR. These incompletely specified Q cells would then make errors in both their polarization and their *mab-5* expression. The resolution of whether or not *mab-5* is normally activated in Q by an A/P localized signal will most likely result from examining the expression pattern of the candidate positional signal, *egl-20*/Wnt, and testing whether localized *egl-20* expression is required for correct *mab-5* expression the Q descendants.

MATERIALS AND METHODS

General methods and genetics

C. elegans strains were maintained and genetically manipulated as described (Sulston and Hodgkin, 1988).

All alleles of *unc-40*, *dpy-19*, and *unc-73* examined were temperature sensitive for their polarization and *mab-5* expression phenotypes. The phenotypes at 15, 20 and 25°C in these mutants were qualitatively similar, but more penetrant at higher temperatures. Because *unc-40(e1430)* and *dpy-19(n1348)* are likely to be null alleles, the temperature dependence presumably reflects the temperature sensitivity of some underlying process. Wild-type worms were not temperature sensitive for any of the phenotypes examined here. All data were collected at 20°C, with the following exceptions: *unc-40(e271)* and *unc-40(e1430)* were scored at 25° in Figure 2.3, 2.7, and 2.8 to more clearly illustrate their phenotypes; *dpy-19(n1348)* was scored at 15° in Figs. 3 and 8 because the strain was extremely unhealthy at 20°. The time at which the Q cell shape was scored in animals grown at 15 or 25° was adjusted appropriately to compensate for different developmental rates at these temperatures.

Because *unc-73(gm33)* animals have few or zero progeny, *unc-73(gm33)* strains were maintained using sDp2, a free duplication that contains *unc-73*(+). *unc-73(gm33)* progeny from *unc-73(gm33);sDp2* worms were identified by the shortened HSN migration phenotype of *unc-73* mutants (Desai, et al., 1988) and then scored for Q cell shape (in Figure 2.3) or MAB-5 staining (in Figure 2.7).

Microscopy and scoring of cell shapes and positions

Animals were staged by washing the hatched worms from a plate of eggs with M9 at 30 minute intervals. These "hatchoffs" were filtered through 13µm Nytex mesh to remove eggs accidentally carried up in the wash and then spotted on seeded NG plates. To measure the degree of polarization, animals were mounted on agarose pads starting at 2 hours after hatchoff collection and scored for the next 30 minutes.

To photograph Q cell shapes, animals were mounted on agarose pads containing 2uM sodium azide. Long-term exposure to sodium azide sometimes caused retraction of cell outlines, so animals were examined within 15 minutes of mounting. Most images were collected using a BioRad MRC-600 confocal microscope, and then later rotated and contrast-enhanced using Adobe Photoshop.

For Figure 2.4, in which the cell shape was followed over time in individual animals, 0-30 minute old worms were mounted on agarose pads. Every 15 or 20 minutes, the Q cells were brought into focus using Nomarski optics, and then exposed for 100-200 msec using the Zeiss fluoroscein filter set and a Uniblitz shutter (Vincent Associates) connected to an Apple Macintosh computer. Custom macros in NIH Image were used to open and close the shutter and control image accumulation on a Photometrics Imagepoint CCD camera. Images were stored on laser videodisc for later analysis. Multiple fluorescence exposures in a short period caused the worms to move rapidly away from the illumination and also caused significant photobleaching; thus only one snapshot per timepoint was possible.

To measure the length of the QL and QR migrations, animals were mounted on 2mM sodium azide pads starting at 2.75 hours after hatchoff collection and continuing for the next 30 minutes. Straight, non-moving worms were selected and Nomarski video images of the left and right sides

were acquired using a Scion LG framegrabber for later analysis. Using NIH Image, the center of the nucleoli of QL and QR were marked, and the straight-line distance between these two points was calculated. The distances of QL and QR from a fixed point on the animal, the posterior end of the intestine, was also measured. From these data, we found that all mutants described here affected the migration of QL and QR equally, and so we have used the QL-QR distance as our single metric.

The final position of the Q descendants was determined in late L1 larvae using standard Nomarski optics. QL.paa and QL.pap (also known as PVM and SDQL) were scored on the left side and QR.paa and QR.pap (also known as AVM and SDQR) were scored on the right side. The QL.ap and QR.ap cells migrate into body regions with many other neurons, and therefore cannot be scored reliably. Cells were positioned relative to the epidermal cells V1-V6, each of which have divided once at the end of L1.

HSN, CAN, M and ALM cell positions were scored in 0-3 hour old animals, relative to the V and P epidermal cells. The following positions were defined as wild-type. HSN: between P5,6 and V5. CAN: between V3 and V4. M: between P7,8 and V5. ALM: between V2 and V3. DTC and Linker cell migrations were scored at 36 hours after hatching and compared to wild type (Sulston and Horvitz, 1977).

MAB-5 antibody staining

Performed as described in Salser, et al., 1993.

Cloning _dpy-19_

The strain MT3128 *dpy-19(n1347)* was found by M. Finney to contain a Tc1 transposon insertion in *dpy-19*. DNA adjacent to all the Tc1 insertions in

this strain was amplified by PCR and this mix of amplified fragments was then probed against a Southern blot of cosmids in the *dpy-19* region (S. Collums and R. Plasterk, personal communication). This led to the tentative mapping of *dpy-19* to the predicted gene F22B7.10, which had been identified by the *C. elegans* genome sequencing project (Sulston, et al., 1992). We used RT-PCR and 3' RACE (Frohman, 1993) to amplify cDNAs containing sequences from F22B7.10 and were able to define a single SL1-spliced transcript (Figure 2.6). The sequence of this transcript matched the computer-predicted splice sites in F22B7.10, with the exception of the first exon and intron.

For Northern analysis, RNA from N2 (wild type) and *dpy-19(n1347n1348)* was prepared using Trizol (Gibco-BRL) according to the protocol of R. Burdine and M. Stern, personal communication. 20 µg of total RNA/lane was blotted using standard techniques (Sambrook, et al., 1989) and the blot was probed with digoxigenin labeled RNA, according to manufacturer's instructions (Genius Kit, Boerhinger). The *dpy-19* anti-sense probe was generated by in vitro transcription, using an RT-PCR product spanning exons 6-9 as template.

We rescued the Dpy and Q phenotypes of *dpy-19(mu78)* by injecting the cosmid C27E4 (which overlaps F22B7) at 12.5 µg/mL using standard techniques (Mello, et al., 1991). We then narrowed the rescuing activity to a 10 kb Bgl-II fragment (injected at 12.5 µg/mL) that contains 1.5 kb upstream and 1.0 kb downstream of the *dpy-19* gene.

To identify the mutations in *dpy-19* alleles, genomic sequences covering the *dpy-19* coding region were PCR amplified from the *dpy-19* alleles *mu78, mu79, e1259,* and *e1314*. DNA was either amplified with Taq (Roche) and sequenced directly or amplified with Pwo hi-fidelity polymerase

(Boerhinger), purified using Geneclean (Bio101), treated with Taq and dATP to add A overhangs, and then subcloned into pGEM-T vector (Promega) for sequencing. In all cases, mutations were confirmed by sequencing from a second PCR amplification. We confirmed that *dpy-19(n1347)* contained a Tc1 insertion in the *dpy-19* gene by PCR with *dpy-19* and Tc1 specific primers. The approximate endpoints of the deletion in *n1347n1348* were determined by Southern analysis.

GFP fusion constructs

mig-2::GFP: The rescuing, NH2-terminal tagged *mig-2::GFP* fusion construct described in Zipkin, et al., 1997was coinjected with the cosmid *C14G10 [unc-31(+)]* into *unc-31(e169); him-5(e1490)* worms using standard techniques (Mello, et al., 1991). We selected an extrachromosomal array carrying line and integrated the array using 3600 R of gamma-irradiation at 300 R/min, as described (Zipkin, et al., 1997). Of 10 integrated lines, we chose the one with highest *mig-2::GFP* expression levels and outcrossed it three times to *unc-31(e169); him-5(e1490)*, selecting at each generation for animals with high levels of *mig-2::GFP* expression. The outcrossed strain, *unc-31(e169); him-5(e1490); muIs28[mig-2::GFP+unc-31(+)]*, had wild-type Q descendant final positions (n=100). *muIs28* was then crossed into *dpy-19*, *unc-40*, and *unc-73* mutants. We found that *muIs28* partially supressed *unc-40* and *unc-73* mutations. At 20°C, *unc-40(e271)* had 18% QL descendants anterior (n=50) while *unc-40(e271);muIs28* had 8% QL descendendants anterior (n=50). *unc-73(e936)* had 4% QL descendants anterior (n=50) while *unc-73(e936);muIs28* had 0% QL descendants anterior (n=200). *unc-73(e936);muIs28* animals also appeared less Unc than *unc-73(e936)* alone, but *muIs28* did not suppress the shortened HSN and QR descendant

migration phenotypes of *unc-73(e936)*. Because we were concerned that *muIs28* could qualitatively change the Q cell shape phenotype in *unc-73* mutants, we used *unc-73::GFP* to visualize the Q cells in all *unc-73* mutant strains.

unc-73::GFP: The non-rescuing fusion *evIn80[unc-73::GFP + rol-6D]* fusion (described in Steven, et al., 1998) was crossed into *unc-73* mutants using standard techniques. *evIn80* has no affects on the Q descendants migrations in *unc-73(e936) [unc-73(e936);evIn80*: 6% QL.pax anterior, n=50]. We did not use *unc-73::GFP* for all cell shape assays because it was not as reliably expressed in the Q cells as *mig-2::GFP* and because *unc-73::GFP* expression in the intestine caused high background fluorescence.

unc-40::GFP: *evEx66[unc-40::GFP + rol-6D]*, from (Chan, et al., 1996)

dpy-19::GFP. We constructed a plasmid with 4.4kb upstream and 1.0 kb downstream of *dpy-19*. For the COOH-terminal GFP tagged construct, we used site-directed mutagenesis (Tomic, et al., 1990) to make a silent change in the 3rd from last codon of *dpy-19* which introduced a unique restriction site. We then inserted S65T GFP with 3 introns (from pPD95.85). We also used site-directed mutagenesis to insert a unique BamHI site after the 2nd codon of *dpy-19*. For the NH2-terminal GFP tagged construct, we then inserted F64L S65T GFP with 3 introns (from pPD114.35). For the transcriptional fusion, we used the BamHI site to excise the 4.4kb of upstream sequence, and then inserted the upstream sequence into a vector containing NLS::GFP::lacZ and the *unc-54* 3'UTR (derived from pPD96.04). These fusions were all injected at 100µg/mL with *C14G10(unc-31(+))* at 30µg/mL . The GFP-tagged constructs were injected into *dpy-19(mu78);unc-31(e169)*. The transcriptional fusion was injected into *unc-31(e169)*. All pPD vectors were provide by A. Fire.

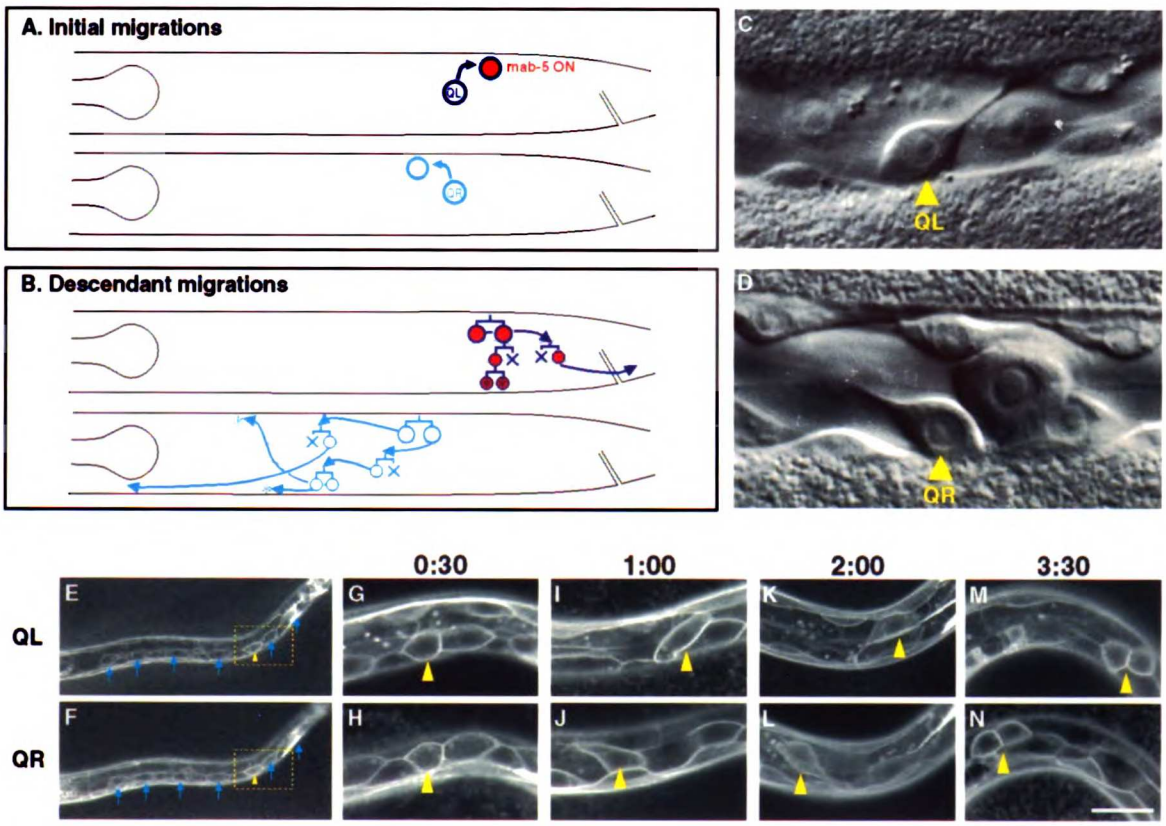

Figure 2.1 Wild type Q cell polarization and migration
(A) The migration of QL toward the posterior and QR toward the anterior. The epidermal cells V1-V6 are shown as landmarks. MAB-5 expression (shown in red) begins in QL after its migration.
(B) Pattern of divisions and further migrations of the Q descendants. X's indicate cell deaths. *'s indicate the stopping points of the Q.paa and Q.pap cells; these are scored to determine the final position of the Q descendants.
(C,D) QL and QR polarization in opposite directions visualized using *clr-1(e1745ts)* Animals were shifted from 20° to 25°C at 60 minutes after hatching (to elicit Clear phenotype) and viewed 60 minutes later using Nomarski optics.
(E,F) *mig-2::GFP* expression on the left and right side of the worm at hatching. The Q cell can be identified by position and by its stronger GFP expression compared to the neighboring V and P epidermal cells. Blue arrows show V1-V6 for reference. Area in yellow box is shown in more detail in G-N.
(G-N) *mig-2::GFP* expression showing typical QL and QR cell shapes from 30 minutes after hatching until the Q cells divide (M,N) at ~3.5 hours after hatching. Each time point shows left and right sides of the same animal. Arrowheads indicate QL on the left and QR on the right.
Scale bar: 5 μm in C-D, 30 μm in E-F, and 10 μm in G-N. C-N are confocal images. Anterior is to left, dorsal is up in all figures.

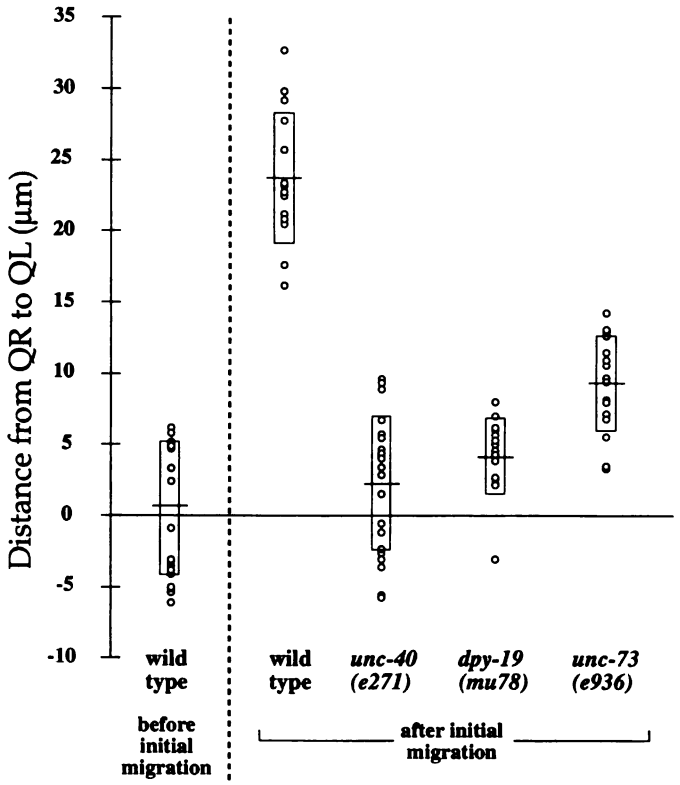

Figure 2.2. Extent of the Q cell migrations in wild type and in *unc-40*, *dpy-19*, and *unc-73* mutants.

Each circle represents the straight-line distance along the A/P axis between the centers of the QL and QR nucleoli in an individual animal. Negative values indicate that QR's nucleolus was more anterior than QL's. Horizontal bars and boxes show mean and standard deviation, respectively. In all three mutants, the Q cells divided at 3.5-4 hours after hatching, the same timing as in wild type, so the prevention of the Q migrations is not the result of slowed development. *dpy-19(mu78)* animals are not significantly Dpy as L1's.

Figure 2.3. Polarization of QL and QR in *unc-40*, *dpy-19*, and *unc-73* mutants

(A-H) Examples of Q cell shape in *unc-40;mig-2::GFP* and *dpy-19;mig-2::GFP* animals at 2 hours after hatching (compare with wild type, Figure 2.1K,L).

(I-K) Example of Q cell shape in *unc-73;mig-2::GFP* animals. Similar cell shapes are seen in *unc-73; unc-73::GFP*. Scale bar: 10μm. A-J are confocal images.

(L,M) Summary of the distance the Q cells extend toward the anterior and posterior at 2-3 hours after hatching. Each dot represents a single animal. The distance reached by the Q cells was scored relative to neighboring V cells in the following categories: [-] Q was round or irregularly shaped; [>] Q pointed toward V5, but did not reach as far as the A/P midpoint of V5; [>>] Q's most posterior tip extended to the midpoint of V5; [>>>] Q's most posterior tip extended past the midpoint of V5. <, <<, and <<< are defined similarly for the right side, except relative to a point which is 1/3 the distance from the posterior to anterior edge of V4. (The cell P7,8 is positioned between Q and V4, so polarization toward the anterior does not reach as far relative to V4.) Data in L and M were collected by visualizing the shape of Q using *mig-2::GFP* for *dpy-19* and *unc-40* mutants and *unc-73::GFP* for *unc-73* mutants. n≈ 50 animals for each strain.

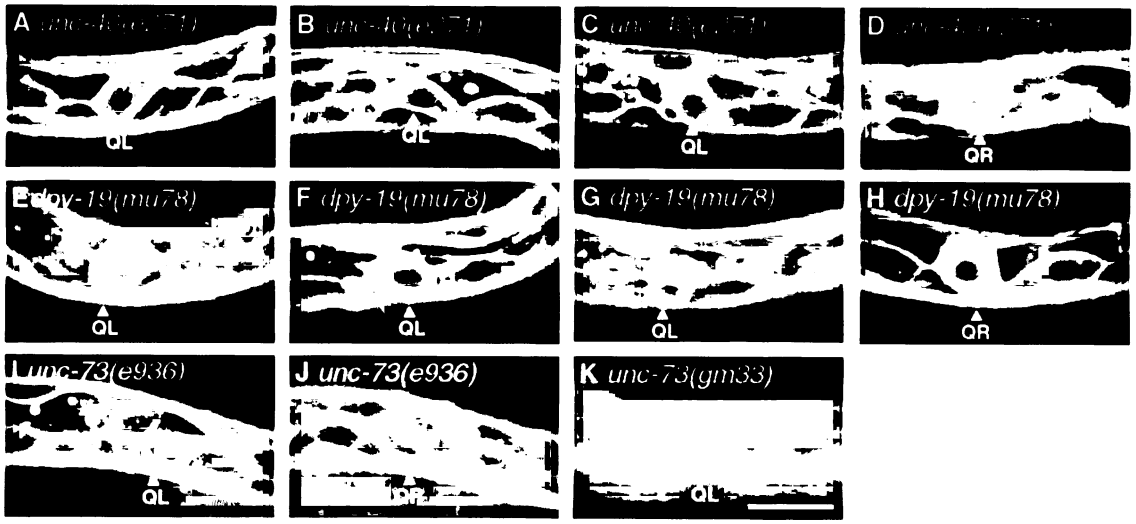
A
QL
B
QL
C
QL
D
QR
E dpy-19(mu78)
QL
F dpy-19(mu78)
QL
G dpy-19(mu78)
QL
H dpy-19(mu78)
QR
I unc-73(e936)
QL
J unc-73(e936)
QR
K unc-73(gm33)
QL

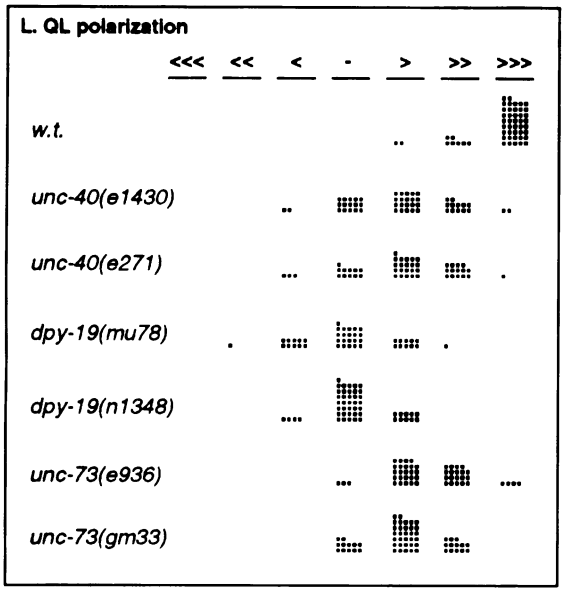
L. QL polarization
<<< << < - > >> >>>
w.t.
unc-40(e1430)
unc-40(e271)
dpy-19(mu78)
dpy-19(n1348)
unc-73(e936)
unc-73(gm33)

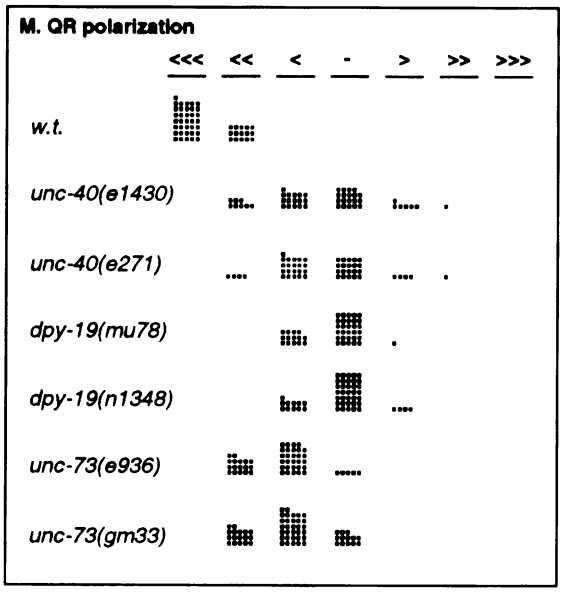
M. QR polarization
<<< << < - > >> >>>
w.t.
unc-40(e1430)
unc-40(e271)
dpy-19(mu78)
dpy-19(n1348)
unc-73(e936)
unc-73(gm33)

Figure 2.3

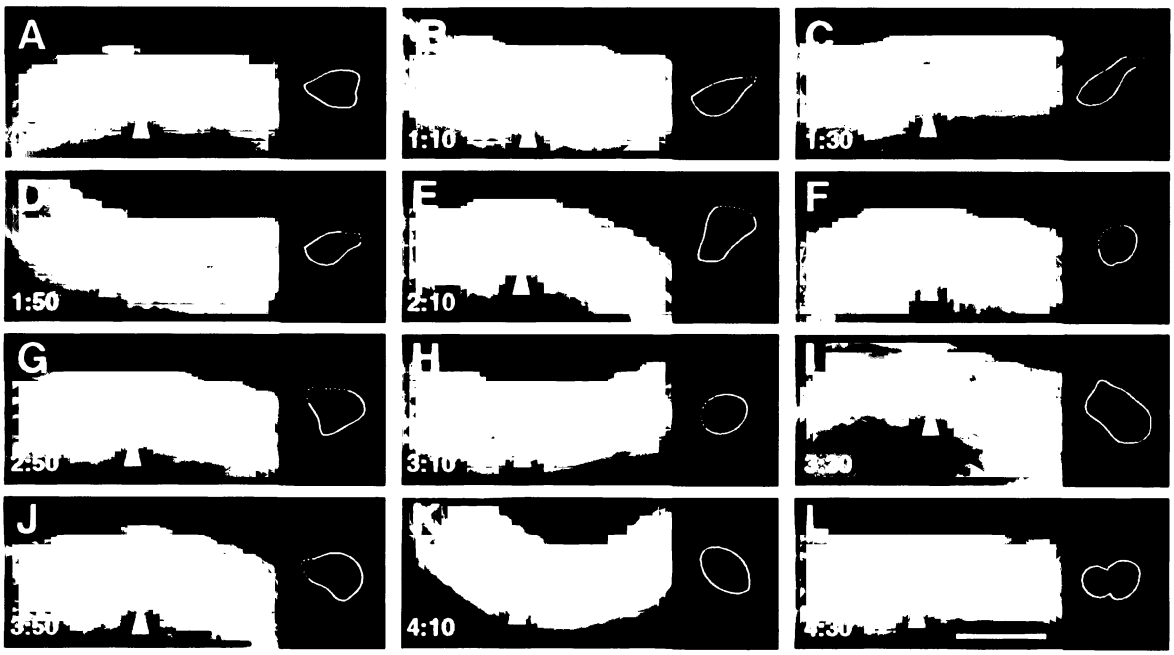

Figure 2.4. A single Q cell can polarize in multiple directions over time in an *unc-40* mutant.

Fluorescent images showing Q cell shape were collected every 20 minutes in an *unc-40(e1430);mig-2::GFP* animal. Tracings of the Q cell are shown to the right of each image. When the edge of the Q cell was out of focus or blurred by motion of the worm, dotted lines indicate estimates of the cell shape. Fluorescent time-lapse imaging sometimes slowed the rate of development (the Q cell shown here divided about 1 hour later than normal), but polarization reversals occurred in animals with normal developmental rates as well (16/31 *dpy-19* or *unc-40* mutant animals had normal timing of the Q division, and we saw polarization reversals in 3 out of these 16 animals). In addition, fluorescent imaging caused delayed development in 2/4 wild-type animals, yet we never saw polarization reversals in wild type.

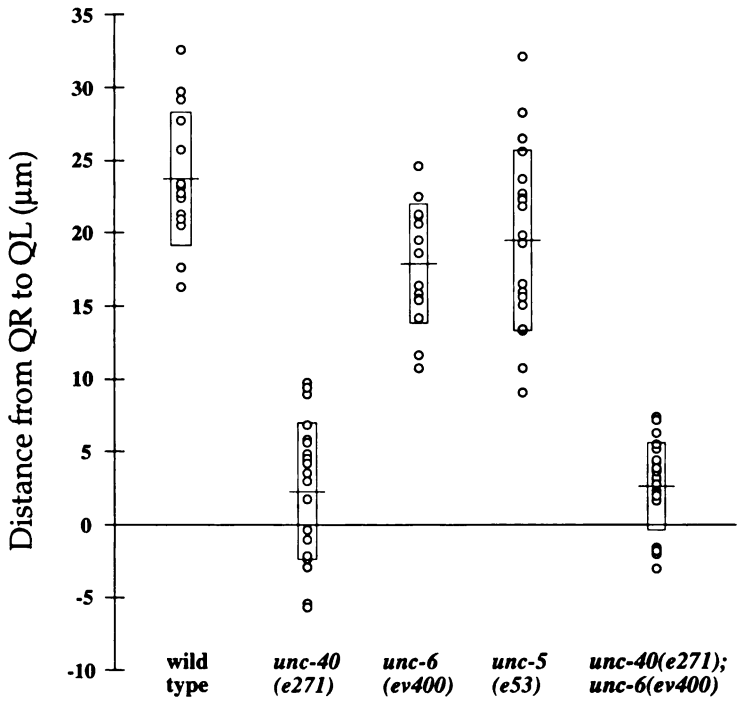

Figure 2.5. The Q migrations do not require *unc-5* or *unc-6*/Netrin.

Q cell migration distances were measured as in Figure 2.2. Data from wild type and *unc-40(e271)* are repeated here for comparison. *unc-6(ev400)* animals are variably small or misshapen. This may contribute to the slight reduction in the separation of the Q cells in *unc-6(ev400)* (17.9 +/- 4.1 µm) compared to wild type (23.7 +/- 4.1 µm).

Figure 2.6. Cloning of *dpy-19*

(A) Schematic diagram showing intron and exon boundaries in *dpy-19*. Shading within exons shows the location of 13 potential membrane spanning domains. The membrane topology predicting program "TopPredict II" favors a model in which only 11 of these cross the membrane, with a cytoplasmic N terminus (Claros and von Heijne, 1994). Shading above exons shows two regions which contain similarities to multiple randomly sequenced human cDNAs, including those shown in panel C. Arrows mark sites of point mutations found in four different *dpy-19* alleles. Open arrows mark sites of mutations found in intragenic revertants of *dpy-19(e1259)*. Exact mutation sites: *mu78*(L218->F), *e1259*(G185->D), *e1314*(splice acceptor mutation disrupts protein after R517), *mu79*(W653->STOP), *e1259mu298*(G185->N), *e1259mu300*(P127->S, G185->D).

(B) Northern blot of total RNA probed with sequences from the *dpy-19* gene. *n1347n1348* lane contains RNA from the deletion allele, *dpy-19(n1347n1348)*. (White bands reflect a decrease in background from excess rRNA.)

(C) Alignments to the two best human EST matches (Complete Genbank accession#'s: AA644618 and AA553359.). The AA64 region is 70% identical over 70 amino acids and the AA55 region is 44% identical over 158 amino acids.

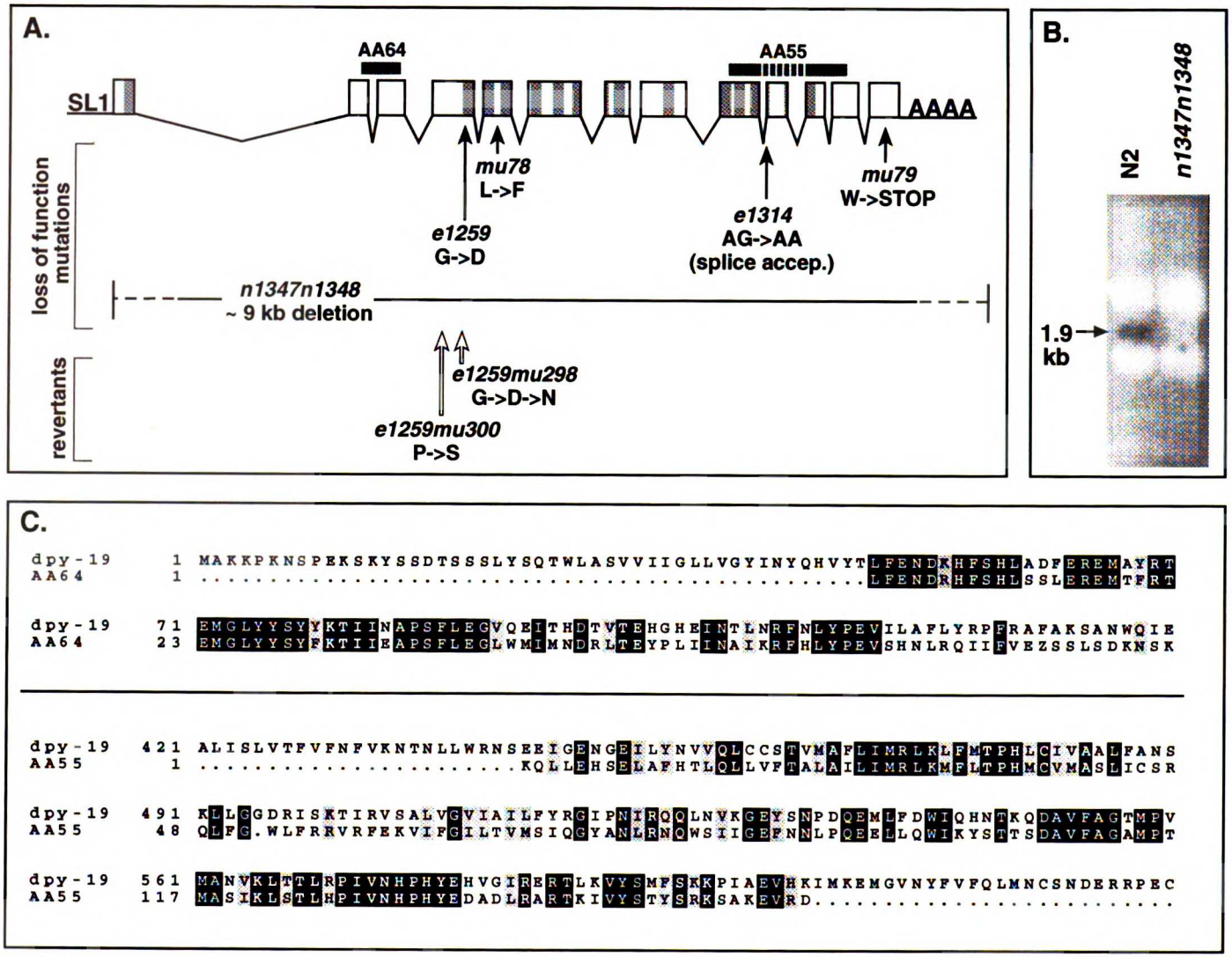
A.
AA64
AA55
SL1
AAAA
mu78
L->F
mu79
W->STOP
e1259
G->D
e1314
AG->AA
(splice accep.)
loss of function mutations
n1347n1348
~ 9 kb deletion
revertants
e1259mu298
G->D->N
e1259mu300
P->S
B.
N2
n1347n1348
1.9 kb
C.
dpy-19 1 MAKKPKNSPEKSKYSSDTSSSLYSQTWLASVVIIGLLVGYINYQHVYTLFENDKHFSHLADFEREMAYRT
AA64 1 .....LFENDRHFSHLSSLEREMTFRT
dpy-19 71 EMGLYYSYYKTIINAPSFLEGVQEITHDTVTEHGHEINTLNRFNLYPEVILAFLYRPFRAFAKSANWQIE
AA64 23 EMGLYYSYFKTIIEAPSFLEGLWMIMNDRLTEYPLIINAIKRFHLYPEVSHNLRQIIFVEZSSLSDKNSK
dpy-19 421 ALISLVTFVFNFVKNTNLLWRNSEEIGENGEILYNVVQLCCSTVMAFLIMRLKLFMTPHLCIVAALFANS
AA55 1 .....KQLLEHSELAFHTLQLLVFTALAILIMRLKMFLTPHMCVMASLICSR
dpy-19 491 KLLGGDRISKTIRVSALVGVIAILFYRGIPNIRQQLNVKGEYSNPDQEMLFDWIQHNTKQDAVFAGTMPV
AA55 48 QLFG.WLFRRVRFEKVIFGILTVMSIQGYANLRNQWSIIGEFNNLPQEELLQWIKYSTTSDAVFAGAMPT
dpy-19 561 MANVKLTTLRPIVNHPHYEHVGIRERTLKVYSMFSKKPIAEVHKIMKEMGVNYFVFQLMNCSNDERRPEC
AA55 117 MASIKLSTLHPIVNHPHYEDADLRARTKIVYSTYSRKSAKEVRD.....

Figure 2.6

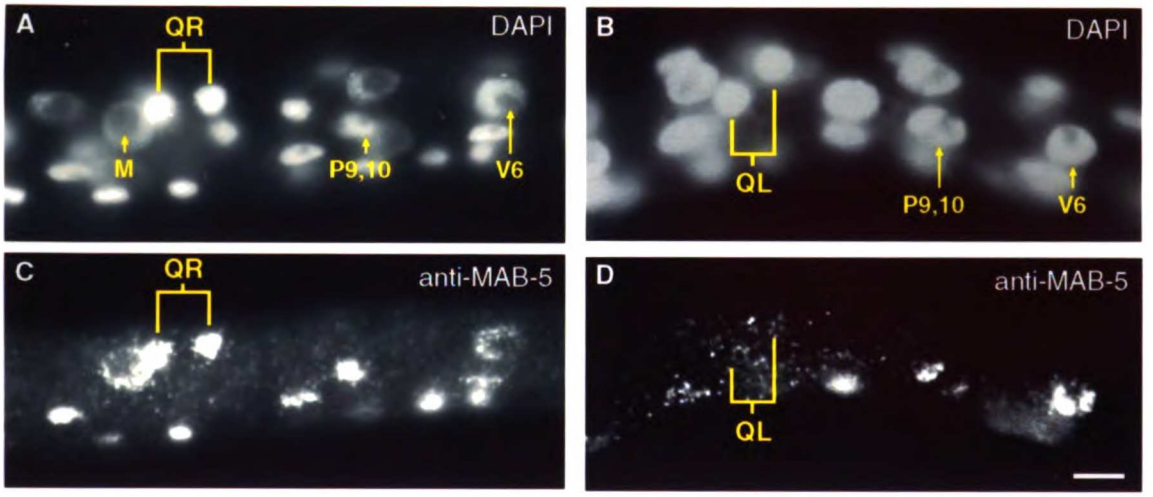

E.

genotype	QL mab-5 staining % none	% weak	% strong	n	% desc. post.	QL mab-5 staining % none	% weak	% strong	n	% desc. post.
w.t.	0.0	0.0	100.0	94	100.0	100	0.0	0.0	170	0.0
unc-40(e271)	20.7	41.4	37.9	29	43.8	89.3	10.7	0.0	28	0.0
dpy-19(mu78)	40.0	25.7	34.3	35	38.4	84.8	3.0	12.1	33	6.0
unc-73(e936)	6.7	6.7	86.7	90	95.8	98.8	1.3	0.0	80	0.0
unc-73(gm33)	22.9	10.4	66.7	48	n.d.	97.1	0.0	2.9	35	n.d.

Figure 2.7. MAB-5 protein expression in the Q descendants.

(A,C) QR.a and QR.p inappropriately expressing MAB-5 in a *dpy-19(mu78)* mutant. (B,D) QL.a and QL.p failing to express MAB-5 in a *dpy-19(mu78)* mutant. DAPI (A,B) stains all nuclei. M, P9/10, and V6 are shown for reference. Out of focus staining is in posterior body muscle and ventral cord motoneurons, cells that normally express MAB-5. Scale bar: 5 μm.

(E) Percentage of worms with anti-MAB-5 staining in the Q.a and Q.p descendants. Animals were fixed and stained at 3.5-5.5 hours after hatching. To control for worm permeabilization, we scored only animals in which V6 showed anti-MAB-5 staining. Strong = Q descendants staining as bright or brighter than V6 in the same animal. Weak = Q descendants staining, but not as bright as V6. % desc. post. = percentage of animals with QL.pax descendants posterior to V4.a.

Figure 2.8. Final position of the Q descendants.

Histograms show the distribution of the final positions of the QL.pax and QR.pax cells (see *'s in Figure 2.1B) relative to the daughters of the epidermal cells V1-V6. All graphs have the same x-axis scale as wild type. Allele names where not shown: *mab-5(e2088)*, *unc-40(e271);mab-5(e2088)*, *dpy-19(mu78);mab-5(e2088)*, *unc-40(e271)*; *dpy-19(mu78)*, *unc-73(e936);mab-5(e2088)*. The final position of the Q descendants in the stronger *unc-73* allele, *gm33*, is not shown because these animals were too sick and disorganized to score. n=50 worms for each genotype, except *mab-5 dpy-19* right side, n=100.

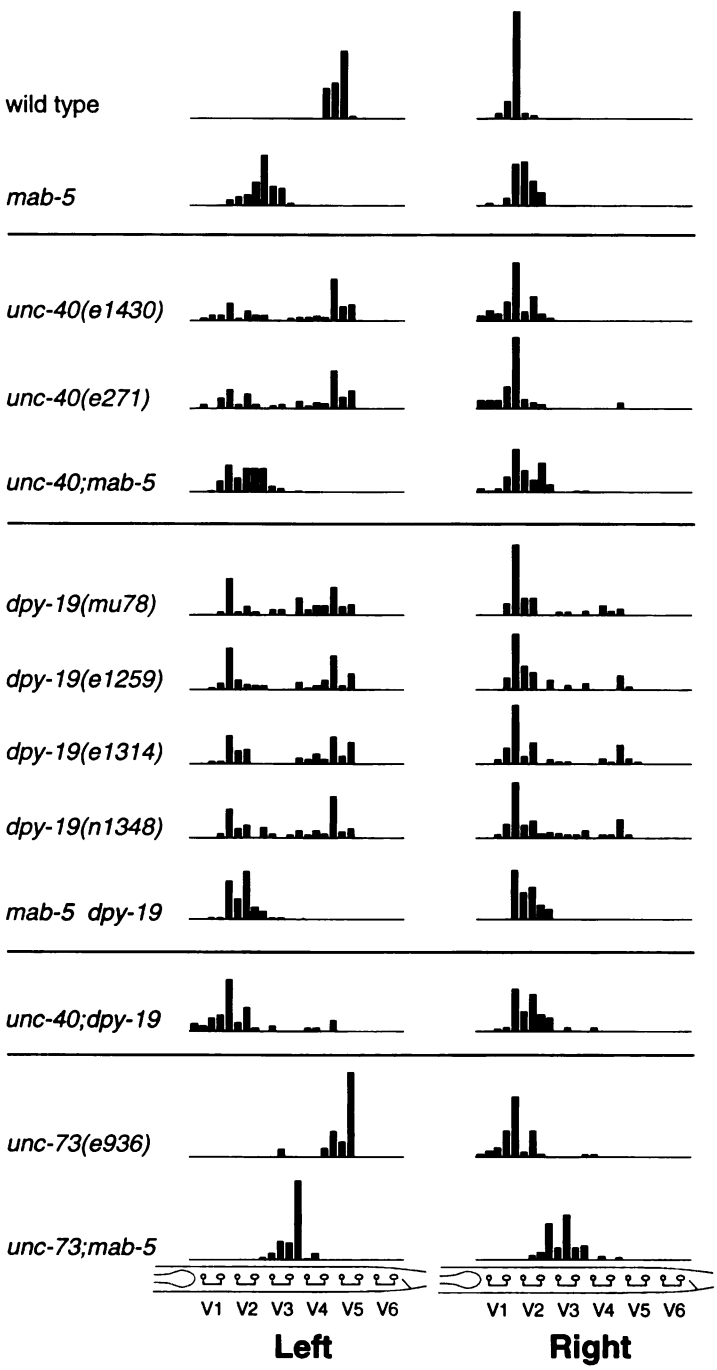
wild type
mab-5
unc-40(e1430)
unc-40(e271)
unc-40;mab-5
dpy-19(mu78)
dpy-19(e1259)
dpy-19(e1314)
dpy-19(n1348)
mab-5 dpy-19
unc-40;dpy-19
unc-73(e936)
unc-73;mab-5
V1 V2 V3 V4 V5 V6
V1 V2 V3 V4 V5 V6
Left
Right

Figure 2.8

Figure 2.9. Direction of Q cell polarization direction correlates with final position of Q descendants.

(A) Animals from the same staged population were scored at 2 hours to determine the percentage of QL cells that pointed toward the posterior and at 11 hours to determine the percentage of QL.pax descendants that remained in the posterior (indicating that the QL descendants expressed *mab-5*). To allow visualization of the shape of the QL cells, all strains in this graph also contained *mig-2::GFP*, except *unc-73(e936)*, which contained *unc-73::GFP*. QL.pax descendants were scored as "posterior" if they were posterior to V4.a. n= 50 worms for each genotype.

(B) Polarization over time toward the posterior correlates with the Q descendants remaining in the posterior. *dpy-19(mu78);mig-2::GFP* and *unc-40(e1430); mig-2::GFP* animals were examined every 20 minutes as in Figure 2.4. The cell shape at each time point was assigned an integer score from -2 to +2 corresponding to the degree of polarization toward the anterior (-) or posterior (+). The average of these polarization scores for each animal is plotted vs. the final position of the Q descendants in that animal. The unpredictability of the final positions for Q cells with intermediate levels of polarization over time may reflect the relatively coarse resolution of our assay for polarization.

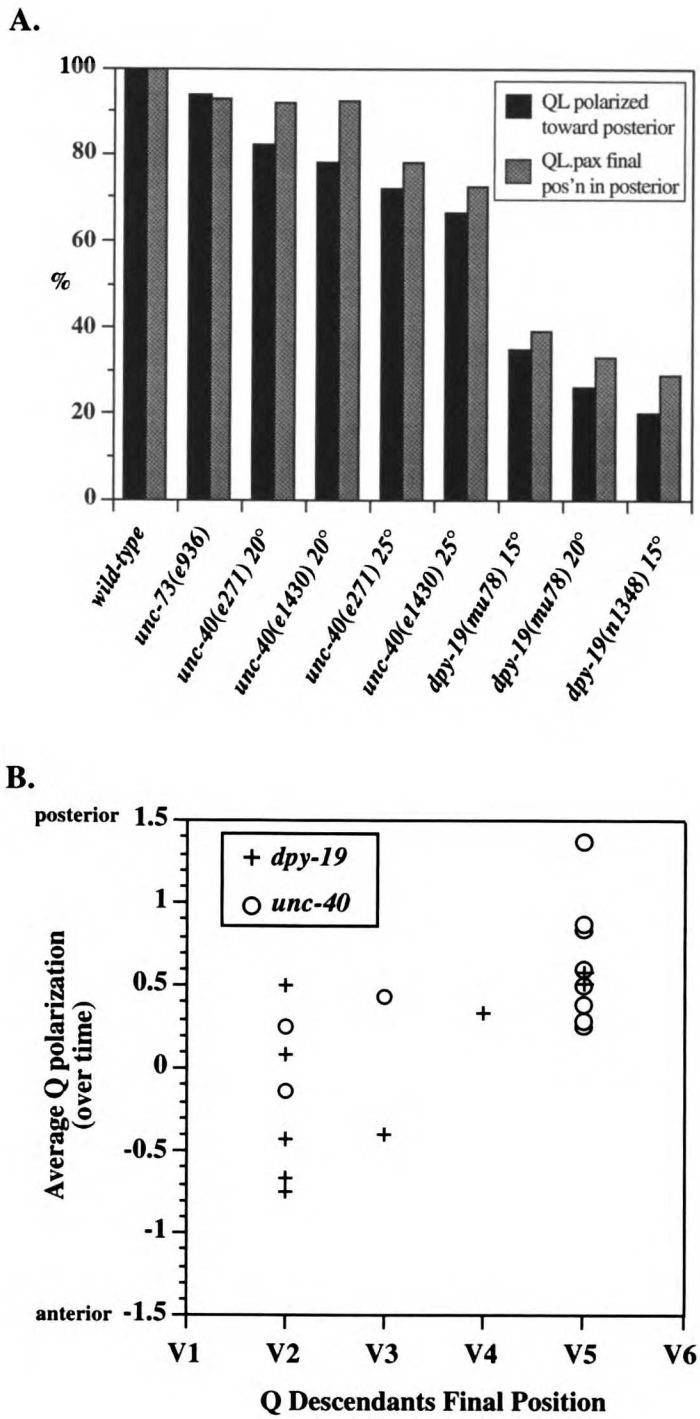
A.
100
80
60
%
40
20
0
QL polarized toward posterior
QL.pax final pos'n in posterior
wild-type
unc-73(e936)
unc-40(e271) 20°
unc-40(e1430) 20°
unc-40(e271) 25°
unc-40(e1430) 25°
dpy-19(mu78) 15°
dpy-19(mu78) 20°
dpy-19(n1348) 15°
B.
posterior
anterior
1.5
1
0.5
0
-0.5
-1
-1.5
+ dpy-19
O unc-40
Average Q polarization (over time)
V1
V2
V3
V4
V5
V6
Q Descendants Final Position

Figure 2.9

Figure 2.10. Expression of GFP constructs at the time of the Q cell migrations

(A,B) *unc-40::GFP* is expressed in QL and QR. Expression in the ventral nerve cord and in a commisural axon is also visible (arrows).

(C,D) *unc-73::GFP*.

(E) COOH-terminal GFP-tagged *dpy-19::GFP*. Arrows mark dorsal (hyp7) and ventral (P) epidermal nuclei. Arrowheads mark lateral (V) epidermal nuclei. Rings of GFP expression are coincident with cell nuclei outlines. This construct fully rescues the Dpy and Q phenotypes of *dpy-19(mu78)*. The final position of QL.pax cells was posterior to V4.a in 50/50 worms carrying the array.

(F) Transcriptional fusion of the *dpy-19* promoter region to a nuclear localized *GFP::lacZ* fusion. Bottom panel shows Nomarski image of the same worm. The lack of expression in V5 is presumably due to loss of the extrachromasomal array carrying *dpy-19::GFP*. (Other animals from the same strain showed robust expression in V5.) In animals with the array, 5/15 QL cells and 9/18 QR cells expressed GFP faintly during the time of the Q migrations.

Arrows mark dorsal (hyp7) and ventral (P) epidermal nuclei. Arrowheads mark V cell nuclei.

Scale bar: 10 μm for A-B, 7.5 μm for C,D,F, and 5 μm for E. C-F are confocal images.

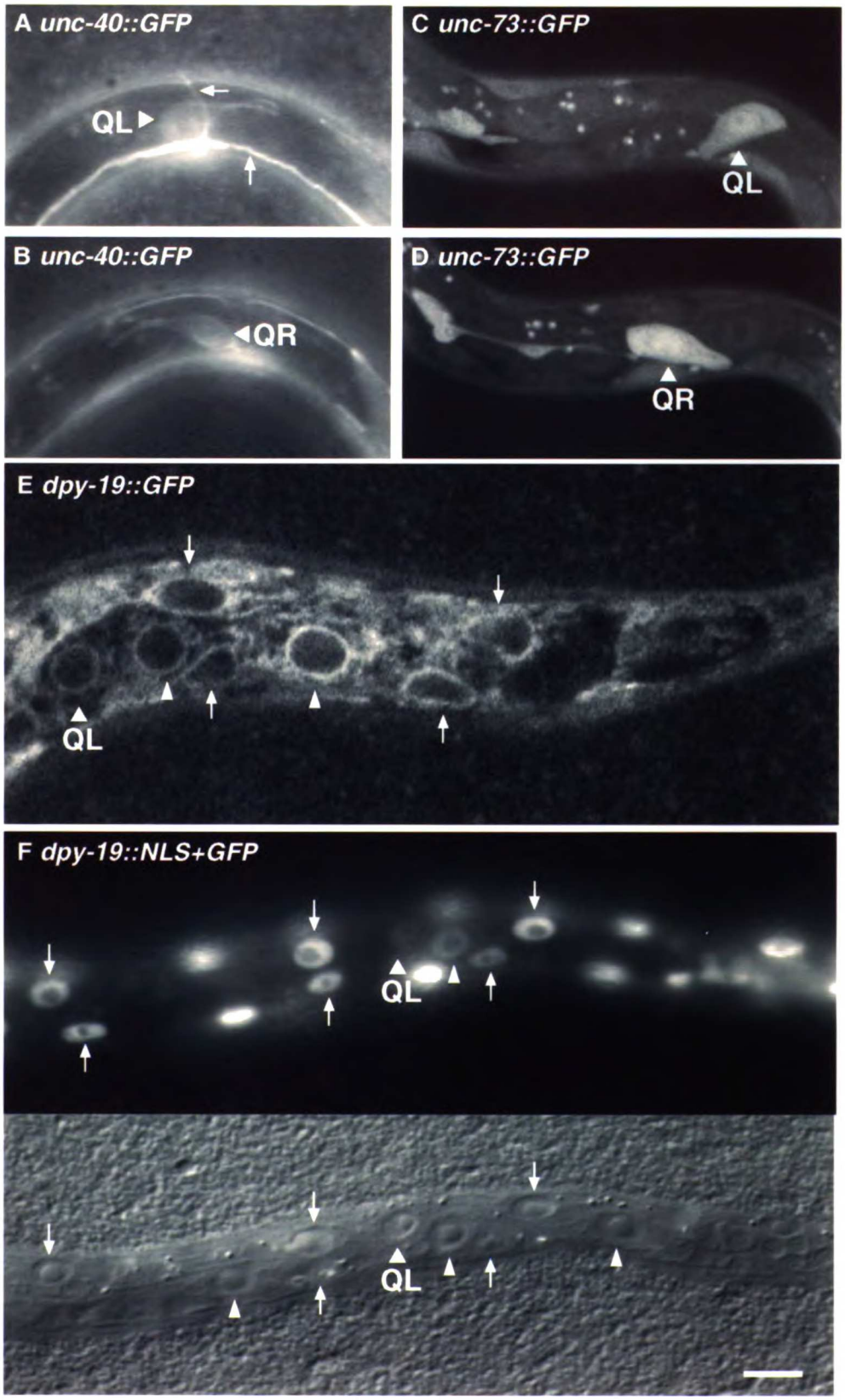
A unc-40::GFP
QL
C unc-73::GFP
QL
B unc-40::GFP
QR
D unc-73::GFP
QR
E dpy-19::GFP
QL
F dpy-19::NLS+GFP
QL
QL

Figure 2.10

Figure 2.11. Models for the polarization of the Q cells and the control of *mab-5* expression.

(A,B) Possible signals for orienting the left/right asymmetric polarization and migration of the Q cells.

(C) The patterned area is a hypothetical A/P localized signal to activate *mab-5*. The signal would have to be sharply defined since polarization, without migration, is sufficient to detect the signal.

(D) In order to explain the correlation between Q cell shape and mab-5 expression without invoking the positional model, these two aspects of the Q cell asymmetry would have to be controlled by an upstream regulator, X. Intermediate levels of X would cause the Q cells to adopt fates that were part QL-like and part QR-like.

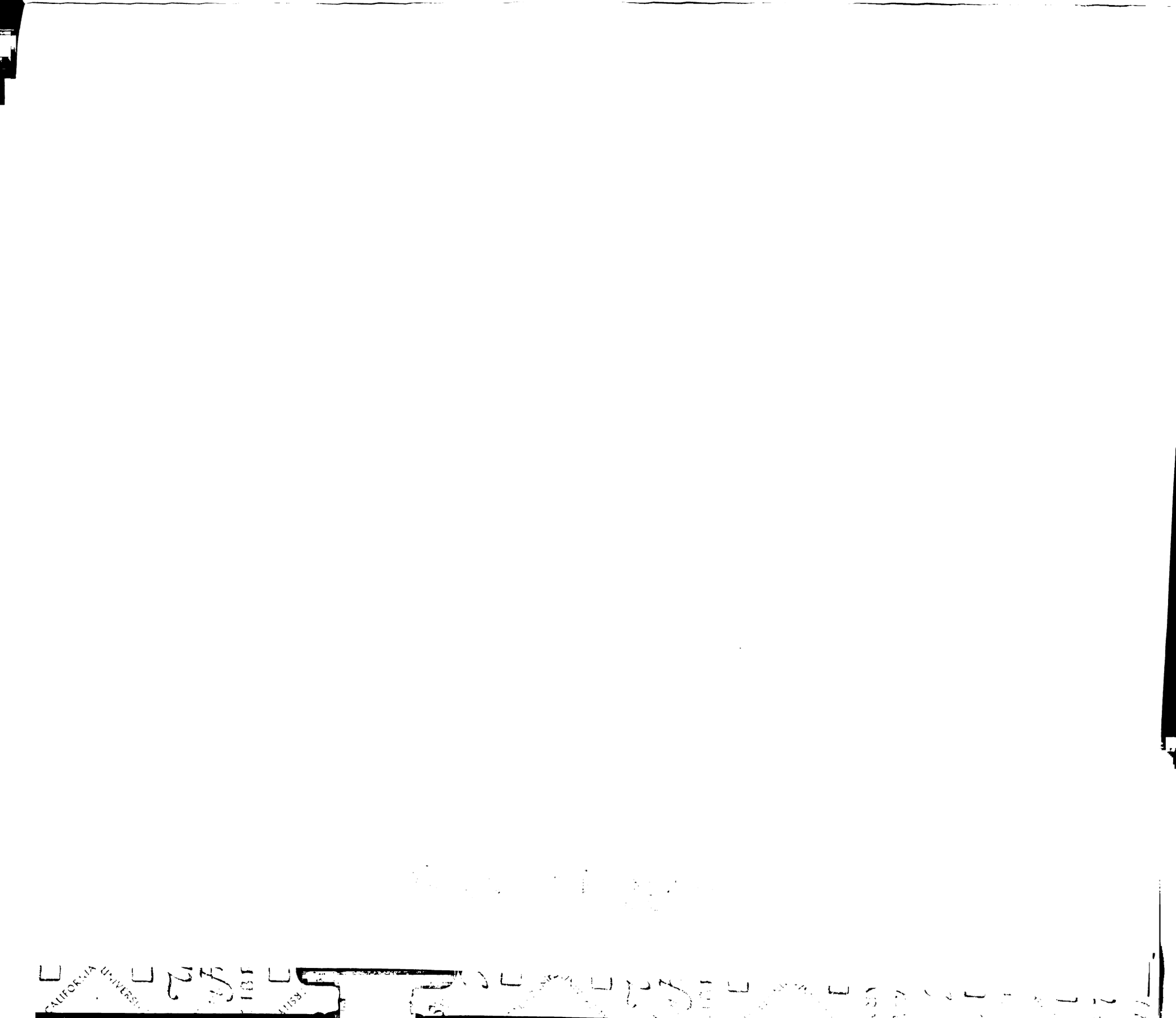

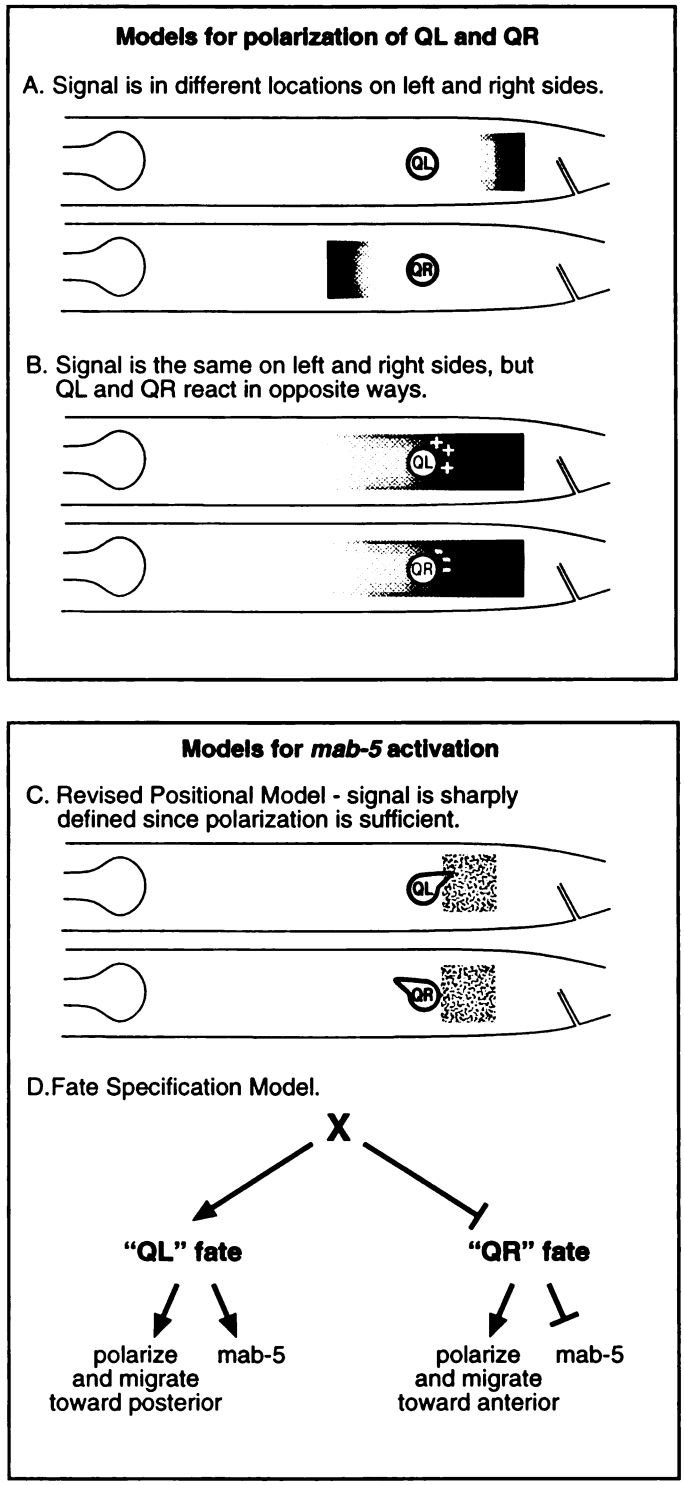
Models for polarization of QL and QR
A. Signal is in different locations on left and right sides.
QL
QR
B. Signal is the same on left and right sides, but QL and QR react in opposite ways.
QL
QR
Models for mab-5 activation
C. Revised Positional Model - signal is sharply defined since polarization is sufficient.
QL
QR
D.Fate Specification Model.
X
"QL" fate
"QR" fate
polarize and migrate toward posterior
mab-5
polarize and migrate toward anterior
mab-5

Figure 2.11

REFERENCES

Brenner, S. (1974). The genetics of C. elegans. *Genetics* **77**, 71-94.

Chalfie, M., N. J. Thomson and J. Sulston (1983). Induction of neuronal branching in *Caenorhabditis elegans*. *Science* **221**, 61-63.

Chan, S. S., H. Zheng, M. W. Su, R. Wilk, M. T. Killeen, et al. (1996). UNC-40, a C. elegans homolog of DCC (Deleted in Colorectal Cancer), is required in motile cells responding to UNC-6 netrin cues. *Cell* **87**, 187-95.

Claros, M. G. and G. von Heijne (1994). TopPred II: an improved software for membrane protein structure predictions. *Comput Appl Biosci* **10**, 685-6.

de la Torre, J., V. H. Hopker, G. L. Ming, M. M. Poo, M. Tessier Lavigne, et al. (1997). Turning of retinal growth cones in a netrin-1 gradient mediated by the netrin receptor DCC. *Neuron* **19**, 1211-24.

Desai, C., G. Garriga, S. L. McIntire and H. R. Horvitz (1988). A genetic pathway for the development of the Caenorhabditis elegans HSN motor neurons. *Nature* **336**, 638-46.

DeVore, D. L., H. R. Horvitz and M. J. Stern (1995). An FGF receptor signaling pathway is required for the normal cell migrations of the sex myoblasts in C. elegans hermaphrodites. *Cell* **83**, 611-20.

Fazeli, A., S. L. Dickinson, M. L. Hermiston, R. V. Tighe, R. G. Steen, et al. (1997). Phenotype of mice lacking functional Deleted in colorectal cancer (Dcc) gene. *Nature* **386**, 796-804.

Forrester, W. C. and G. Garriga (1997). Genes necessary for C. elegans cell and growth cone migrations. *Development* **124**, 1831-43.

Frohman, M. A. (1993). Rapid amplification of complementary DNA ends for generation of full-length complementary DNAs: thermal RACE. *Methods Enzymol* **218**, 340-56.

Guthrie, S. (1997). Axon guidance: netrin receptors are revealed. *Curr Biol* **7**, R6-9.

Harris, J., L. Honigberg, N. Robinson and C. Kenyon (1996). Neuronal cell migration in C. elegans: regulation of Hox gene expression and cell position. *Development* **122**, 3117-31.

Hedgecock, E. M., J. G. Culotti and D. H. Hall (1990). The unc-5, unc-6, and unc-40 genes guide circumferential migrations of pioneer axons and mesodermal cells on the epidermis in C. elegans. *Neuron* **4**, 61-85.

Hedgecock, E. M., J. G. Culotti, D. H. Hall and B. D. Stern (1987). Genetics of cell and axon migrations in *Caenorhabditis elegans*. *Development* **100**, 365-382.

Hutter, H. and R. Schnabel (1995). Establishment of left-right asymmetry in the Caenorhabditis elegans embryo: a multistep process involving a series of inductive events. *Development* **121**, 3417-24.

Ishii, N., W. G. Wadsworth, B. D. Stern, J. G. Culotti and E. M. Hedgecock (1992). UNC-6, a laminin-related protein, guides cell and pioneer axon migrations in C. elegans. *Neuron* **9**, 873-81.

Keino, M. K., M. Masu, L. Hinck, E. D. Leonardo, S. S. Chan, et al. (1996). Deleted in Colorectal Cancer (DCC) encodes a netrin receptor. *Cell* **87**, 175-85.

Kenyon, C. (1986). A gene involved in the development of the posterior body region of *C. elegans*. *Cell* **46**, 477-487.

Kolodziej, P. A., L. C. Timpe, K. J. Mitchell, S. R. Fried, C. S. Goodman, et al. (1996). frazzled encodes a Drosophila member of the DCC immunoglobulin subfamily and is required for CNS and motor axon guidance. *Cell* **87**, 197-204.

Leonardo, E. D., L. Hinck, M. Masu, M. K. Keino, S. L. Ackerman, et al. (1997). Vertebrate homologues of C. elegans UNC-5 are candidate netrin receptors. *Nature* **386**, 833-8.

Leung, H. C., A. M. Spence, B. D. Stern, Y. Zhou, M. W. Su, et al. (1992). UNC-5, a transmembrane protein with immunoglobulin and thrombospondin type 1 domains, guides cell and pioneer axon migrations in C. elegans. *Cell* **71**, 289-99.

Luo, L., Y. J. Liao, L. Y. Jan and Y. N. Jan (1994). Distinct morphogenetic functions of similar small GTPases: Drosophila Drac1 is involved in axonal outgrowth and myoblast fusion. *Genes Dev* **8**, 1787-802.

McIntire, S. L., G. Garriga, J. White, D. Jacobson and H. R. Horvitz (1992). Genes necessary for directed axonal elongation or fasciculation in C. elegans. *Neuron* **8**, 307-22.

Mello, C. C., J. M. Kramer, D. Stinchcomb and V. Ambros (1991). Efficient gene transfer in C.elegans: extrachromosomal maintenance and integration of transforming sequences. *Embo J* **10**, 3959-70.

Nobes, C. D. and A. Hall (1995). Rho, rac, and cdc42 GTPases regulate the assembly of multimolecular focal complexes associated with actin stress fibers, lamellipodia, and filopodia. *Cell* **81**, 53-62.

Salser, S. and C. Kenyon (1991). Activation of a *C. elegans Antennapedia* homolog within migrating cells controls their direction of migration. *Nature* **355**, 255-258.

Salser, S. J., C. M. Loer and C. Kenyon (1993). Multiple HOM-C gene interactions specify cell fates in the nematode central nervous system. *Genes Dev* **7**, 1714-24.

Sambrook, J., T. Maniatis and E. F. Fritsch (1989). Molecular cloning : a laboratory manual. (Cold Spring Harbor, N.Y.: Cold Spring Harbor Laboratory).

Sawa, H., L. Lobel and H. R. Horvitz (1996). The Caenorhabditis elegans gene lin-17, which is required for certain asymmetric cell divisions, encodes a putative seven-transmembrane protein similar to the Drosophila frizzled protein. *Genes Dev* **10**, 2189-97.

Segall, J. E. (1993). Polarization of yeast cells in spatial gradients of alpha mating factor. *Proc Natl Acad Sci U S A* **90**, 8332-6.

Steven, R., T. J. Kubiseski, H. Zheng, S. Kulkarni, J. Mancillas, et al. (1998). UNC-73 activates the Rac GTPase and is required for cell and growth cone migrations in C. elegans. *Cell* **92**, 785-95.

Sulston, J., Z. Du, K. Thomas, R. Wilson, L. Hillier, et al. (1992). The C. elegans genome sequencing project: a beginning. *Nature* **356**, 37-41.

Sulston, J. and J. Hodgkin (1988). Methods. *In* "The Nematode Caenorhabditis elegans" (W. B. Wood, Ed.), Vol. pp. 587-605. Cold Spring Harbor Laboratory, Cold Spring Harbor, N.Y.

Sulston, J. and H. Horvitz (1977). Post-embryonic cell lineages of the nematode, *C elegans*. *Developmental Biology* **56**, 110-156.

Tomic, M., I. Sunjevaric, E. S. Savtchenko and M. Blumenberg (1990). A rapid and simple method for introducing specific mutations into any position of DNA leaving all other positions unaltered. *Nucleic Acids Res* **18**, 1656.

Wadsworth, W. G., H. Bhatt and E. M. Hedgecock (1996). Neuroglia and pioneer neurons express UNC-6 to provide global and local netrin cues for guiding migrations in C. elegans. *Neuron* **16**, 35-46.

Way, J. C., J. Q. Run and A. Y. Wang (1992). Regulation of anterior cell-specific mec-3 expression during asymmetric cell division in C. elegans. *Dev Dyn* **194**, 289-302.

Way, J. C., L. Wang, J. Q. Run and M. S. Hung (1994). Cell polarity and the mechanism of asymmetric cell division. *Bioessays* **16**, 925-31.

Zigmond, S. H. (1977). Ability of polymorphonuclear leukocytes to orient in gradients of chemotactic factors. *J Cell Biol* **75**, 606-16.

Zipkin, I. D., R. M. Kindt and C. J. Kenyon (1997). Role of a new Rho family member in cell migration and axon guidance in C. elegans. *Cell* **90**, 883-894.

CHAPTER 3: Neuronal Cell Migration in *C. elegans*: Regulation of Hox Gene Expression and Cell Position

This work was done in collaboration with Jeanne Harris and Naomi Robinson. I performed the laser-induced single cell heat-shock experiments and wrote the sections of this paper that refer to those experiments. I also did all the experiments involving *mig-14*. Lastly, I scored the ALM, CAN, M, and muIntR migrations of mig-1 mutants. Naomi followed the migrations of QL in *mig-1* mutants, constructed and analyzed the *mig-1;mab-5(gf)* strain, and constructed the *egl-20;mig-13* and *mab-5;egl-20;mig-13* strains. Jeanne Harris did everything else, including the writing.

SUMMARY

In *C. elegans*, the Hox gene *mab-5*, which specifies the fates of cells in the posterior body region, has been shown to direct the migrations of certain cells within its domain of function. *mab-5* expression switches on in the neuroblast QL as it migrates into the posterior body region. *mab-5* activity is then required for the descendants of QL to migrate to posterior rather than anterior positions. What information activates Hox gene expression during this cell migration? How are these cells subsequently guided to their final positions? We address these questions by describing four genes, *egl-20*, *mig-14*, *mig-1* and *lin-17*, that are required to activate expression of *mab-5* during migration of the QL neuroblast. We find that two of these genes, *egl-20* and *mig-14*, also act in a *mab-5*-independent way to determine the final stopping points of the migrating Q descendants. The Q descendants do not migrate toward any obvious physical targets in wild-type or mutant animals. Therefore, these genes appear to be part of a system that positions the migrating Q descendants along the anteroposterior axis.

INTRODUCTION

Cell migrations play an important role in development. Concerted movements of large numbers of cells help to establish the different tissue layers during gastrulation and the migrations of individual cells contribute to tissue organization and body pattern. For example, cells of the vertebrate neural crest migrate from their birth place over the neural tube to different locations throughout the body, generating widely distributed neuronal and non-neuronal tissues. Invertebrates such as *Hydra*, *C. elegans*, and *Drosophila* all require cell migration to develop

normally (Hedgecock *et al.*, 1987; Teragawa and Bode, 1990; Montell, 1994). For cell movement to be a reproducible part of development, the migrations of these cells must be guided. Some cells migrate towards a visible target which supplies a guidance cue; for example, germ cells are attracted to and migrate towards the genital ridge in mammals (Godin *et al.*, 1990). However, many migrating cells stop at positions that are not associated with any obvious physical structures.

A number of genes required for cell migration have been identified in the nematode *C. elegans*. The migrations of the sex myoblasts in hermaphrodites are guided by an attractive signal from the developing gonad mediated by an FGF receptor (Devore *et al.*, 1995). Dorsoventral (D/V) migrations in *C. elegans* are guided by the netrin UNC-6 (Hedgecock *et al.*, 1990; Ishii *et al.*, 1992) in a highly conserved process that has also been shown to guide D/V migrations of axons in the developing vertebrate nervous system (Kennedy *et al.*, 1994; Serafini *et al.*, 1994). The guidance of migrations along the anteroposterior (A/P) axis in *C. elegans* has been shown to involve the gene *vab-8*, which is required for the posterior migration of many cells and axons (Wightman *et al.*, 1996). However, in general, the guidance of cells along the A/P axis is less well-understood.

We have chosen to focus on the migrations of the neuroblasts QL and QR, which migrate along the A/P body axis in *C. elegans*. The Q cells are similar to neural crest cells in that they delaminate from an epidermal epithelium and go on to populate regions of the body with sensory neurons (Sulston and Horvitz, 1977; Chalfie and Sulston, 1981). The Q cells and their descendants migrate to highly reproducible positions in a relatively uniform region of the body. QL and QR are born in the same

A/P position on opposite sides of the animal: QL on the left and QR on the right. Although they undergo an identical sequence of cell divisions, the two Q cells and their descendants migrate in opposite directions: QL and its descendants migrate towards the posterior, whereas QR and its descendants migrate towards the anterior (Sulston and Horvitz, 1977) (Fig. 3.1).

The *C. elegans* Hox genes *lin-39* and *mab-5* play important roles in regulating the migrations of cells in the Q lineages. *lin-39*, the *C. elegans Sex combs reduced* homolog that specifies cell fates in the mid-body region, is required for the anterior migration of the QR descendants (Clark *et al.*, 1993; Wang *et al.*, 1993). *mab-5*, the *C. elegans Antennapedia* homolog that specifies cell fates in the posterior body region, is required for the posterior migration of the QL descendants (Chalfie and Sulston, 1981; Kenyon, 1986). Salser and Kenyon (1992) have shown that *mab-5* acts as a switch to determine the direction of migration. If *mab-5* is ON, the Q descendants migrate towards the posterior; if *mab-5* is OFF, the Q descendants migrate towards the anterior (Salser and Kenyon, 1992; Fig. 3.1). Here, we extend these results by using a laser microbeam to activate a *heat-shock-mab-5* fusion gene (Salser and Kenyon, 1992) exclusively within a migrating cell. Our findings, together with previous genetic mosaic analysis (Kenyon, 1986) argue that *mab-5* acts within migrating Q descendants to determine their direction of migration.

The state of *mab-5* expression within QL or QR determines whether their descendants will migrate to anterior or posterior positions. However, additional information is required to specify the final positions of these cells, since each QL descendant migrates to a characteristic position in the posterior and each QR descendant migrates to a characteristic position in

the anterior. There are no obvious cellular targets located at these stopping points.

To understand better how these cells find their characteristic positions along the A/P axis, we have identified and characterized mutants in which cells in the Q lineage migrate to incorrect positions. Here we show that four of these genes, *egl-20*, *mig-14*, *mig-1* and *lin-17*, are required to activate the Hox gene *mab-5* in the migrating QL cell. When these gene activities are reduced or eliminated, QL and its descendants do not express *mab-5* and consequently QL's descendants migrate towards the anterior. Two of the genes, *egl-20* and *mig-14*, also act in a *mab-5*-independent way to determine the final stopping points of the migrating Q descendants along the A/P axis. Whether or not cells in the Q lineage are provided with *mab-5* activity, in the absence of *egl-20* or *mig-14* gene activities, they migrate to positions shifted posterior to the positions that they would otherwise seek: cells that would migrate posteriorly go too far and cells that would migrate anteriorly stop short. In addition, cells that would remain stationary migrate posteriorly, and cells that would only migrate a short distance anteriorly instead reverse direction and migrate posteriorly. Thus, in addition to activating *mab-5* expression in the migrating QL cell, *egl-20* and *mig-14* appear to participate in a guidance system that determines the final stopping points of cells in the Q lineage.

The gene *lin-17*, which we show activates expression of the Hox gene *mab-5* in the neurobast QL, is homolgous to the *Drosophila* tissue polarity gene *frizzled* (Sawa et al., 1996) and is required for the generation and orientation of cellular asymmetry in many tissues (Sternberg and Horvitz, 1988). Similarly, *egl-20* and *mig-14* also regulate the orientation of certain asymmetric cell divisions (J. H., Jennifer Whangbo and C. K.,

manuscript in preparation). Thus *egl-20, mig-14, mig-1* and *lin-17* are part of a regulatory system that may be similar to the signaling systems that regulate tissue and segment polarity in *Drosophila*.

RESULTS

Wild-type Q lineage migrations

The QR and QL neuroblasts are born at the same time, in the same A/P position on opposite sides of the animal (Sulston and Horvitz, 1977). These cells each undergo an identical sequence of divisions (Fig. 3.1) to produce one mechanosensory neuron (AVM/PVM), one putative interneuron (SDQR/SDQL), a ciliated neuron (AQR/PQR) and two cells that undergo programmed cell death (Sulston and Horvitz, 1977; Chalfie and Sulston, 1981; White *et al.*, 1986). Approximately one hour after the worm hatches, QL and QR begin their migrations: QL towards the tail and QR towards the head. After these initial migrations, QL and its descendants activate expression of the Hox gene *mab-5*. The *mab-5*-expressing cells then remain in the posterior: QL's posterior daughter, QL.p, and its descendants stop migrating, while QL's anterior daughter, QL.a, and its descendant continue migrating towards the posterior. In contrast, QR and its descendants do not express *mab-5* (Salser and Kenyon, 1992) and migrate towards the anterior (Fig. 3.1).

In mutants lacking *mab-5* activity, the initial migrations of QL towards the tail and QR towards the head are unaffected, but the descendants of both QL and QR migrate towards the head, just as the descendants of QR do in wild type (Fig. 3.1) (Kenyon, 1986; Salser and Kenyon, 1992). In animals that express *mab-5* ectopically, such as *mab-5(gf)* mutants (Hedgecock *et al.*, 1987; Salser and Kenyon, 1992) or animals

carrying *heat-shock-mab-5* (Salser and Kenyon, 1992), the initial migration of QR is still towards the head, but now QR.p and its descendants stop and QR.a and its descendants migrate towards the tail, just as QL.p, QL.a and their descendants do in wild type (Fig. 3.1). In this paper, we will refer to the daughters of QL and QR and all of their subsequent descendants collectively as QL.(d) and QR.(d) cells.

Previous mosaic analysis has shown that *mab-5* activity is required within the AB.p branch of the *C. elegans* lineage for QL's descendants to migrate posteriorly (Kenyon, 1986). Since QL is derived from AB.p, this finding is consistent with the cell autonomous action of *mab-5*. This interpretation is strengthened by the observation that *mab-5* expression is activated in QL, but not QR (Salser and Kenyon, 1992). However, the possibility remained that *mab-5* activity in some other AB.p descendant, such as V3, V5, or the P cells, might influence the QL.(d) migrations. Therefore, to ask whether *mab-5* activity within a migrating Q.(d) cell is sufficient to direct its posterior migration, we used an attenuated laser microbeam to activate *hs-mab-5* within a single cell (see Materials and Methods). We found that focusing the laser beam on the anteriorly migrating QR.a cell, but not surrounding cells, caused QR.a to reverse direction and migrate towards the posterior (Fig. 3.2).

Despite the fact that in wild-type animals all three QL-derived neurons express *mab-5*, each cell comes to occupy a characteristic position along the body axis (Fig. 3.1). Similarly, all three QR-derived neurons fail to express *mab-5*, yet each of them migrates to a different characteristic position (Fig. 3.1). Thus, although *mab-5* expression plays an important role in determining whether these cells ultimately reside in the posterior

or the anterior of the body, it does not appear to be sufficient to specify their precise locations.

Genes affecting Q descendant migration: Overview

In this paper we describe four genes that affect the migrations of the Q.(d) cells along the A/P body axis. A number of mutants had been identified previously in which the descendants of QL were located in anterior body regions (*mig-1*: Hedgecock *et al.*, 1987; *lin-17*: Way *et al.*, 1992; *egl-20*: G. Garriga, personal communication), and we identified additional mutants with this phenotype (Fig. 3.3A; see Materials and Methods). Mutations in three of these genes were previously identified on the basis of other mutant phenotypes: *egl-20* mutants are **Egg**-laying detective, *mig-1* mutants have other **Mig**ration derects, and *lin-17* mutants are **Lin**eage abnormal. Mutations in *egl-20*, *mig-1*, *mig-14*, and *lin-17* can cause the QL.(d) cells, which normally migrate posteriorly, to reverse direction and migrate anteriorly instead. In addition to their effect on the direction of migration, mutations in two of these genes, *egl-20* and *mig-14*, affect a second aspect of cell positioning of both the QL.(d) and QR.(d) cell migrations: namely, that subsequent anterior migrations are shortened and posterior migrations are lengthened. We will discuss these two different mutant phenotypes in turn, beginning with the change in direction of migration.

Mutations in *egl-20*, *mig-1*, *mig-14*, and *lin-17* reverse the direction of migration of QL's descendants

The QL.(d) cells in *egl-20*, *mig-1*, *mig-14*, and *lin-17* mutants migrate towards the anterior just as they do in *mab-5* mutants (Fig. 3.3A). Are

these reversals due to a failure of the *mab-5* switch? *mab-5* mutations do not affect the initial posterior migration of QL, only that of the descendants. Thus, if *mab-5* activity in QL were blocked, one would expect QL to migrate posteriorly, but its descendants to migrate anteriorly, as they do in *mab-5* mutants (Fig. 3.1). To ask whether QL migrated posteriorly in these mutants, we observed its migration in living animals using Nomarski microscopy. We found that in these mutants, QL initially migrated towards the posterior, the same trajectory observed in wild type, but its descendants migrated towards the anterior, as in *mab-5(-)* mutants (Fig. 3.3B). Thus, these four genes, *egl-20*, *mig-1*, *mig-14*, and *lin-17*, were likely to function in the *mab-5* pathway.

Mutations in *egl-20*, *mig-14*, *mig-1* and *lin-17* prevent MAB-5 expression in QL

In principle, the QL.(d) cells could migrate anteriorly in these mutants either because they fail to express *mab-5*, or because they fail to respond correctly to *mab-5*. To distinguish between these two possibilities, we first used polyclonal antisera against *mab-5* protein (MAB-5) (Salser *et al.*, 1993) to determine whether QL and its daughters, QL.a and QL.p, produced MAB-5. We found that although QL.a and QL.p always expressed *mab-5* strongly in wild-type worms, they produced no detectable MAB-5 in *egl-20(n585)* and *mig-14(mu71)* mutants (Fig. 3.4 and Table 3.2).

The effect on *mab-5* expression at this stage seemed to be fairly specific for QL.a and QL.p: surrounding cells (V6, P9/10, P11/12, M and the seven most posterior juvenile motoneurons) appeared to produce MAB-5 as in wild type (data not shown). We also found that in general, *mab-5*-dependent cell fates in four other tissues (the hermaphrodite M-derived

coelomocytes, male spicules, rays 1-6 and hooks) (Kenyon, 1986) were normal in *egl-20*, *mig-14* and *mig-1* mutants (exceptions are described in Materials and Methods). These tissues were defective in *lin-17* mutants, but had a phenotype that differed from that of *mab-5* mutants (see Materials and Methods). Therefore these genes are not required globally for *mab-5* expression.

When we examined MAB-5 expression in *mig-1(e1787)* and *lin-17(n671)* mutants, we found that the QL daughters showed decreased MAB-5 staining in 83% of *mig-1* mutants and 48% of the *lin-17* mutants (Fig. 3.4 and Table 3.2). As in *egl-20* and *mig-14* mutants, staining appeared normal in surrounding cells. Since these *mig-1* and *lin-17* mutants have an incompletely penetrant migration defect, the QL.(d) cells that remain in the posterior in *mig-1* mutants could do so as a result of *mab-5* activity. To test this, we removed *mab-5* activity using a *mab-5* null mutation, *e1239* (Salser and Kenyon, 1996). We found that the QL.pa daughters were located in full anterior positions (anterior to V3.a) in 98% (n=67) of the *mig-1(e1787); mab-5(e1239)* double mutants. The same was true for *lin-17(n671); mab-5(e1239)* double mutants constructed and analyzed previously by Way et al. (1992). These observations indicate that the QL descendants that remain in the posterior, or in intermediate positions, in *mig-1* and *lin-17* mutants do so largely as a result of *mab-5* activity.

If the QL.(d) cells in *mig-1* and *lin-17* mutants migrate incorrectly because they fail to express MAB-5, then they would be expected to migrate correctly if provided with MAB-5. To test this, we used a *mab-5* gain-of-function mutation, *e1751gf*, a regulatory mutation that causes ectopic production of MAB-5 (Salser and Kenyon, 1992; Salser *et al.*, 1993). In *e1751gf* mutants, both QL and QR produce MAB-5, and both the QL and

QR descendants migrate to posterior positions (Hedgecock *et al.*, 1987; Salser and Kenyon, 1992) (Fig. 3.5). We found that in double mutant combinations between *mab-5(e1751gf)* and *egl-20*, *mig-1* or *mig-14* mutations, the QL.pa descendants remained in the posterior (Fig. 3.5). This shows that the QL.(d) cells in *egl-20*, *mig-1*, and *mig-14* mutants can respond correctly to MAB-5. This finding, together with the MAB-5 expression data, indicates that the QL.(d) cells migrate towards the anterior in *egl-20*, *mig-1*, and *mig-14* mutants because they fail to express MAB-5.

We were unable to maintain *lin-17(n671)*; *mab-5(e1751gf)* double mutants because the animals were very sick. However, the frequency of QL daughters in *lin-17* mutants that have little or no MAB-5 staining correlates well with the percentage of QL descendants that migrate into the anterior, as it does for *mig-1* mutants (Table 3.2), and the QL.(d) cells that remain in the posterior require *mab-5* activity to do so (Way *et al.*, 1992). Together, these observations suggest that a lack of *mab-5* expression in the QL.(d) cells causes them to migrate into the anterior.

In *egl-20* and *mig-14* mutants the anterior migrations of the QR descendants are shortened

In addition to their failure to express *mab-5* in QL, *egl-20* and *mig-14* mutants also exhibit a second migration phenotype. In the wild type, the three QR-derived neurons each stop at unique and characteristic positions in the anterior, just as the three QL-derived neurons do in the posterior. Interestingly, we found that in *egl-20* and *mig-14* mutants, but not *mig-1* and *lin-17* mutants (data not shown), the final positions of most of the QR.pa daughters were consistently shifted posteriorly relative to wild type (Fig. 3.6, column 1). When we observed the QR.(d) migrations in living

animals using Nomarski microscopy, we found that, in general, these cells stop migrating prematurely (Fig. 3.7A). We also noticed a similar alteration in the QL.(d) migrations: for example, in *egl-20* or *mab-5; egl-20* double mutants the final positions of these cells were generally shifted significantly posteriorly relative to the positions in the anterior that they would come to occupy in *mab-5(lf)* mutants (Fig. 3.3 and data not shown). Since the anterior-directed QL.(d) migrations of *egl-20* and *mig-14* mutants are shorter than those of *mab-5(lf)* mutants, the *egl-20* and *mig-14* mutant phenotypes cannot be completely explained by a loss of *mab-5* expression in the QL lineage. Because *egl-20* and *mig-14* influence *mab-5* expression as well as this additional aspect of cell position in the QL lineage, in the following sections we will describe the shortening of the anterior migrations on the right side only, where cells in the QR lineage do not express *mab-5*.

The shortening of the anterior migrations of the QR descendants in *egl-20* and *mig-14* mutants is not due to a defect in motility

What causes the QR descendants to stop short in *egl-20* and *mig-14* mutants? These cells may be specifically defective in anterior migration, or they may simply be unable to migrate well in any direction. Alternatively, these mutations may direct cells to migrate to positions shifted posterior to normal. To distinguish between these possibilities, we asked what effect *egl-20* or *mig-14* mutations would have on a mutant in which QR.p did not migrate at all. In worms carrying the *mab-5* gain-of function mutation, *e1751gf*, QR.p and its descendants do not migrate and QR.a and its daughter migrate towards the posterior (Fig. 3.7). We found that when an *egl-20* or *mig-14* mutation was introduced into this strain, the QR.p cell

now migrated towards the tail (Fig. 3.7), thus shifting the positions of the QR.pa daughters towards the posterior (Fig. 3.6, column 3). This meant that a loss of *egl-20* or *mig-14* activity could cause a normally stationary cell to migrate posteriorly. We also observed that in *mab-5(gf); egl-20* double mutants, QR.a and its daughter, QR.ap, now migrated further posteriorly than in the *mab-5(gf)* single mutant (Fig. 3.7A, black triangles). These new findings are not consistent with the hypothesis that *egl-20* mutants are defective in cell motility. Instead, they imply that *egl-20* and *mig-14* mutations cause cells to migrate to positions located posterior to their normal stopping points.

In another mutant, *mig-13(mu31)*, QR.p and its descendants only migrate a short distance to the anterior (Robinson, 1995) (Fig. 3.7B). The *mu31* mutation is recessive and the severity of the phenotype does not increase *in trans* to a deficiency (Robinson, 1995). Thus, the wild-type function of *mig-13* is probably to allow QR.(d) cells to migrate anteriorly. Since mutations in *egl-20* and *mig-14* shift the positions of the QR.pa daughters toward the posterior in wild-type, *mab-5(lf)* and *mab-5(gf)* mutants, we wondered whether they would shift the QR.pa daughters toward the posterior in a *mig-13* mutant as well: specifically, might they cause the QR.p cell to actually reverse direction and migrate posteriorly? We found that the positions of the QR.pa daughters in *mig-13* mutants carrying *egl-20* or *mig-14* mutations were consistently shifted posterior relative to the *mig-13* single mutants (Fig. 3.6, column 4), and some, most strikingly in the *egl-20; mig-13* double mutant, were actually posterior to the birthplace of QR (denoted by asterisks at the bottom of Fig. 3.6). We followed the migrations of QR and its daughters in both *egl-20; mig-13* and *mig-14; mig-13* double mutants and found that QR.p always migrated in

the reverse direction, towards the posterior, whereas in *mig-13* single mutants, QR.p either stopped or migrated towards the anterior (Fig. 3.7B). These observations indicate that loss of *egl-20* or *mig-14* activity can cause a QR.(d) cell to change its direction of migration from anterior to posterior.

In the wild type, posterior migration of Q.(d) cells requires *mab-5* activity. Is *mab-5* required for the posterior migration caused by *egl-20* mutations? To ask whether the posterior migration of these cells required *mab-5* activity, we constructed and analyzed *mab-5(e2088); egl-20(n585); mig-13(mu31)* triple mutants. We found that in these mutants QR.p migrated towards the posterior in 3 out of 4 animals (Fig. 3.7B). This observation indicates that *mab-5* is not absolutely required for posterior migration.

The known Hox gene functions are not responsible for the shortened migrations of the QR descendants in *egl-20* and *mig-14* mutants

Both *egl-20* and *mig-14* mutations affect the expression of the Hox gene *mab-5*. Could the posterior shift in the positions of the QR.pa daughters in *egl-20* and *mig-14* mutants be explained by altered activities of the Hox genes? Of the four *C. elegans* Hox genes, three, *lin-39*, *mab-5* and *egl-5*, are known to be required for wild-type Q.(d) migrations (Kenyon, 1986; Costa *et al.*, 1988; Chisholm, 1991; Clark *et al.*, 1993; Wang *et al.*, 1993). There are no mutations in the fourth gene, *ceh-13*, and its function is unknown (Shaller *et al.*, 1990; Wang *et al.*, 1993).

The Hox gene *lin-39* is required for patterning the central body region and for the anterior migrations of QR and its descendants (Clark *et al.*, 1993; Wang *et al.*, 1993). In *lin-39* mutants, the anterior migrations of QR and its descendants are shortened. To determine whether reduced *lin-*

39 activity in *egl-20* and *mig-14* mutants is responsible for shortening anterior QR.(d) migrations, we first examined the expression of a *lin-39-lacZ* fusion gene (Wang *et al.*, 1993) in *egl-20* and *mig-14* mutants. *lin-39-lacZ* is normally expressed in both QL and QR (Wang *et al.*, 1993) and we found that its expression in both cells was unaffected by *egl-20* or *mig-14* mutations (data not shown). Second, we examined the QR.(d) migrations in a double mutant containing *egl-20(n585)* and a *lin-39* null allele, *mu26,*, (Wang *et al.*, 1993; J. Maloof and C. Kenyon, unpublished data). If the shortened anterior migrations of the QR.(d) cells in *egl-20* mutants were due to a loss of *lin-39* activity, then the migrations in the *lin-39; egl-20* double mutant should be the same as those in the *lin-39* single mutant. We found that the positions of the QR.pa daughters in the double mutant were further posterior than in the *lin-39(mu26)* single mutant (data not shown). Since the presence of an *egl-20* mutation shortened the anterior-directed migrations of the QR.(d) cells in a *lin-39* null mutant, the failure of these cells to migrate to their normal positions in *egl-20* mutants cannot be explained simply by a loss of *lin-39* activity.

Another possibility is that the QR.(d) cells did not migrate as far anteriorly as normal because they misexpressed the Hox genes *mab-5* or *egl-5*. These two genes are required for the posterior migrations of the QL.(d) cells: *mab-5* activity is required in all animals (Kenyon, 1986; Salser and Kenyon, 1992) whereas *egl-5* activity is required in approximately 9% of wild-type animals (Chisholm, 1991). To test whether ectopic *mab-5* or *egl-5* activity could be responsible for the shortened anterior migrations and lengthened posterior migrations of the QR descendants in *egl-20* and *mig-14* mutants, we made double mutants between *mab-5(e2088)* or *egl-5(n945)* and *egl-20(n585)* or *mig-14(mu71)*. We found that neither Hox

mutation rescued the shortened QR.(d) migrations of *egl-20* and *mig-14* mutants (Fig. 3.6 and data not shown). These observations demonstrate that the posteriorly shifted positions of the QR.pa daughters in *egl-20* and *mig-14* mutants are not due to ectopic *mab-5* or *egl-5* activity.

The phenotypes of mutations in *egl-20* and *mig-14* are additive

We examined the positions of the QR.pa descendants in *mig-14(mu71); egl-20(n585)* double mutants, and found that they were shifted even further posterior than either single mutant (Fig. 3.6B). Further genetic and molecular analysis of these alleles should help us to determine whether these genes function in the same or in parallel pathways to determine the stopping points of the migrating QR.(d) cells.

Effect of *egl-20, mig-14, mig-1* and *lin-17* mutations on other cell migrations

To ask whether these mutations affected other cell migrations, we examined the positions of the migratory cells HSN, ALM, CAN, muIntR, ccLa/p, ccRa/p, and M (Fig. 3.8). Mutations in *egl-20, mig-14, mig-1* and *lin-17* affected a few migrating cells but did not produce a consistent posterior shift. Since we have not examined the position of every cell in these mutants, the possibility remains that *egl-20, mig-14, mig-1* and *lin-17* may also play a broader role in cell migration than we have so far determined.

DISCUSSION

Our experiments address two important questions: First, what initiates expression of a Hox gene in a migrating cell, and second, what directs migrating cells to their final positions? We have identified four

genes required to activate *mab-5* in QL (Fig. 3.9A). Two of these genes, *egl-20* and *mig-14*, are also required independently of *mab-5* activity to position the migrating Q descendants correctly along the A/P axis (Fig. 3.9A).

Activation of the Hox gene *mab-5* within the migrating QL neuroblast

egl-20, *mig-14*, *mig-1* and *lin-17* act in the same pathway as the Hox gene *mab-5* to direct descendants of QL to migrate towards the posterior. All four of these genes act upstream of *mab-5*, and mutations in these genes appear to affect *mab-5* expression primarily in QL. None of these mutations appear to affect *mab-5* expression or activity globally; thus they are not likely to be general activators of *mab-5* unless their functions in other cells are redundant with other factors. These genes could act either at the level of transcription or of protein stability; however, the latter possibility seems less likely since mutations in these genes also block appearance of B-galactosidase in QL.a and QL.p in worms carrying *mab-5-lacZ* fusions encoding only the first seventeen amino acids of the MAB-5 protein (Salser and Kenyon, 1992; data not shown).

How might *egl-20*, *mig-14*, *mig-1* and *lin-17* function to activate *mab-5*? One possibility is that these genes are part of a system that creates left/right (L/R) asymmetries since, in wild type, QL but not QR expresses *mab-5*. Alternatively, these genes could be part of a system that is involved with the establishment of, or the response to, A/P positional information. In this model, the asymmetric initial migration would place QL and QR in different A/P positions, creating an A/P difference in addition to a L/R asymmetry. Signals present in QL's new posterior location would then instruct it to activate *mab-5*, allowing the A/P patterning system to

distinguish the fate of QL from that of QR. Finally, it is possible that these genes act to specify aspects of Q cell fate in a manner independent of either A/P or L/R position.

One of these genes, *lin-17*, a homolog of the *Drosophila* tissue polarity gene *frizzled* (Sawa et al., 1996), is required for many asymmetric cell divisions. For example, in *lin-17* mutants, many cells that normally divide to generate two different cell types (A and B) instead generate two similar cells (A and A) (Sternberg and Horvitz, 1988; Way *et al.*, 1992). Although QL's ability to express *mab-5* is altered in *lin-17* mutants, it does not adopt the fate of its sister, the epidermal cell, V5. It is not clear how, or if, *lin-17*'s role in the generation and orientation of cellular asymmetry is related to its role in activating *mab-5* expression in QL. Molecular analysis of *lin-17*, as well as *egl-20*, *mig-14* and *mig-1*, should help to understand how *mab-5* gene expression is activated during the migration of QL.

The *egl-20* and *mig-14* genes influence the stopping points of the migrating Q descendants along the A/P axis

Two of the genes required for *mab-5* activation in QL, *egl-20* and *mig-14*, are also required in a *mab-5*-independent process to position cells correctly along the body axis. Mutations in these two genes cause the Q descendants to stop at positions that are further posterior than wild-type (Fig. 3.6). This shift is not due to misregulation of the Hox genes *mab-5*, *lin-39* or *egl-5*. Nor is the posterior shift due to a defect in motility, since mutations in *egl-20* and *mig-14* lengthen the posterior-directed migration of QR.ap in *mab-5(gf)* mutants, cause the non-migratory QR.p cell to migrate posteriorly in *mab-5(gf)* mutants, and reverse the direction of the anteriorly migrating QR.p cell in *mig-13* mutants (Fig. 3.7). The *egl-20* and

mig-14 mutations we have analyzed all appear to reduce or eliminate gene function. Thus, it appears that the wild-type function of *egl-20* and *mig-14* is to allow the QR.(d) cells to migrate to more anterior positions.

Thus, in addition to directing both the QL and the QR descendants to more anterior positions, *egl-20(+)* and *mig-14(+)* also activate expression of *mab-5* in QL, which, in turn, promotes posterior migration. Since *mab-5* is not active in QR and its descendants, only the additional anterior increment is visible in the QR.(d) cell migrations, which migrate farther towards the head. In the QL lineage, however, *egl-20(+)* and *mig-14(+)* promote both anterior migration (in a *mab-5*-independent way) and posterior migration (via *mab-5* regulation). Thus, in *egl-20* mutants, in which the *mab-5*-activation defect caused by *egl-20* is specifically suppressed by a *mab-5(gf)* mutation, the QL.(d) cells migrate too far posteriorly (Fig. 3.5), just as the QR.(d) cells do in this same double mutant (Fig. 3.6). This observation suggests that in the wild-type, the anterior-directing and *mab-5*-activation (posterior-directing) functions of *egl-20* (and *mig-14)* combine to direct QL.p to stop and QL.a to migrate to its normal posterior position.

In migrations directed by signals from target cells, the attraction of migrating cells or growth cones to a specific target determines both their direction of migration and their stopping or turning point. In contrast, the Q.(d) cells do not migrate towards any apparent target, and yet they stop at precise positions. This situation is reminiscent of the targeting of chick retinal axons to specific positions in the optic tectum. Axons from cells in different regions of the retina map to specific locations on a tectum that morphologically appears relatively uniform. Graded expression of cell-surface molecules across the tectum may direct the migrating growth

cones to different locations (reviewed in Tessier-Lavigne, 1995). If a similar graded signal guides the Q descendants, then *egl-20* and *mig-14*'s role must be relatively specific for Q.(d) cell migration, since many other A/P migrations are unaffected by mutations in these genes (Fig. 3.8).

Positioning migrating Q descendants along the A/P axis

How might *egl-20* and *mig-14* act to tell the migrating Q.(d) cells where to stop? There are at least three possibilities. 1) The Q.(d) cells might seek out specific positional values, perhaps defined by a specific concentration or combination of guidance molecules whose composition changes with position along the A/P axis. Mutations in *egl-20* and *mig-14* could act by shifting positional values, or the cell's perception of these values, towards the posterior (Fig. 3.9B). This model could also explain the failure of QL to activate *mab-5* if the decision to activate *mab-5* is based on a positional cue that is shifted out of the range of QL in *egl-20* or *mig-14* mutants. 2) Opposing forces within the Q.(d) cells could simultaneously promote both anterior and posterior-directed migration. During this "tug-of-war", the relative strength of the two opposing forces determines the final position of the migrating cell along the A/P axis (Fig. 3.9B). In this model, the wild-type function of *egl-20* and *mig-14* would be to promote anterior migration or inhibit posterior migration. 3) Mutations in *egl-20* and *mig-14* might disrupt fine-scale A/P patterning, in the manner of *Drosophila* segment polarity mutants (Howard, 1990; Ingham, 1991). *C. elegans* is not a segmented animal, but there are repeating patterns of cells along the body (for a discussion, see Kenyon and Wang, 1991). In this model, other gene products would guide Q.(d) cells to the correct region of the body, and then *egl-20* and *mig-14* would position them correctly

within each metameric unit (Fig. 3.9B). Interestingly, mutations in *egl-20* can reverse the A/P polarity of certain epidermal cells (Jeanne Harris, Jennifer Whangbo and Cynthia Kenyon, manuscript in preparation) and cells in the Q lineage (Fig. 3.3, legend), much as mutations in segment polarity genes do in the fly (Ma and Moses, 1995; Wehrli and Tomlinson, 1995).

Why do *egl-20* and *mig-14* mutations cause posterior shifts in the positions of cells in the Q lineage but not in the positions of all cells that migrate along the A/P axis? Migrations along the D/V axis are coordinately affected by *unc-5* and *unc-6* mutations, and migrations along the A/P axis, including the Q.(d) cells, are coordinately affected by mutations in *vab-8*. If common external cues guide all A/P cell migrations, then *egl-20* and *mig-14* might act to modify the response of the Q descendants to these signals. However, it remains possible that separate cell-extrinsic signals guide a subset of A/P cell migrations, such as those of the QL and QR descendants.

A new look at *mab-5*'s role in cell migration

Our analysis of the *egl-20* and *mig-14* mutant phenotypes suggests a new interpretation of *mab-5*'s role in cell migration. The starting point for the experiments presented here was the hypothesis that *mab-5* acts as a directional migration switch: if *mab-5* is on, the Q.(d) cells migrate towards the posterior, if *mab-5* is off, the Q.(d) cells migrate towards the anterior. In this model, it was assumed that *mab-5* acts to specify the direction of migration. Thus it was somewhat surprising to find that *mab-5* is not absolutely required to migrate posteriorly (in *mig-13; egl-20* double mutants; Fig. 3.7b).

This analysis of *egl-20* and *mig-14* mutations suggests the possibility that cells in the Q lineages are instructed to migrate to specific positions rather than in specific directions. In *egl-20* and *mig-14* mutants the target positions adopted by migratory cells are shifted posteriorly. In some cases this positional shift involves a change in the direction of cell migration from anterior to posterior (Fig. 3.7). Perhaps this type of guidance system, that is, specifying cell position rather than direction of migration, governs Q.(d) cell migration. If so, then other mutations that alter the migrations of the Q.(d) cells would also act by respecifying target position rather than altering the direction of migration. Perhaps *mab-5*, rather than directing cells to migrate in a specific direction (i.e. towards the posterior), acts by directing cells to migrate to specific positions: positions that just happen to be posterior to the cells' starting points. The observation that intermediate levels of *mab-5* (as in a *mab-5*/+ heterozygote) direct cells to intermediate positions (Salser and Kenyon, unpublished data), also suggests that *mab-5* may not act as a simple ON/OFF-type directional switch. Our results suggest that there are at least two ways to promote posterior migration of the Q descendants: through *mab-5* activity or by inhibiting the promotion of anterior migration by the *egl-20*/*mig-14* system, which can act independently of *mab-5*. Further analysis of *egl-20*, *mig-14*, *mig-1* and *lin-17*, both genetic and molecular, should provide a greater understanding of how guidance information is encoded in this system.

ACKNOWLEDGEMENTS

We thank members of our lab for discussions and comments on the manuscript and Raffi Aroian and Marc Tessier-Lavigne for comments on the manuscript. We are grateful to the anonymous reviewers for many

helpful suggestions. We would also like to thank K. Nishiwaki for *mig-14(k124)*, M. Chalfie for the *mec-7-lacZ* transgenic worms, G. Xie and E. Aamodt for the *pag-1* mutant and advice on the *mec-7-lacZ* screen and G. Garriga for several *mig-1* mutants and the outcrossed *egl-20(n1437)* strain. We are grateful to Drs. S. and K. Kocherlakota for advice on statistical analysis. Thanks to Judy Silber and Julin Maloof in the the Kenyon lab for the *egl-20* alleles *mu25* and *mu39*, to rotation students Monica Gerber and Martha Stark for constructing two double mutant strains and assisting in their analysis and to Steve Salser for much patient assistance and advice on the beta-galactosidase and antibody staining protocols. Some *C. elegans* strains were provided by the *Caenorhabditis* Genetics Center which is funded by the NIH National Center for Research Resources (NCRR). This work was supported by NIH grant GM37053 and a grant from the Packard Foundation to C.K. ,an NSF predoctoral fellowship to N.T.R. and a UC Regents Fellowship to L.H.

MATERIALS AND METHODS

General Procedures, Nomenclature, and Strains

Methods for routine culturing and genetic analysis are described in Brenner, (1974) and Sulston and Hodgkin, (1988). Analyses were performed at 25°C, unless otherwise noted. The wild-type strain N2 is the parent of all strains used with the exception of *egl-20(n1437)*, which was isolated in an MT2878 background (G. Garriga, pers. comm.). Mutations not described in this paper are described by (Hodgkin *et al.*, 1988) or are noted below.

Mutations used:

LG I: *lin-17(n671), lin-17(n677), lin-17(e1456)* (Ferguson and Horvitz, 1985) *mig-1(e1787), mig-1(mu72), mig-1(n687), mig-1(n1354), mig-1(n1652),* (Desai *et al.*, 1988) *lin-6(e1466), dpy-5(e61), jeIn1[mec-7-lacZ+pRF4(rol-6d)]* (Hamelin *et al.*, 1992)

LG II: *mig-14(mu71), mig-14(k124)* (Kiyoji Nishiwaki, personal communication), *rol-1(e91), unc-52(e444).*

LG III: *mab-5(e1239), mab-5(e2088), mab-5(e1751gf)* (Hedgecock *et al.*, 1987; Salser and Kenyon, 1992), *pag-1(ls2)* (Xie et al., 1995).

LG IV: *unc-24(e138), dpy-20(e1282), egl-20(n585), egl-20(n1437),* (Desai *et al.*, 1988) *egl-20(mu25), egl-20(mu27), egl-20(mu39), unc-31(e169), muIs6 [lin-39-lacZ + pRF4(rol-6d)]* (Wang *et al.*, 1993).

LG V: *him-5(e1490)*

LG X: *mig-13(mu31)* (Robinson, 1995), *muIs5 [lin-39-lacZ + pRF4(rol-6d)]* (Wang *et al.*, 1993), *muIs9[hs-mab-5 + C14G10(unc-31$^+$)]* (Salser *et al.*, 1993).

Rearrangements: *eDf19 , tDf3 , tDf4* (Ahn and Fire, 1994), *jDf1, jDf2, jDf4* (Jacobson *et al.*, 1988)

Isolation of mutants with misplaced QL descendants

mig-14(mu71) and *mig-1(mu72)* were isolated in a screen for mutants with misplaced Q descendants. In order to visualize the Q descendants using a dissecting microscope, we used a *mec-7-lacZ* fusion, which is expressed in the touch receptor neurons AVM (QR.paa) and PVM (QL.paa) (Hamelin *et al.*, 1992) and an X-gal staining protocol that does not kill the eggs inside a stained hermaphrodite (Xie *et al.*, 1995). EA23 *jeIn1[mec-7-lacZ+pRF4(rol-6d)]; pag-1(ls2)* hermaphrodites were mutagenized with ethyl methanesulfonate (EMS; Brenner, 1974). (*pag-1(ls2)* increases the intensity of *mec-7-lacZ* expression (Xie et al., 1995))

3500 F2 descdendants from these animals were screened for the absence of a staining cell in the posterior where PVM is normally found.

egl-20(mu25) is an EMS-induced allele isolated in a screen using Nomarski optics to visualize animals with misplaced Q descendants. *egl-20(mu39)* was isolated in a screen for EMS-generated mutations affecting the expression of a *mab-5-lacZ* fusion gene, which will be described elsewhere (Maloof and Kenyon, unpublished data).

egl-20(mu27) was the only *egl-20* allele isolated in a non-complementation screen. EMS-mutagenized *him-5(e1490)* L4 males were mated to *unc-24(e138) egl-20(n585)* hermaphrodites. Approximately 2100 F1 non-Unc L4 hermaphrodites were picked away from their male siblings, grown to adulthood and screened for the Egl phenotype. Their progeny were screened for a QL.(d) migration (Mig) defect. Since *unc-24(e138) egl-20(n585)/eDf19* are viable, fertile and Egl, we should have been able to identify and recover complete loss-of-function alleles in this screen.

Forty-eight percent of *mab-5(e2088)/+; egl-20(n585)/+* animals have QL.pa daughters in anterior positions (i.e. in the V1-V3 region; n=56). To rule out the possibility that these new mutations were unlinked non-complementing mutations, we mapped *mu25, mu27* and *mu39* to the *egl-20* region, using *unc-24(e138)* and *dpy-20(e1282)* (see next section and data not shown).

Genetic Mapping

egl-20. The *egl-20* gene maps to LG IV (Trent *et al.*, 1983). We mapped *egl-20* between the genes *unc-24* and *dpy-20.* From heterozygotes of genotype *unc-24(e138) + dpy-20(e1282)/ + egl-20(n585) +*, 9/14 Dpy non-Unc

recombinants and 8/20 Unc non-Dpy recombinants segregated Mig progeny. We also found that the deficiency *eDf19* failed to complement *egl-20(n585)* (data not shown).

mig-14. *mig-14(mu71)* was mapped to the right arm of LGII using STS markers (Williams *et al.*, 1992). Three-factor mapping placed it between *rol-1* and *unc-52*: from *rol-1(e91) unc-52(e444)/mig-14(mu71)* heterozygotes, 4/25 Rol non-Unc recombinants segregated Mig progeny. None of the known deficiencies in the region (*jDf1, jDf2, jDf4*) delete *mig-14.*

mig-1. Two-factor map data had placed *mig-1* on the left arm of LGI (Hodgkin *et al.*, 1988). Three-factor mapping was used to further define the map position of *mig-1.* From heterozygotes of genotype + *lin-6(e1466) dpy-5(e61)/ mig-1(e1787)* + +, 21/21 Dpy non-Lin recombinants segregated Mig animals. *lin-17*, whose QL.(d) cell mutant phenotype is similar to that of *mig-1* mutants, also maps to the left arm of LGI. However, deficiencies *tDf3* and *tDf4*, which delete the *lin-17* locus, both complement *mig-1(e1787)* (data not shown). Together, these data suggest that the map position of *mig-1* is near or to the left of *lin-6*, consistent with the two-factor map data, and confirm that *mig-1* and *lin-17* are two distinct genes.

Genetic analysis of gene activity

egl-20. Four of the five *egl-20* alleles, *n585, n1437, mu25,* and *mu27* have similar phenotypes at 20° C: severe QL descendant migration defects and HSN migration defects. At 25° C, *mu25* has a weaker QL descendant migration defect (see Table 3.1). The QL descendant migration defects are less severe in *egl-20(mu39)* mutants (see Table 3.1), which also fail to exhibit some of the other *egl-20* mutant phenotypes such as crumpled

spicules, incomplete migration of rays 1 and 2 into the tail, and the A/P reversal of cells in the V5 lineage (data not shown).

We found that the *egl-20* allele *n585* is semi-dominant due to haploinsufficiency (Table 3.1) and behaves as a strong reduction-of-function mutation by genetic criteria. Placing the allele *n585* in trans to a deficiency for the region, *eDf19*, did not increase the severity of the QL descendant defect, the HSN defect or the polarity reversal. These data suggest that the *n585* mutation may completely eliminate gene activity. In addition, placing the weak allele *mu39 in trans* to either *n585* or *eDf19* increased the penetrance of the QL descendant and HSN migration defects to approximately the same degree. However, the polarity reversal phenotype was more severe in *mu39/eDf19* worms than in *mu39/n585* (data not shown). Thus the *n585* allele, although it is a strong reduction of function allele, may not represent the *egl-20* null phenotype.

To generate *egl-20* heterozygotes for gene dosage analysis (Table 3.1), hermaphrodites of genotype *unc-24(e138) egl-20* were crossed with N2 males, and their non-Unc progeny were scored. *eDf19* heterozygotes were identified as non-Unc, non-Dpy progeny from an *eDf19/unc-24(e138) dpy-20(e1282)* strain. As a control, *unc-24(e138) dpy-20(e1282)* hermaphrodites were crossed to N2 males and their non-Unc, non-Dpy progeny scored.

***mig-14, mig-1* and *lin-17*.** The alleles of *mig-14*, *mig-1* and *lin-17* that we studied are all recessive (Ferguson and Horvitz, 1985; Desai *et al.*, 1988; data not shown). Both alleles of *mig-14*, *mu71* and *k124*, have a QL descendant migration defect that is more than 95% penetrant (Fig. 3.3 and data not shown), although some of the other migration defects appear to be more severe in *k124* than *mu71* (K. Nishiwaki, pers. comm. and data not shown). The QL descendant migration defects in *mig-1* and *lin-17*

mutants are less penetrant than those of *egl-20* and *mig-14* mutants, and some alleles of *mig-1* have no associated QL descendant migration defect at all. The positions of the QL.pa daughters are anterior to wild type in greater than 75% of worms homozygous for the *mig-1* alleles *e1787* (Fig. 3.3), *n687* and *mu72*, but less than 2% of worms homozygous for *n1354* and *n1652* (data not shown; Maloof and Kenyon, unpublished data). All *lin-17* alleles examined, *n671*, *n677*, and *e1456*, have similar QL descendant migration phenotypes. However, the *lin-17(n671)* and *n677* mutations, reported to be the most severe *lin-17* alleles with respect to vulva formation (Ferguson and Horvitz, 1985), are both temperature sensitive for the QL descendant migration defect (data not shown). Interestingly, the *e1456* allele, reported to be weaker than *n671* and *n677* for other phenotypes (Ferguson and Horvitz, 1985), exhibits the migration defect at lower temperatures (data not shown). Thus, it is difficult to infer what the *lin-17* null phenotype might be and whether any of these alleles are null.

Since more than one allele of each of these genes caused a QL.(d) migration defect, the simplest explanation for all these mutations is that they reduce or eliminate gene function, and therefore function during normal development to activate *mab-5* expression in QL.

Scoring the positions of the Q.pa daughters

The positions of the Q.pa daughters were determined in late L1 after the descent of the last P nucleus into the ventral nerve cord. The positions of the QL descendants along the A/P axis were determined relative to those of the stationary Vn.p and Vn.a epidermal cells. QL/R.paa and its sister QL/R.pap migrate to nearby A/P positions and they are sometimes very close together. Since it was not always possible to determine which

cell was which without observing the division of Q.pa, the positions of both cells were plotted on the same graphs. By convention, anterior is always to the left in all graphs and diagrams. All strains were examined at 25°C except *mig-14(mu71); mab-5(e1751gf)* which was examined at 20°C.

Direct observation of Q lineage migrations

Worms were mounted for long-term observation as described by Sulston and Horvitz, (1977). Unhealthy strains were observed at lower temperatures: *mig-1(e1787)* and *mig-14(mu71); mab-5(e1751gf)* mutants at 20°C, and *mab-5(gf); egl-20(n585)* mutants at 22.5°C. All other strains were observed at 25°C.

Determination of Mab-5-like phenotypes

We examined *egl-20(n585)*, *mig-14(mu71)*, *mig-1(e1787)* and *lin-17(n671)* mutants at 25° for other Mab-5 phenotypes (Kenyon, 1986). Tissues examined were: adult coelomocytes in hermaphrodites, and spicules, hooks and sensory rays 1-6 in males. More than 20 worms of each genotype were examined for each phenotype.

***egl-20*, *mig-14*, and *mig-1*.** All tissues examined were essentially wild-type, except for two tissues in *egl-20* mutants: the coelomocytes, which were often missing (20/43), and the spicules, which were often crumpled (16/26).

***lin-17*.** *lin-17* mutations are known to cause many asymmetric cell divisions to become symmetric or to adopt a reversed polarity. The lineage of the M mesoblast was abnormal in *lin-17* mutants (Sternberg and Horvitz, 1988); however, we found that 21 out of 25 animals produce adult coelomocytes, unlike *mab-5* mutants. Male tails have few rays, often with

severely abnormal morphology (Hodgkin *et al.*, 1988; and data not shown), but, unlike *mab-5* mutants, do not replace rays with alae (data not shown). *lin-17* mutations affect the formation of the hook and the organization of the spicules, as do mutations in *mab-5*; however, the defects in these structures are due to different developmental abnormalities in *lin-17* and *mab-5* mutants (Kenyon, 1986; Sternberg and Horvitz, 1988).

Antibody staining of whole mount larvae

Larvae were fixed and stained with a rabbit polyclonal antisera to MAB-5 as described in (Salser and Kenyon, 1996). The DNA stain DAPI, which labels all nuclei, was used to confirm the identity of both *mab-5* immunoreactive and non-immunoreactive cells.

Single-Cell Activation of *hs-mab-5*

To induce *heat-shock-mab-5 (hs-mab-5)* expression in a migrating Q descendant, we heated it using a laser microbeam. Experiments were performed as described by Stringham and Candido (1993) with the modification that laser strength was calibrated daily by inserting neutral density filters in the laser light path until 15-25 pulses were needed to burst an *E. coli* cell. We then further attenuated the laser by placing a glued stack of 10 or 12 microscope slides perpendicular to the laser's path. The laser was focused on a single cell for 3 minutes at a pulse rate of 2.5 Hz. After testing several different integrated lines carrying *hs-mab-5*, we chose the strain CF301 *mab-5(e2088); unc-31(e169); him-5(e1490); muIs9[hs-mab-5 + C14G10(unc-31$^+$)]* (Salser *et al.*, 1993) because of its high sensitivity and low background in whole-animal heat-shocks. Animals were kept at 20°C throughout the experiments. 3.5-4 hour old L1 larvae were mounted on

agarose pads containing 2 mM azide to immobilize them. After laser treatment, animals were allowed to recover for 1 hour on a seeded NG plate and then were remounted on agarose pads. The migrating cells were followed until QR.a or QR.ap had remained stationary for at least 2 hours, usually about 8 hours total. Reversals were defined as migrations in which QR.a or QR.ap moved towards the posterior and passed more than one nucleus in the surrounding epidermis. The data presented in Figure 2 represents all experiments carried out once conditions were found that caused QR.a migration reversals. To insure that the reversals were dependent on the laser heat-shock of QR.a, we carried out controls in parallel in which animals were mounted on azide for the same amount of time but without laser pulsing. Controls in which QR.a was targeted in N2 (wild-type) worms were also done in parallel. We found that the laser intensity necessary for inducing QR.a reversals had the side-effect of delaying or blocking the division of QR.a. This effect was independent of *mab-5*, however, because focusing the laser on QR.a in wild-type worms also delayed or blocked the division but did not induce reversals. We did not test the effect of laser induction of *mab-5* in QR.p and QL.p because *mab-5* expression in this branch of the QL and QR lineage causes these cells to stop migrating (Fig. 3.1), a result indistinguishable from that caused by cell damage.

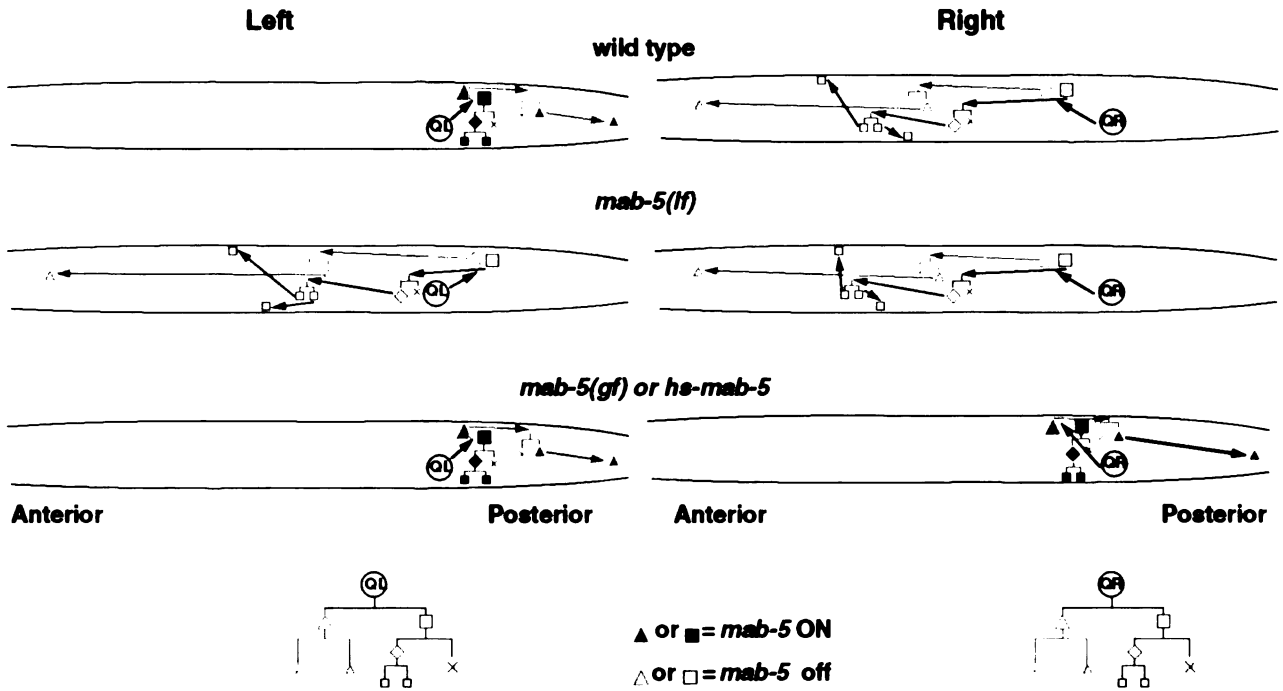

Figure 3.1 Migration of the Q neuroblasts and their descendants in wild type (Sulston and Horvitz, 1977; Chalfie and Sulston, 1981) , *mab-5(lf)* (Kenyon, 1986; Salser and Kenyon, 1992) and *mab-5(gf)* (Salser and Kenyon, 1992) mutants. Data are from Salser and Kenyon, (1992). Each cell in the lineage is denoted by a different shape (see lineage diagrams at bottom of figure): QL/R, circle; QL/R.a, large triangle; QL/R.ap (PQR/AQR), small triangle; QL/R.p, large square; QL/R.pa, diamond; QL/R.paa (PVM/AVM) and QL/R.pap (SDQL/R), small squares. Cells undergoing programmed cell death are marked with an x. Cell migrations are indicated by arrows. All cells divide and migrate along the A/P axis except for the daughters of the anteriorly migrating QR.pa cell, which also have a dorsoventral component to their migration. The divisions of cells other than QL or QR are symbolized by cell lineage diagrams. In all figures, anterior is to the left. Filled symbols indicate *mab-5* expression as determined by antibody staining (S. Salser and C. Kenyon, unpublished data; see also Fig. 4). This pattern is the same as that determined using *mab-5-lacZ* (Salser and Kenyon, 1992) . The brief expression of MAB-5 in the QL neuroblast just before division is not depicted.

Figure 3.2. Laser activation of *hs-mab-5* in QR.a as it migrates anteriorly causes the cell to reverse direction and migrate posteriorly.

During the anterior migrations of QR.a and QR.p, an attenuated laser beam was focused on a single nucleus for three minutes in order to activate *mab-5* expression, and the resulting cell migrations were observed during the following 8-10 hours (see Materials and Methods). The symbols indicating cells in the QR lineage are the same as those in Fig 3.1. The QR.p lineage (square) was unaffected and is omitted. Gray ovals show Vn.a and Vn.p epidermal cells and correspond to the horizontal axis of Figure 3. The targeted cell is indicated with radiating lines.

(A) Sample lineage from a *mab-5(e2088); muIs9(hs-mab-5)* animal in which the laser was focused on QR.a (red triangle). QR.a continued to migrate anteriorly, then reversed direction and migrated toward the posterior, divided as QR.a normally does, and then migrated a short distance to the anterior (presumably due to decay of the *hs-mab-5* activity (Salser and Kenyon, 1992).

(B) Sample lineage from *mab-5(e2088); muIs9(hs-mab-5)* animal in which the laser was focused on a nearby cell, V3.p. At that time, QR.a (dashed triangle) was just dorsal of V3.p but was unaffected, continuing its normal anterior migration pattern.

(C) Summary of all laser heat-shock experiments. In all cases the laser was focused on cells on the right side of the animal during the time that QR.a was migrating anteriorly (between V3 and V4). The targeted "nearby" epidermal cells were: V3, V3.a, and V3.p (n= 3, 2 and 4, respectively). "Distant" epidermal cells were: V1, V2, V2.a, V2.p, V6, and P1/2 (n= 1, 1, 1, 1, 2 and 2, respectively). Dorsal syncytial nuclei were: the

hyp7 nucleus between V2 and V3 (n=4) and the hyp7 nucleus between V1 and V2 (n=1). Using the positions of the Vn.a and Vn.p cells as a ruler (see horizontal axis for Fig. 3.3, in which each tick mark is defined as one unit) the distance migrated toward the posterior in the QR.a reversals ranged from 4 to 13 units, mean = 7.9.

A.

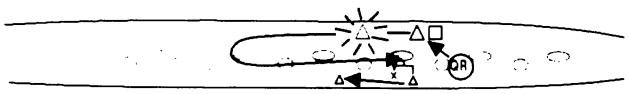

B.

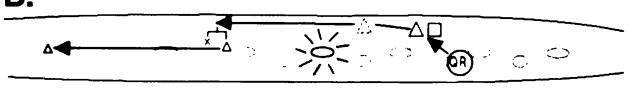

C.

genotype	targeted cell	QR.a reversed
hs-mab-5	QR.a	18/38
"	"nearby" hypodermal cell (V3)	0/9
"	"distant" hypodermal cell (V1,V2,V6, or P1-2)	0/8
"	dorsal syncytial nucleus	0/5
"	QR.p	0/2
"	none	0/17
wild type	QR.a	0/16

Figure 3.2

Figure 3.3. The migrations of the QL descendants in wild-type and *mab-5(e2088)*, *egl-20(n585)*, *mig-14(mu71)*, *mig-1(e1787)* and *lin-17(n671)* mutants.

The positions of the QL descendants along the A/P axis were determined relative to that of the stationary Vn.a and Vn.p epidermal cells, shown at the bottom of the figure (see Materials and Methods). (A) Final positions of the QL.pa daughters, AVM and SDQL, at 25°C. The asterisk above V5.a marks the birthplace of QL. Fifty animals of each genotype were scored. (B) The migrations of QL and its descendants in representative animals of each genotype. The migrating cells were followed in living animals using Nomarski (DIC) optics. The different cells are depicted by different shapes (see lineage diagram at bottom of figure) as described in Fig. 3.1. The cells in the Q.p branch of the lineage are labelled blue and in the Q.a branch are labelled pink. We observed the complete migrations in 5 *egl-20*, 3 *mig-14*, and 4 *mig-1* mutants. Data for wild-type and *mab-5* mutant migrations are from Salser and Kenyon (1992). Illustrated lineages are representative. The following variation was seen: ***egl-20.*** QL.p did not migrate at all in one *egl-20* mutant, although its daughter, QL.pa, did. QL.pa migrated anteriorly in 3/5 animals and did not migrate at all in the other two. In one animal, QL.ap did not migrate into the head but stopped in the body, just posterior to V1.p. In addition, in one animal, the polarity of the QL.a division was reversed: QL.aa migrated and QL.ap died. The migration of QL.aa in this animal was quite unusual; first it migrated anteriorly past three nuclei, then changed direction and migrated posteriorly past four nuclei, then changed direction again and migrated anteriorly past seven nuclei to a position just adjacent to V3.a,

where it stopped. ***mig-14.*** In one animal QL.ap did not migrate into the head, but stopped in the body between V1.a and V1.p. ***mig-1.*** In one *mig-1* mutant the QL.(d) cells migrated as in wild type. ***lin-17.*** *lin-17* mutants were not observed continuously, since their development at 25°C, where the Mig defect is observed, is greatly retarded. Instead, the initial migration of QL was observed and then the final positions of the QL.pa descendants were scored the following day. In all 8 *lin-17* mutants examined, QL migrated towards the posterior; in four of those animals the QL.pa daughters migrated to positions anterior to wild-type.

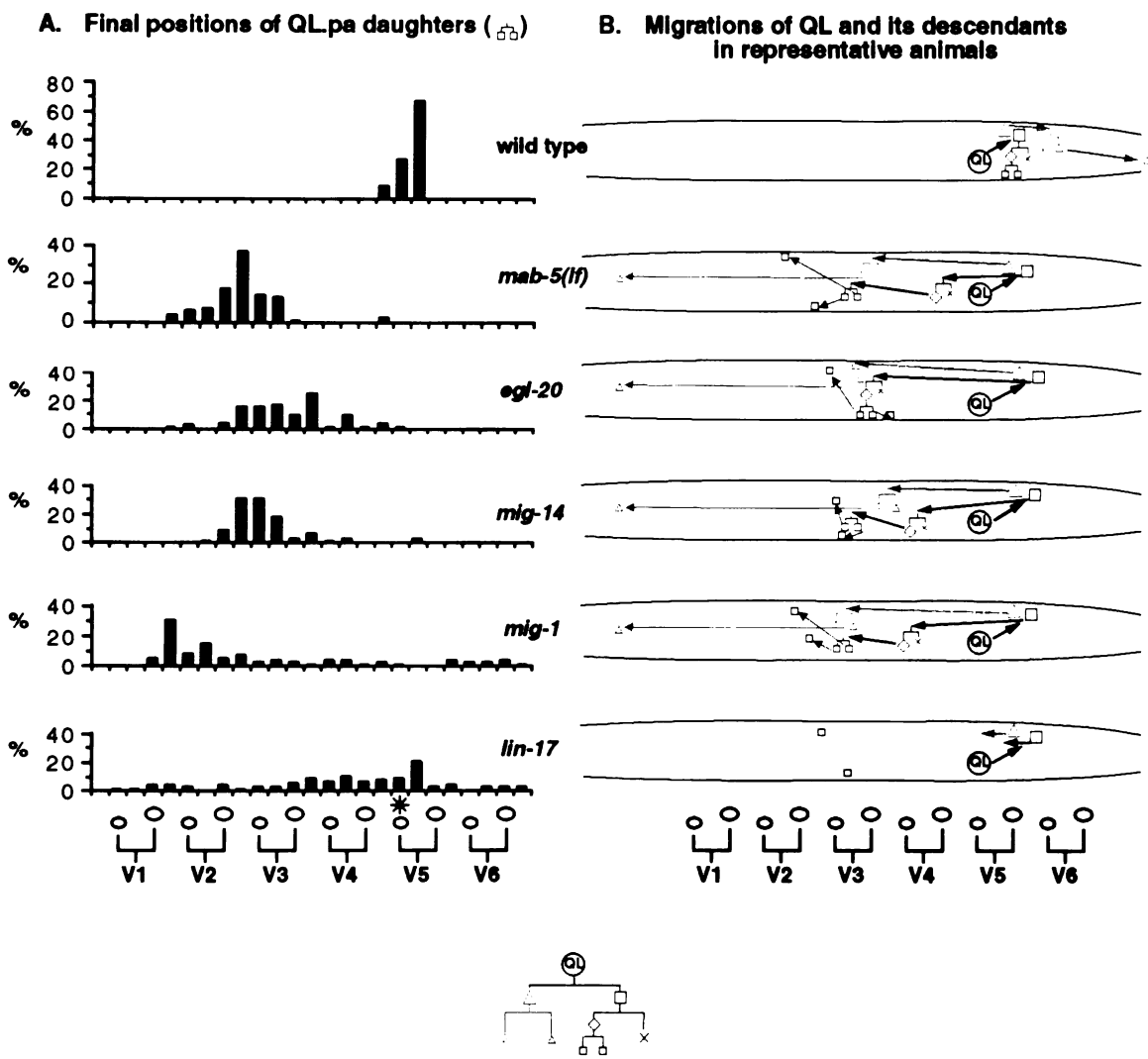
A. Final positions of QL.pa daughters ( )
B. Migrations of QL and its descendants in representative animals
%
80
60
40
20
0
wild type
mab-5(lf)
egl-20
mig-14
mig-1
lin-17
V1
V2
V3
V4
V5
V6
QL

Figure 3.3

Figure 3.4. MAB-5 expression in QL.a and QL.p.

Whole mount larvae, 3-6 hours post-hatching (raised at 25°C), were stained with polyclonal anti-MAB-5 antisera and the DNA stain DAPI (Salser *et al.*, 1993). At this time, QL has just divided and both daughters stain brightly with anti-MAB-5 antisera in wild type (top panels). In the *egl-20*, *mig-14* and *mig-1* mutants depicted above, QL.a and QL.p did not stain with anti-MAB-5 antisera. The *lin-17* mutant shown here demonstrates the faint MAB-5 staining occasionally seen in QL.a and QL.p in *mig-1* and *lin-17* mutants. Some other MAB-5-immunureactive cells are labeled for reference: arrow indicates V6, left arrowhead indicates P9/10, right arrowhead indicates P11/12.

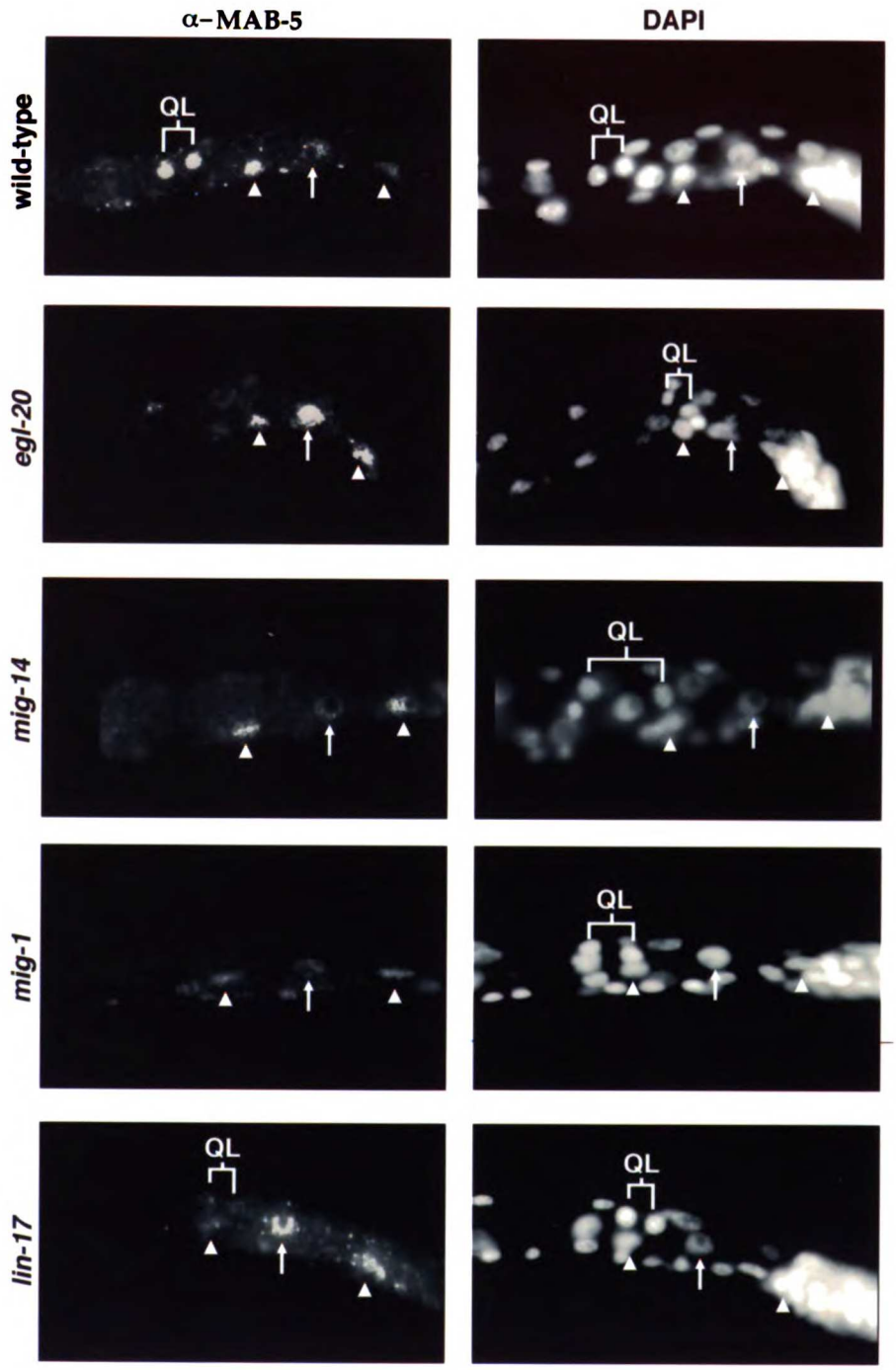

Figure 3.4

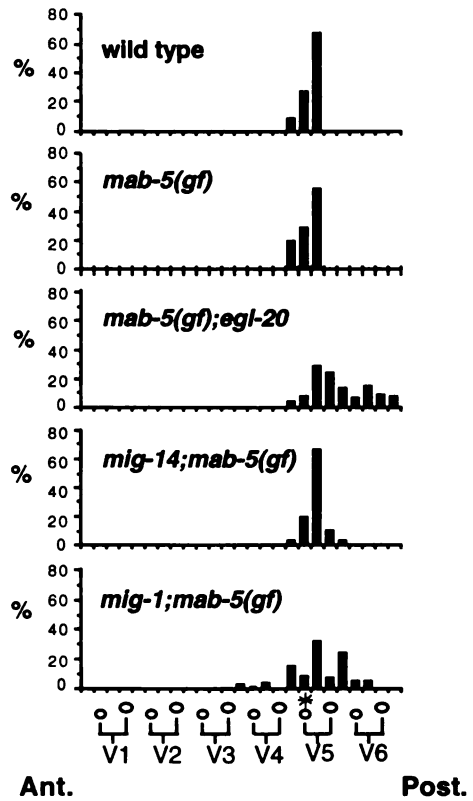

Figure 3.5. A *mab-5(gf)* mutation suppresses the anterior migrations of the QL.(d) cells in *egl-20*, *mig-14* and *mig-1* mutants.

Final positions of the QL.pa daughters (small blue squares in Figs 1 and 3) in worms carrying *mab-5(e1751gf)* alone and in combination with *egl-20(n585)*, *mig-14(mu71)* and *mig-1(e1787)*. The positions in wild type are shown for comparison. The star above V5.a marks the birthplace of QL. n=35 for *mig-14; mab-5(gf)*. n=50 for all other genotypes. In *egl-20*, *mig-14*, *mig-1* and *lin-17* mutants, but not in *mab-5* mutants, the migration of QL towards the posterior was lengthened, so that it often divided next to P9/10 or even V6 instead of over V5. *egl-20* L1 larvae are slightly Dumpy, so distances between cells are shorter, but the other three mutants are of normal length. The lengthened QL migration may be responsible, at least in part, for the QL.pa daughters which are posterior to wild-type in *mab-5(e1751gf)* double mutants (shown here), and in the *mig-1* and *lin-17* mutants which have sufficient *mab-5* activity to remain in the posterior (Fig. 3).

Figure 3.6. Mutations in*egl-20* and *mig-14* shift the QR.pa daughters towards the posterior.

The positions of the QR.pa daughters are shifted towards the posterior in (A)*egl-20(n585)* and *mig-14(mu71)* mutants, in double mutant combinations, and further posterior in (B) *mig-14(mu71); egl-20(n585)* double mutants. The star above V5.a marks the birthplace of QR. n $\geq$ 50 animals of each mutant genotype except: *mab-5(lf)*, n=35; *mig-14; mab-5(gf)*, n=37; and *egl-20; mig-13*, n=42. A dashed line is drawn through each column of graphs to make it easier to compare the distribution in different genotypes. The lines are drawn such that for each column, the final positions of the QR.pa daughters in 95% or more of control worms (top histogram of each column) are anterior to this line. The percentage of worms of each genotype with QR.pa descendants posterior to the line are noted at the right of each histogram. The QR.pa daughters in *egl-20* and *mig-14* mutant strains (second and third rows of A) are significantly different from that of control strains (top row of A) according to both the Kruskal-Wallis test and Sheffe's test (P<.0001).

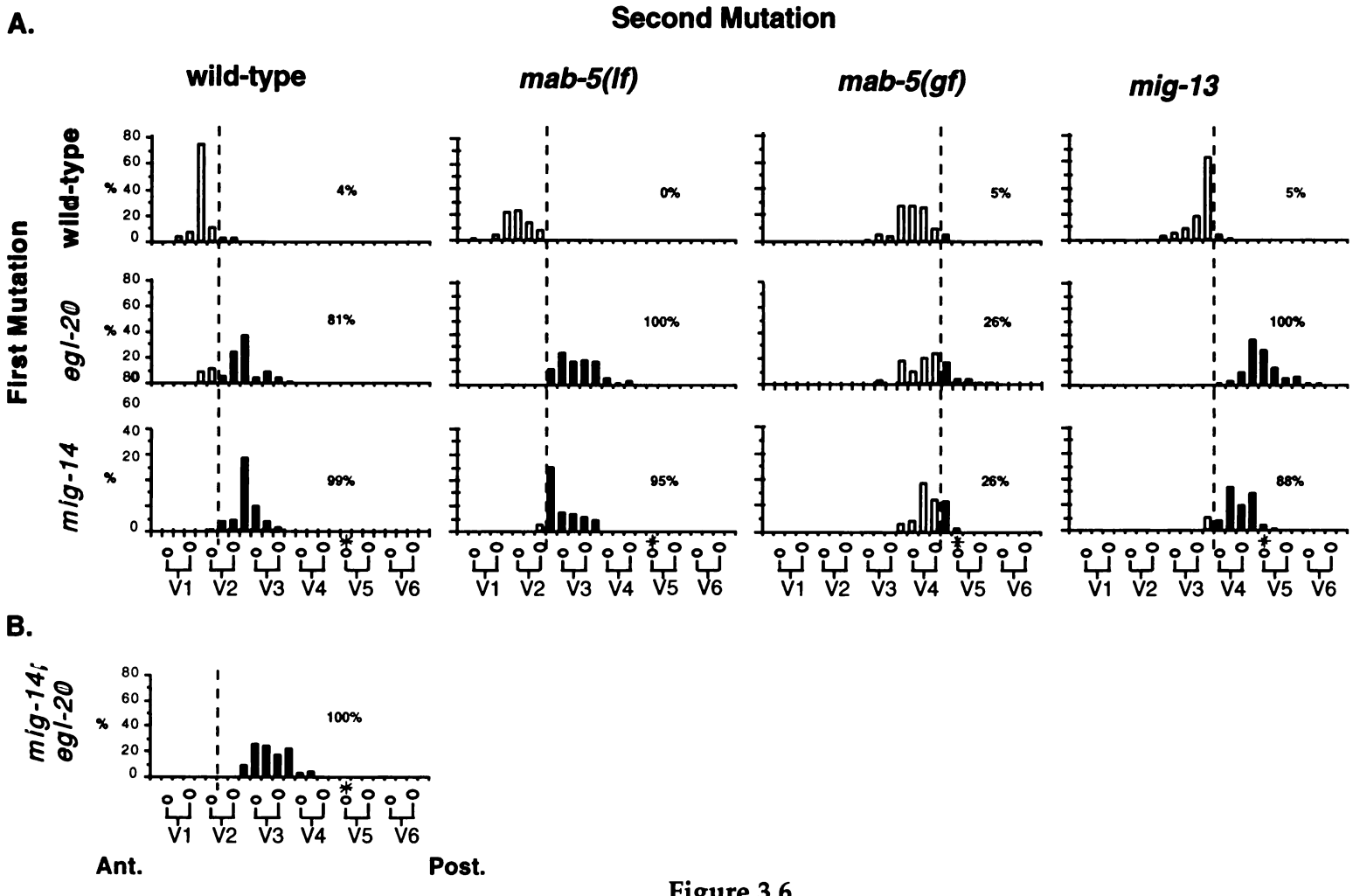
A.
Second Mutation
wild-type
mab-5(lf)
mab-5(gf)
mig-13
First Mutation
wild-type
egl-20
mig-14
4%
0%
5%
5%
81%
100%
26%
100%
99%
95%
26%
88%
V1 V2 V3 V4 V5 V6
B.
mig-14;
egl-20
100%
Ant.
Post.

Figure 3.6

Figure 3.7. The migrations of QR and its descendants.

The migrating cells were observed using Nomarski (DIC) optics. (A) QR lineage migrations in representative wild-type and mutant worms. Cells in the lineage are denoted by different shapes, as described in Fig. 3.1 (see lineage diagram at bottom of Part A). The final positions of the QR.pa daughters are labelled blue. The QR.p cell and its migration are labelled red. We observed the complete migrations in 2 *egl-20*, 3 *mig-14*, and 3 *mab-5(gf); egl-20* mutants. The data for the wild-type and *mab-5(gf)* mutant migrations are taken from Salser and Kenyon (1992). Diagonal line near tail marks the position of the anus. (B) The migrations of QR.p (red square and arrow in part A) in wild-type and mutant animals. Each arrow represents the migration of QR.p in a different animal. Only cells that passed both a Vn.a/p nucleus and an internuclear interval were defined as having migrated. QR.p cells that did not migrate are indicated with a red circle. The asterisk above V5.a marks the birthplace of QR. The dashed line is for reference and marks the average birthplace of QR.p.

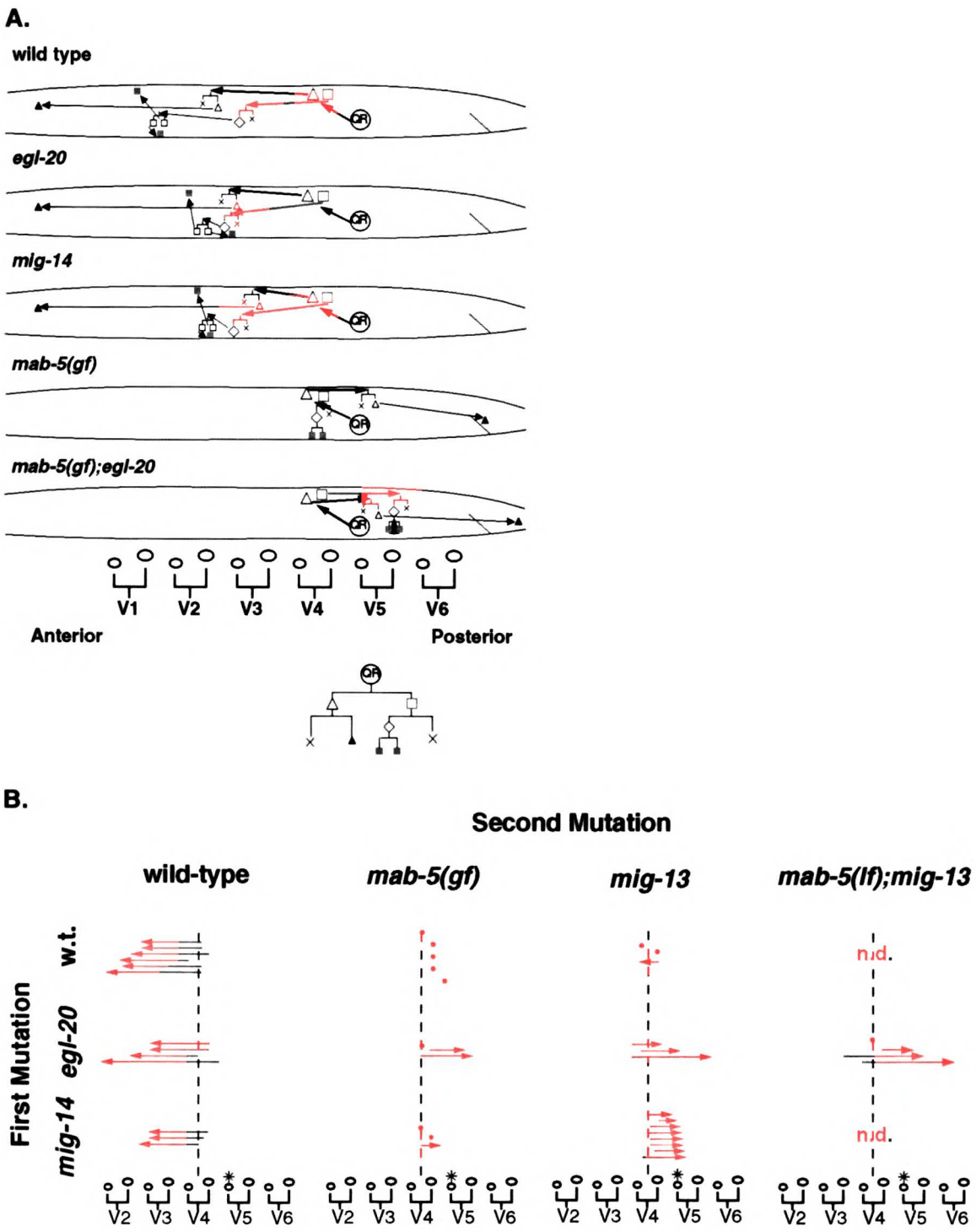
A.
wild type
egl-20
mig-14
mab-5(gf)
mab-5(gf);egl-20
OR
V1
V2
V3
V4
V5
V6
Anterior
Posterior
B.
Second Mutation
wild-type
mab-5(gf)
mig-13
mab-5(lf);mig-13
First Mutation
w.t.
egl-20
mig-14
n.d.
n.d.
V2
V3
V4
V5
V6

Figure 3.7

Figure 3.8. Other cell migrations in wild-type and mutant worms. Cell positions in N2 at 20°C are defined as wild-type (data not shown). (A) The final positions of migratory cells in wild-type worms at 20°C. Range of final positions indicated beneath cell name was determined by examining more than 20 worms. Each worm has two HSN, ALM and CAN neurons, one per side, but only one M and muIntR cell, both found on the right side (Sulston and Horvitz, 1977). There are also two pairs of juvenile coelomocytes found in different A/P positions (Sulston and Horvitz, 1977): ccLa/p on the left side and ccRa/p on the right side. Final positions of all cells were determined relative to the positions of the Vn.p and Vn.a cells (bottom of A) except for M and muIntR, which were determined relative to the positions of the undivided V and P cells and then extrapolated onto this diagram of a later developmental stage. The migrations of all these cells occur during embryogenesis, prior to Q cell migration. Arrows indicate direction of migration. Diagonal line near tail marks the position of the anus. (B) The percentage of worms grown at 25°C which have misplaced migratory cells. Note the effect of temperature on some migrations in wild-type animals. n, number of sides scored. **a.** mostly anterior to wild type. **p.** mostly posterior to wild type. The HSN position observed in *egl-20* and *mig-1* mutants at 25°C is similar to that previously observed in worms grown at 20°C (Garriga *et al.*, 1993). The position of M is unaffected by mutations in *mab-5* (data not shown). **Other migration defects.** In addition to the defects described above, all four mutants have variable defects in the migrations of the distal tip cells (Kiyoji Nishiwaki, pers. comm and J. H., L. H., N. R., and C. K., data not shown). Also, in *mig-14(mu71)* mutants, the position of the neuron BDU, which undergoes a short anterior migration (J. Sulston, pers. comm.), was posterior to wild type 45% of the time (n=49).

A.

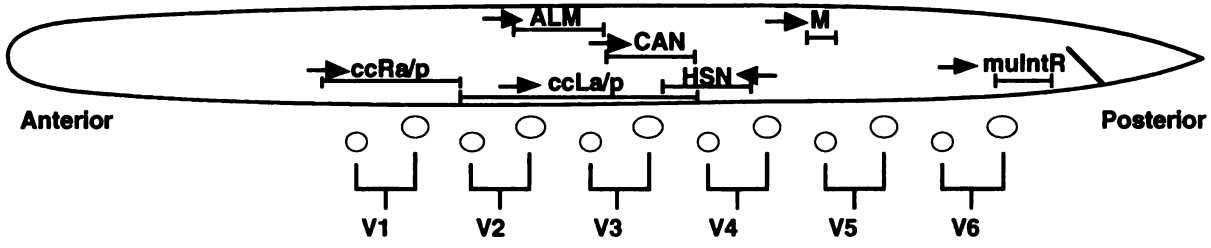

B.

Mig. Cells	% misplaced (n) wild type	*egl-20(n585)*	*lin-17(n671)*	*mig-1(e1787)*	*mig-14(mu71)*
HSN	4% (99)	81% (98) P	18% (77) a,P	38% (97) P	95% (43) P
ALM	0% (50)	5% (38)	10% (21)	2% (40)	26% (50) P
CAN	8% (50)	5% (40)	0% (22)	0% (40)	2% (50)
muIntR	0% (40)	2% (42)	0% (40)	6% (31)	0% (25)
ccLa/p	0% (38)	10% (47)	6% (40)	10% (40)	4% (23)
ccRa/p	3% (43)	18% (41) a	10% (41)	10% (40)	6% (33)
M	18% (34) a	68% (34) a	20% (40) a,P	35% (31) P	40% (25) a

Figure 3.8

Figure 3.9. Models for the function of *egl-20, mig-14, mig-1* and *lin-17*

(A) A diagram summarizing the roles of *egl-20, mig-14, mig-1* and *lin-17* in the migrations of the QL and QR descendants. These four genes activate *mab-5* expression in QL and its descendants, not QR and its descendants. Both *egl-20* and *mig-14*, however, promote anterior migration of the descendants of both QL and QR.

(B) Alternative models to explain the posterior shift in *egl-20* and *mig-14* mutants. Large circle indicates the birthplace of QR. Arrows indicate the sum of the QR and QR.(d) migrations. Small circles indicate the positions of the QR.pa daughters. The position of the gonad primordium, represented by the gray oval, is not shifted in *egl-20* and *mig-14* mutants and is used as a reference point for Q.(d) cell position in these diagrams. **1. Positional Model.** The QR.(d) cells seek out specific positional values. *egl-20* and *mig-14* mutations either shift positional values toward the posterior (values shifted) or direct cells to migrate to more posterior positional values (response altered). In the former case, the cells continue to migrate to their wild-type positional value, but that value is now in a more posterior position in the worm. **2. Tug-of-War Model.** Proteins involved in anterior- and posterior-directed migrations compete for control of the QR.(d) cells. *egl-20* and *mig-14* mutations act by increasing the relative activity levels of proteins that promote posterior-directed migrations. **3. Fine-scale Patterning Model.** QR.(d) cells migrate to the correct region of the body, then *egl-20* and *mig-14* help to position these cells correctly within that region. Mutations in *egl-20* and *mig-14* might disrupt fine-scale patterning, for example, by locally reversing A/P polarity.

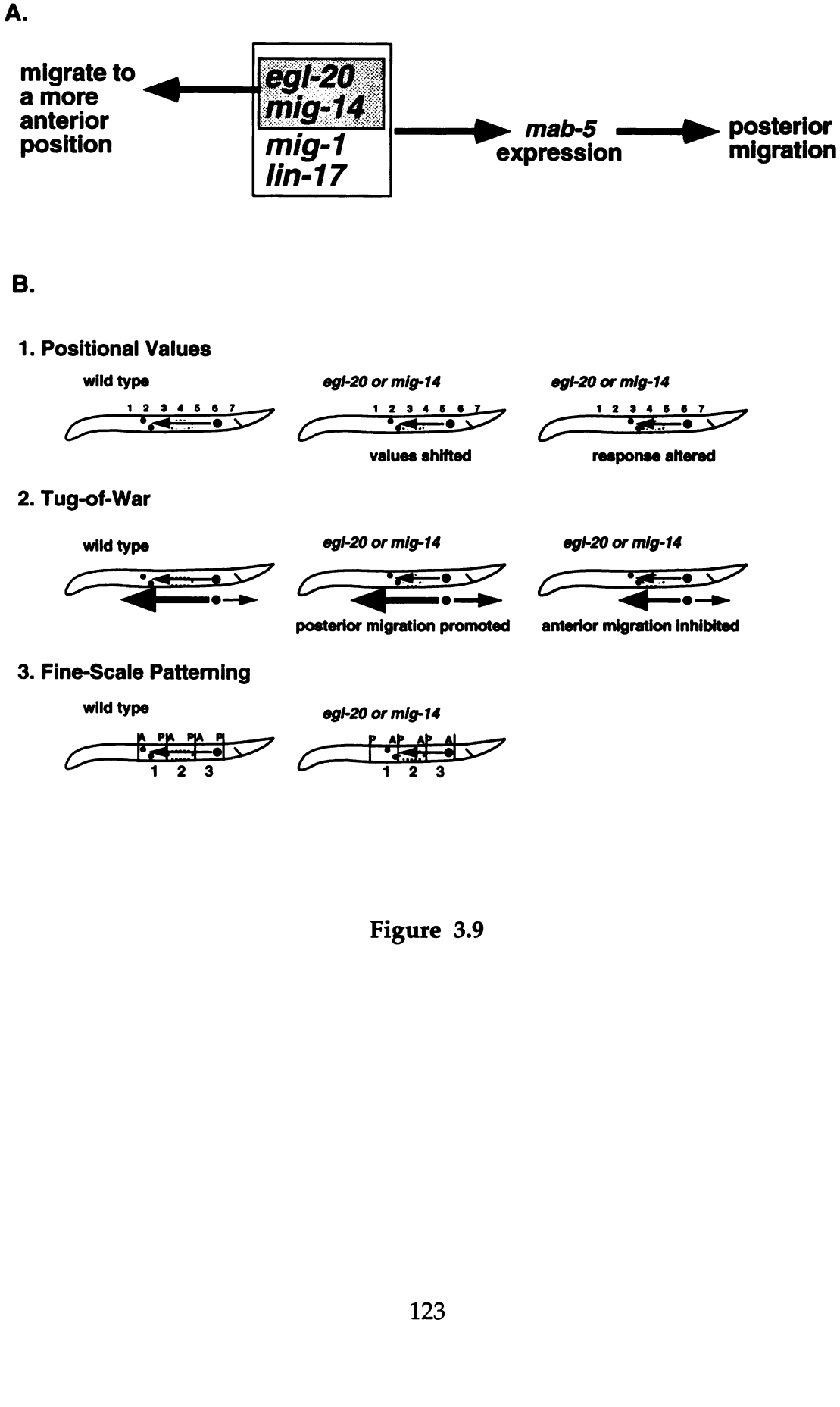
A.
migrate to a more anterior position
egl-20
mig-14
mig-1
lin-17
mab-5 expression
posterior migration
B.
1. Positional Values
wild type
egl-20 or mig-14
values shifted
egl-20 or mig-14
response altered
2. Tug-of-War
wild type
egl-20 or mig-14
posterior migration promoted
egl-20 or mig-14
anterior migration inhibited
3. Fine-Scale Patterning
wild type
egl-20 or mig-14

Figure 3.9

genotype	% QL desc. anterior	n
egl-20 (n585)	96%	50
mu27	100%	25
n1437	96%	36
mu25	83%	35
mu39	66%	25
eDf19/+	9%	123
egl-20 (n585)/+	7%	100
mu27/+	5%	114
n1437/+	3%	107
mu25/+	3%	181
mu39/+	0%	114
control +/+	0%	279

Table 3.1. Gene dosage analysis of *egl-20.*

Strong *egl-20* mutations are haploinsufficient for the QL descendant migration defect. The positions of the QL.pa daughters were scored in L2 and late L1 larvae. Positions were scored as anterior if they were anterior to the V4.pp or V4.ppa nuclei in L2 or the posterior end of the V4.p nucleus in L1. *egl-20* heterozygotes were generated using the *unc-24(e138)* mutation to distinguish self- from cross-progeny (see Materials and Methods). The *eDf19* deficiency is maintained in trans to *unc-24(e138)* and *dpy-20(e1282)*. As a control, we examined *unc-24(e138) dpy-20(e1282)/+* animals. n, number of animals scored for each genotype. The percentage of QL.pa daughters that migrate into the anterior in *egl-20* heterozygotes is significantly different from that of control animals according to the one-tailed Fisher Exact Test for all *egl-20* alleles except *mu39* (*eDf19*, P<

0.000002; *n585*, P<0.0001; *mu27*, P<0.0005; *n1437*, P<0.02; *mu25*, P<0.01, *mu39*, P<1.00).

	A. *mab-5* Ab staining in QL.a and QL.p				B. Position of QL.pa desc.	
genotype	**% bright**	**% faint**	**% none**	**(n)**	**% posterior**	**(n)**
wild type	**98**	2	0	(94)	**100**	(50)
egl-20(n585)	**0**	0	100	(27)	**4**	(50)
mig-14(mu71)	**0**	0	100	(31)	**2**	(50)
mig-1(e1787)	**17**	11	72	(72)	**15**	(50)
lin-17(n671)	**52**	27	21	(52)	**48**	(50)

Table 3.2. Correlation of MAB-5 expression in QL.a and QL.p with posterior positions of the QL.pa daughters.

n, number of sides scored. All worms were grown at 25°C. (A) The percentage of worms with QL.a and QL.p staining brightly with antisera to MAB-5 (see Materials and Methods). All worms were fixed at 3-6 hours after hatching except for *mig-14* mutants which were fixed at 3.5-4.5 hours. Staining was only scored in animals in which QL had divided. (B) The percentage of animals in which the final position of the QL.pa descendants at the end of L1 was posterior to V4.p. Data taken from Fig. 3.3.

We did not examine *mab-5* expression and final position in the same animals since *mab-5*-expressing QL.(d) cells which migrate into the anterior stop expressing *mab-5* (Salser and Kenyon, unpublished data). Thus we scored *mab-5* expression in QL.a and QL.p before they had migrated very far.

REFERENCES

Ahn, J. and Fire, A. (1994). A Screen for Genetic Loci Required for Body-Wall Muscle Development During Embryogenesis in *Caenorhabditis elegans*. *Genetics* **137,** 483-98.

Brenner, S. (1974). The genetics of *C. elegans*. *Genetics* **77,** 71-94.

Chalfie, M. and Sulston, J. (1981). Developmental genetics of the mechanosensory neurons of *C. elegans*. *Dev. Biol.* **82,** 358-370.

Chisholm, A. (1991). Control of cell fate in the tail region of *C. elegans* by the gene *egl-5*. *Development* **111,** 921-32.

Clark, S. G., Chisholm, A. D. and Horvitz, H. R. (1993). Control of cell fates in the central body region of *C. elegans* by the homeobox gene *lin-39*. *Cell* **74,** 43-55.

Costa, M., Weir, M., Coulson, A., Sulston, J. and Kenyon, C. (1988). Posterior pattern formation in *C. elegans* involves position-specific expression of a gene containing a homeobox. *Cell* **55,** 747-56.

Desai, C., Garriga, G., McIntire, S. L. and Horvitz, H. R. (1988). A genetic pathway for the development of the *Caenorhabditis elegans* HSN motor neurons. *Nature* **336,** 638-46.

Devore, D. L., Horvitz, H. R. and Stern, M. J. (1995). An FGF receptor signaling pathway is required for the normal cell migrations of the sex myoblasts in *C. elegans* hermaphrodites. *Cell* **83,** 611-20.

Ferguson, E. and Horvitz, H. (1985). Identification and characterization of 22 genes that affect the vulval cell lineages of the nematode *C. elegans*. *Genetics* **110,** 17-72.

Garriga, G., Desai, C. and Horvitz, H. R. (1993). Cell interactions control the direction of outgrowth, branching and fasciculation of the HSN axons of *Caenorhabditis elegans*. *Development* **117,** 1071-87.

Godin, I., Wylie, C. and Heasman, J. (1990). Genital ridges exert long-range effects on mouse primordial germ cell numbers and direction of migration in culture. *Development* **108,** 357-363.

Hamelin, M., Scott, I. M., Way, J. C. and Culotti, J. G. (1992). The *mec-7* beta-tubulin gene of *Caenorhabditis elegans* is expressed primarily in the touch receptor neurons. *EMBO Journal* **11,** 2885-93.

Hedgecock, E. M., Culotti, J. G. and Hall, D. H. (1990). The *unc-5, unc-6* and *unc-40* genes guide circumferential migrations of pioneer axons and mesodermal cells on the epidermis in *C. elegans*. *Neuron* **4,** 61-85.

Hedgecock, E. M., Culotti, J. G., Hall, D. H. and Stern, B. D. (1987). Genetics of cell and axon migrations in *Caenorhabditis elegans*. *Development* **100,** 365-82.

Hodgkin, J., Edgley, M., Riddle, D. L. and Albertson, D. G. (1988). Appendix 4, Genetics. In *The Nematode Caenorhabditis elegans*, (ed. W. B. Wood), Cold Spring Harbor, New York: Cold Spring Harbor Laboratory.

Howard, K. (1990). The Blastoderm Prepattern. *Seminars in Cell Biology* **1,** 161-72.

Ingham, P. (1991). Segment Polarity Genes and Cell Patterning within the *Drosophila* body segment. *Current Opinion in Genetics and Development* **1,** 261-7.

Ishii, N., Wadsworth, W. G., Stern, B. D., Culotti, J. G. and Hedgecock, E. (1992). UNC-6, a laminin-related protein, guides cell and pioneer axon migrations in *C. elegans*. *Neuron* **9,** 873-81.

Jacobson, L. A., Jen, J. L., Hawdon, J. M., Owens, G. P., Bolanowski, M. A., Emmons, S. W., Shah, M. V., Pollock, R. A. and Conklin, D. S. (1988). Identification of a putative structural gene for cathepsin D in *Caenorhabditis elegans*. *Genetics* **119,** 355-63.

Kennedy, T. E., Serafini, T., de la Torre, J. R. and Tessier-Lavigne, M. (1994). Netrins are diffusible chemotropic factors for commissural axons in the embryonic spinal cord. *Cell* **78,** 425-35.

Kenyon, C. (1986). A gene involved in the development of the posterior body region of *C. elegans*. *Cell* **46,** 477-487.

Ma, C. and Moses, K. (1995). *wingless* and *patched* are negative regulators of the morphogenetic furrow and can affect tissue polarity in the developing *Drosophila* compound eye. *Development* **121,** 2279-2289.

Montell, D. J. (1994). Moving right along: regulation of cell migration during *Drosophila* development. *Trends Genet.* **10,** 59-62.

Robinson, N. T. 1995. Genetic Analysis of Neuroblast Migration in *Caenorhabditis elegans*. Ph.D., University of California, San Francisco,

Salser, S. and Kenyon, C. (1992). Activation of a *C. elegans Antennapedia* homolog within migrating cells controls their direction of migration. *Nature* **355,** 255-258.

Salser, S., Loer, C. and Kenyon, C. (1993). Multiple HOM-C gene interactions specify cell fates in the nematode central nervous system. *Genes Dev.* **7,** 1714-1724.

Salser, S. J. and Kenyon, C. (1996). A *C. elegans* Hox Gene Switches ON, OFF, ON, and OFF Again to Regulate Proliferation, Differentiation, and Morphogenesis. *Development* **122 (5),** 1651-1661.

Sawa, H., Lobel, L. and Horvitz, H.R. (1996). The *Caenorhabditis elegans* gene *lin-17,* which is required for certain asymmetric cell divisions, encodes a putative seven-transmembrane protein similar to the Drosophila Frizzled protein. *Genes Dev.,* (in Press).

Serafini, T., Kennedy, T. E., Galko, M. J., Mirazayan, C., Jessel, T. M. and Tessier-Lavigne, M. (1994). The netrins define a family of axon outgrowth promoting proteins homologous to *C. elegans* UNC-6. *Cell* **78,** 409-424.

Shaller, D., Wittmann, C., Spicher, A., Muller, F. and Tobler, H. (1990). Cloning and analysis of three new homeobox genes from the nematode *Caenorhabditis elegans. Nucleic Acids Res.* **18,** 2033-6.

Sternberg, P. W. and Horvitz, H. R. (1988). *lin-17* mutations of *Caenorhabditis elegans* disrupt certain asymmetric cell divisions. *Dev Biol* **130,** 67-73.

Stringham, E. G. and Candido, E. P. (1993). Targeted single-cell induction of gene products in *Caenorhabditis elegans*: a new tool for developmental studies. *J. Exp. Zool.* **266,** 227-33.

Sulston, J. and Hodgkin, J. (1988). Methods. In *The Nematode Caenorhabditis elegans,* (ed. W. B. Wood), pp. 587-605. Cold Spring Harbor, New York: Cold Spring Harbor Laboratory.

Sulston, J. and Horvitz, H. (1977). Post-embryonic cell lineages of the nematode, *C elegans. Dev. Biol.* **56,** 110-156.

Teragawa, C. and Bode, H. (1990). Spatial and temporal patterns of interstitial cell migration in Hydra vulgaris. *Dev. Biol.* **138,** 63-81.

Trent, C., Tsung, N. and Horvitz, H. (1983). Egg-laying defective mutants of the nematode *C. elegans. Genetics* **104,** 619-647.

Wang, B. B., Müller-Immergluck, M. M., Austin, J., Robinson, N. T., Chisholm, A. and Kenyon, C. (1993). A Homeotic Gene Cluster Patterns the Anteroposterior Body Axis of *C. elegans. Cell* **74,** 29-42.

Way, J., Run, J. and Wang, A. (1992). Regulation of anterior cell-specific *mec-3* expression during asymmetric cell division in *C. elegans*. *Developmental Dynamics* **194,** 289-302.

Wehrli, M. and Tomlinson, A. (1995). Epithelial planar polarity in the developing *Drosophila* eye. *Development* **121,** 2451-2459.

White, J., Southgate, E., Thomson, J. and Brenner, S. (1986). The structure of the nervous system of the nematode *C. elegans*. *Philosophical Transactions of the Royal Society of London* **314B,** 1-340.

Wightman, B., Clark, S. G., Taskar, A. M., Forrester, W. C., Maricq, A. V., Bargmann, C. I. and Garriga, G. (1996). The *C. elegans* gene *vab-8* guides posteriorly directed axon outgrowth and cell migration. *Development* **122,** 671-682.

Williams, B. D., Schrank, B., Huynh, C., Shownkeen, R. and Waterston, R. H. (1992). A genetic mapping system in *Caenorhabditis elegans* based on polymorphic sequence-tagged sites. *Genetics* **131,** 609-624.

Xie, G. Y., Jia, Y. and Aamodt, E. (1995). A *C. elegans* mutant screen based on antibody or histochemical staining. *Genetic Analysis: Biomolecular Engineering* **12,** 95-100.

CHAPTER 4: Future Directions

INTRODUCTION

In order to learn how cells and axons migrate great distances to precise targets, I have focused on the migration of the two Q neuroblasts of *C. elegans*. As these left/right asymmetric cells divide and migrate, they progress through multiple phases which are controlled by different sets of genes. Understanding the interactions among these genes will enable us to see how left/right asymmetric cell fates are specified, how the direction of cell migration is controlled, and how position along the A/P axis is encoded. I found that the first step in the Q cell migrations is their polarization in opposite directions, and that the shape of these cells can be followed over time. Thus, the Q cells also provide a system for the study of how cells polarize in a chosen direction within the context of a multicellular organism.

In this chapter I will discuss some specific questions raised by the results presented in Chapters 2 and 3 and suggest future experiments to address these questions.

What is the function of the DPY-19 protein?

dpy-19 encodes a transmembrane protein containing two regions with homology to human expressed sequence tags (ESTs) but no other significant sequence similarities. In animals lacking DPY-19 protein, QL and QR polarize in random directions, fail to migrate, and misexpress the Hox gene *mab-5*. This phenotype is similar to that seen in the absence of UNC-40, the Ig-family member that functions as a receptor for UNC-6/Netrin in guiding dorsal-ventral migrations. It is likely that UNC-40 also acts as receptor in the Q cells

to orient their A/P polarization and migration. What part might *dpy-19* play in such a system? Because *unc-6* is not required for the Q migrations, one hypothesis is that DPY-19 could be the ligand for UNC-40 in the Q cells. DPY-19's 12-13 putative transmembrane domains would be an unusual structural configuration for a ligand, but there are other examples of multipass transmembrane proteins that function as ligands (Cagan, et al., 1992, Hart, et al., 1993).

A second hypothesis for the function of *dpy-19* is that it could function in concert with *unc-40* in the Q cells to allow them to detect a polarizing signal or form stable cell polarizations. *unc-40* is required for dorsal guidance directed by the UNC-5 receptor (Colavita and Culotti, 1998), indicating that UNC-40 may indeed function as a co-receptor with other proteins.

The last hypothesis for the function of DPY-19 is that it could be involved in the production of a ligand necessary for the Q cell migration. If *dpy-19* were also involved in the production of collagens or other proteins that make up the cuticle, such a model could also explain the Dpy-ness phenotype of *dpy-19* mutants. The fact that *dpy-19* mutations suppress the Roller phenotype caused by the *rol-6(d)* collagen (L.H. and C.K., unpublished) is one hint that *dpy-19*'s role in Dpyness may not be far removed from cuticle assembly. Another hint that *dpy-19* might be involved in secretion or processing of extracellular proteins is that rescuing *dpy-19*::GFP fusion proteins were localized in a ring around the nucleus and in a reticular pattern within cells, but were not visible at cell membranes. *unc-40* mutations do not suppress *rol-6(d)* (L.H. and C.K., unpublished), suggesting that not all functions of *dpy-19* overlap with functions of *unc-40*.

There are many experiments that would help determine what the function of this novel protein is. Of prime importance is the generation of

anti-DPY-19 antisera to allow a more reliable determination of which cells express *dpy-19* and whether the unusual subcellular localization seen with *dpy-19*::GFP reflects the true location of the protein. It is also essential to determine in what cells *dpy-19* functions. The key question is whether *dpy-19* is required in Q. Standard mosaic analysis is not possible because *dpy-19* is maternally rescued, but expression of *dpy-19(+)* under the control of tissue specific promoters could narrow down the site of action for *dpy-19*.

A second approach to understanding *dpy-19*'s function would be to look more closely at its role in other tissues. Mutations in *dpy-19* cause temperature-sensitive male mating defects, and *dpy-19*::GFP is strongly expressed in many cells that give rise to the male mating structures. Morphogenesis of the male tail involves migration and polarization of many cells and a detailed analysis of the shapes of these cells in wild-type and *dpy-19* mutants would reveal whether there is a generalizable theme to the effects of *dpy-19* mutations. It would be especially interesting to see if mutations in *dpy-19* cause cells in the developing male tail to polarize in random directions over time, as was seen in the Q cells. It is also possible that the Q cells are more sensitive than other cells to the loss of *dpy-19*. Other defects in *dpy-19* mutants might be revealed by careful temperature-shift experiments. Strong *dpy-19* alleles are lethal at 25°C, but it should be possible to shift these mutants to 25°C at times when various larval cell and growth cone migrations are occurring and then look immediately for randomization of polarization in a wider range of cells.

Lastly, the function of *dpy-19* could be studied in other systems. If the human EST matches can be extended to a full length vertebrate *dpy-19* homolog, it would be worth seeing if the vertebrate *dpy-19* is expressed in

tissues that also express *unc-40* or *unc-6*, and where in cells the DPY-19 protein is found.

What makes QL and QR different from one another?

The experiments in Chapter 3 show that *unc-40*, *dpy-19*, and *unc-73* are required for QL and QR to migrate in opposite directions and for the correct expression of the Hox gene *mab-5*. The expression patterns of these genes do not appear to be left/right asymmetric and loss-of-function mutations in these genes do not transform QL into QR or vice versa, but instead prevent migration in both Q cells. The simplest interpretation of these results is that *unc-40*, *dpy-19*, and *unc-73* are required for the left/right asymmetry but do not themselves specify "left" vs. "right" fate in the Q cells. This would imply that another factor must be responsible for the difference between QL and QR. It is possible that a post-translational modification could establish "left" and "right" states for *unc-40*, *dpy-19*, or *unc-73*, but such a model begs the question of what asymmetric factor creates the post-translational modification. Identifying the asymmetric factor is the key to further understanding of the left/right asymmetry in the Q cells. A mutation which transformed QL into QR or vice versa would be an ideal candidate for the factor that distinguishes QL from QR. If such a factor exists, its expression pattern would be extremely informative. Is it inside the Q cells or outside? How does its expression change in *dpy-19* and *unc-40* mutants?

How might one identify such a factor? Screening directly for mutants that disrupt the migration of QL and QR is difficult because the phenotype is scorable only during a one-hour window of development. Mutagenized animals have variable rates of development, making precise staging even more difficult. However, a screen for animals in which the Q cells are

polarized in the wrong direction (rather than just failing to polarize) might be feasible. The other source for mutations affecting the migration of QL and QR is through re-screening mutations identified by their affect on the migration of the Q descendants. (This is how *unc-40*, *dpy-19* and *unc-73* were recognized as being required for the migration of QL and QR. Interestingly, *dpy-19* is maternally rescued, and thus has not appeared in large F2 screens for misplaced Q descendants (Q. Ch'ng, M. Sym., L. Williams, and C. Kenyon unpublished). An F3 screen could identify maternally rescued Q migration mutants and these might be good candidates for interacting with *dpy-19.*)

There is a more challenging possible outcome of screens to identify the asymmetric factor. If the two Q cells are identical and the difference between the left and right sides is in the positioning of a cue toward which the Q cells polarize (Fig 2.11A), then mutations that eliminate the cue would be expected to have a similar phenotype to that of *unc-40*, i.e. neither Q cell migrates. Mutations which move the location of the hypothetical cue would make QL behave like QR (or vice versa), but such mutants may be rare. In such a system, the only way to cause QL/QR fate switching might be to cause whole animal left/right reversals. Although interesting, these mutants would not shed light on the real question, i.e. how the Q cells read the left/right asymmetric information. The lesson from considering such a model is that mutants that could identify the left/right asymmetry might have a symmetric phenotype in the Q cells after all. The only way to know is by examining the expression patterns of the genes defined by such mutants.

How is cell polarization controlled in Q?

The intriguing observation that the Q cells polarize in multiple directions over time in *unc-40* and *dpy-19* mutants suggests that these cells

are capable of dynamic responses to their environment. Because they are among the largest post-embryonic migrating cells in the worm and because they are controlled at some level by a left/right switch, they may be especially well suited for the cell biological study of how the direction of cell polarization is controlled. Small GTPases are key regulators of cell polarization in yeast and vertebrates. Since MIG-2, a rho-GTPase, and UNC-73, which contains guanine-nucleotide exchange factor domains, are required for Q cell polarization, we already know that the Q cells use evolutionarily conserved mechanisms to control cell shape. Solving a few technical problems would allow the Q cells to become a first-rate system for the analysis of cell polarization. First, figuring out a way to immobilize young worms while allowing them to feed (and thus develop) would allow a much higher resolution time-lapse analysis of Q cell shape. Second, GFP or antibody reagents are needed to determine the role of the cytoskeleton in Q cell polarization. Do changes in microtubule or actin organization prefigure the changes in cell shape? How do various mutants affect cytoskeletal organization? Lastly, the most desirable of all reagents would be a molecular marker that is localized toward the direction of polarization, analogous, for example, to the localization of Bud3 in yeast bud site selection. Such a marker would serve as a starting point for ordering the Q cell polarization genes in a pathway. One could ask, for example, whether *dpy-19* and *unc-40* are required for the localization of such a marker.

Does an A/P localized signal control *mab-5* expression in the Q cells?

QL normally starts expressing *mab-5* after it migrates toward the posterior, while QR, which migrates anteriorly does not express *mab-5*. In *dpy-19* and *unc-40* mutants, the shape of the Q cells is variable, but an

individual Q cells which spends more time pointing toward the posterior is more likely to express *mab-5*. The ongoing appearance of these correlations between the polarization of Q toward the posterior and the activation of *mab-5* have supported, but not proven the "positional model," i.e. that QL expresses *mab-5* because it reaches toward the posterior, thus allowing it to contact a localized signal. If the positional model were true, it could offer an interesting explanation for why all *dpy-19* and *unc-40* alleles are temperature sensitive for the activation of *mab-5* in QL: perhaps at higher temperatures, randomized Q cells are less likely to reach far enough toward the posterior for a long enough period of time to allow them to reach some threshold of signaling that activates *mab-5*. Many observations make the positional model attractive, but how can it finally be put to the test? It seems that the best hope for proving the positional model is the identification of the positionally localized signal. *egl-20*, the Wnt homolog that is required for *mab-5* activation in QL is an good candidate for this role. If *egl-20* is the positional signal, its expression should be limited to posterior tissues, and it should be equally available on the left and right sides. The real test of a positional signal is whether its ectopic expression in the anterior (e.g. using a heat-shock promoter) can cause QR to express *mab-5*.

Conversely, the best hope for disproving the positional model would be the discovery of mutants which break the rule of correlation between cell shape and activation of *mab-5*.

How does *mig-14* fit into the Wnt pathway that regulates *mab-5* expression in the Q descendants?

After the migrations of QL and QR discussed above, a second set of genes takes over control of the Q descendants. *egl-20, mig-14, mig-1, lin-17,*

bar-1 are all required to activate *mab-5* in QL, which in turn directs the migration of the Q descendants toward the posterior. Recent work has shown that many of these genes fit into the evolutionarily conserved Wnt/*wingless* signaling pathway (*J. Whangbo, J. Maloof, and C. Kenyon unpublished, (Sawa, et al., 1996), and D. Eisenmann, personal communication). *mig-14* remains un-cloned, but its phenotype is extremely similar to *egl-20*, the Wnt homolog. In both *mig-14* mutants and *egl-20* mutants: QL fails to express *mab-5*, the QR descendants seek out final positions that are shifted toward the posterior, the migrations of the HSN and M cells are shortened, the migration of the distal tip cells are misrouted, and the polarity of the V5 seam cell division is sometimes reversed (*(Harris, 1996),J. Whangbo and C.K. unpublished) Only two differences distinguish these mutants: they behave differently in double mutant combinations with *mig-1* (see Appendix 3 and *(Harris, 1996)) and the BDU cell is posteriorly displaced only in *mig-14* mutants. *mig-14* could be required for the production of *egl-20*/Wnt or it could act somewhere downstream in the reception of the Wnt signal. Examining the *egl-20* expression pattern in a *mig-14* mutant should narrow down the possibilities. What might *mig-14* encode? The *frizzled*, *dishevelled*, and *armadillo* slots of the Wnt cascade controlling *mab-5* expression in Q have already been filled by other genes (*(Guo, 1996, Sawa, et al., 1996) and D. Eisenmann, personal communication). In addition, *C. elegans porcupine* and APC homologs have already been mapped to other genes (Rocheleau, et al., 1997, Thorpe, et al., 1997). (It has not yet been shown that these genes act in the Q cells, leaving open the possibility that multiple worm *porcupine* or APC homologs exist, one of which could be *mig-14*.) Recent work has shown that the UDP-glucose dehydrogenase gene, which functions in proteoglycan synthesis, is required for *wingless* signaling

in *Drosophila* (Binari, et al., 1997, Hacker, et al., 1997, Haerry, et al., 1997). Thus mig-14 might be involved in proteoglycan synthesis or it might encode a completely novel element in Wnt signaling.

Beyond simply placing *mig-14* in the Wnt pathway, there are deeper mysteries concerning the role for *mig-14* and *egl-20* in anterior migration. Mutations in both *egl-20* and *mig-14* cause the anteriorly directed QR descendants to migrate to slightly less anterior positions than normal. Because the QR descendant migrations are still shortened in *mig-14;mab-5* and *mab-5;egl-20* double mutants, this effect is not due to misexpression of *mab-5*. How does a Wnt pathway control the fine-scale positioning of the Q descendants? It simply may be that a currently unknown transcription factor promotes anterior migration and this gene is turned on by Wnt signals (similarly to *mab-5*). Another possibility is that the Q cell migrate relative to cues produced by the epidermal cells V1-V6. Perhaps in *egl-20* and *mig-14*, these signals are shifted, analogous to the segment polarity defects caused by mutations in the *Drosophila* Wnt homolog, *wingless*. An even more exotic possibility is that the migrating Q cells read a long range gradient to measure their A/P position, and that this gradient is directly or indirectly generated by *egl-20*.

CONCLUSION

The goal of the genetic analysis of the Q neuroblast migrations is to produce a pathway that explains how left/right asymmetric signals feed into the Q cells to control the direction and extent of their migration. The characterization of new Q migration genes can build on the genetic analysis described here to provide insight into what makes QL and QR different from

one another. By understanding the Q cells we can hope to identify general principles used in generating left/right asymmetry.

REFERENCES

Binari, R. C., B. E. Staveley, W. A. Johnson, R. Godavarti, R. Sasisekharan, et al. (1997). Genetic evidence that heparin-like glycosaminoglycans are involved in wingless signaling. *Development* **124**, 2623-32.

Cagan, R. L., H. Kramer, A. C. Hart and S. L. Zipursky (1992). The bride of sevenless and sevenless interaction: internalization of a transmembrane ligand. *Cell* **69**, 393-9.

Colavita, A. and J. G. Culotti (1998). Suppressors of ectopic UNC-5 growth cone steering identify eight genes involved in axon guidance in Caenorhabditis elegans. *Dev Biol* **194**, 72-85.

Guo, C. (1996). mig-5, a gene that controls cell fate determination and cell migration in C. elegans, is a member of the DSH family. Ph. D. thesis. Johns Hopkins.

Hacker, U., X. Lin and N. Perrimon (1997). The Drosophila sugarless gene modulates Wingless signaling and encodes an enzyme involved in polysaccharide biosynthesis. *Development* **124**, 3565-73.

Haerry, T. E., T. R. Heslip, J. L. Marsh and M. B. O'Connor (1997). Defects in glucuronate biosynthesis disrupt Wingless signaling in Drosophila. *Development* **124**, 3055-64.

Harris, J. M. (1996). Genes that Control Cell Migration and Cell Polarity in C. elegans. Ph.D. thesis. Univ. of Calif., San Francisco.

Hart, A. C., H. Kramer and S. L. Zipursky (1993). Extracellular domain of the boss transmembrane ligand acts as an antagonist of the sev receptor. *Nature* **361**, 732-6.

Rocheleau, C. E., W. D. Downs, R. Lin, C. Wittmann, Y. Bei, et al. (1997). Wnt signaling and an APC-related gene specify endoderm in early C. elegans embryos. *Cell* **90**, 707-16.

Sawa, H., L. Lobel and H. R. Horvitz (1996). The Caenorhabditis elegans gene lin-17, which is required for certain asymmetric cell divisions, encodes a putative seven-transmembrane protein similar to the Drosophila frizzled protein. *Genes Dev* **10**, 2189-97.

Thorpe, C. J., A. Schlesinger, J. C. Carter and B. Bowerman (1997). Wnt signaling polarizes an early C. elegans blastomere to distinguish endoderm from mesoderm [see comments]. *Cell* **90**, 695-705.

Figure A.1 Hatching is delayed in *dpy-19(n1347n1348)*, but not in *dpy-19(mu78)*

Two cell embryos, isolated by cutting open gravid hermaphrodites, were placed on individual plates and grown at 20°C. 750 minutes later, plates were examined every 5 minutes to see when the embryos hatched. Each horizontal bar corresponds to a single embryo and spans the interval during which the animal was observed to hatch. Embryos which had still not hatched by 900 minutes were checked less frequently thereafter. As expected, wild type animals hatched at very near 800 minutes. The positive control, *hch-1* mutants, caused delayed hatching as expected. The deletion allele of *dpy-19*, *n1347n1348*, also sometimes caused delayed hatching. As described in Figure A.2, *hch-1* mutants disrupt the Q cell migrations, but this phenotype can be rescued by artificially opening the eggshells of *hch-1* animals. We wondered whether delayed hatching was also responsible for the Q migration defects seem in *dpy-19* mutants. However, we found that a weaker *dpy-19* allele, *mu78*, did not cause delayed hatching, even though it still causes mutant (anterior) migrations of the QL descendants (as shown by the color of the bars). Because misregulation of mab-5 can occur in *dpy-19(mu78)* animals with normal hatching rates, this demonstrates that *dpy-19* mutants do not exert their effects on the Q cells by delaying exit from the eggshell.

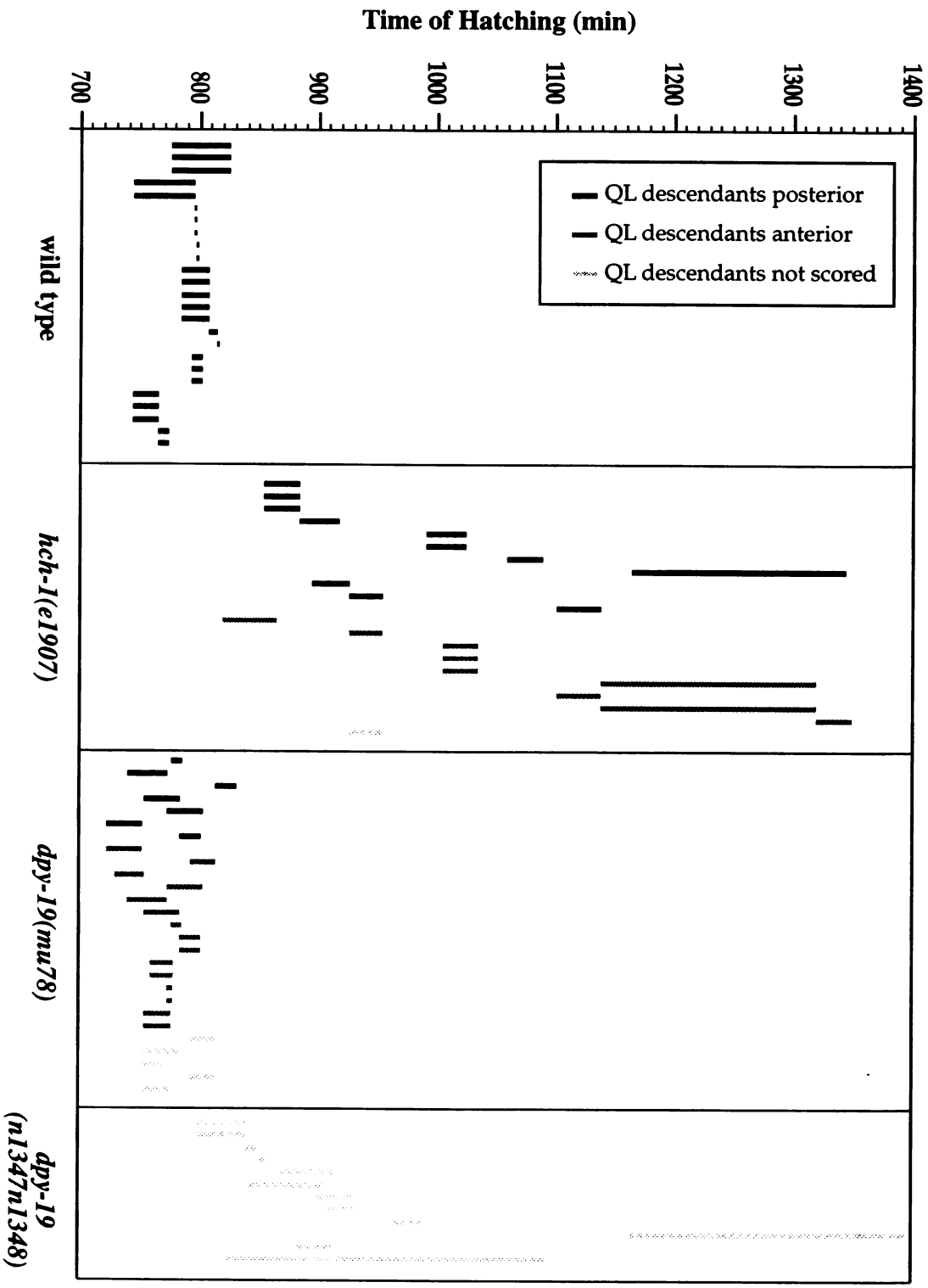
Time of Hatching (min)
700
800
900
1000
1100
1200
1300
1400
QL descendants posterior
QL descendants anterior
QL descendants not scored
wild type
hch-1(e1907)
dpy-19(mu78)
dpy-19 (n1347n1348)

Figure A.1

Figure A.2 Liberation from the eggshell rescues the Q phenotype of *hch-1* mutants.

The Q neuroblasts begin their migrations shortly after hatching. Hedgecock et al found that *hch-1* mutants have delayed hatching as well as Q cell migration defects (Development 100:365-382) and Hishida et al have found that *hch-1* encodes a Zn++ protease (Embo Journal 15:4111-22.) There are two models to explain the *hch-1* mutant phenotype: 1) the HCH-1 protease could be acting both to allow escape from the eggshell and to allow the Q cells to migrate correctly on their substrate or 2) *hch-1* could be just required for timely hatching, and the Q defect could be an indirect result of the delay in hatching. If the Q phenotype is caused indirectly, then artificially liberating *hch-1* animals in a timely fashion should restore normal Q migration. To generate a roughly staged population of eggs, we allowed N2 and *hch-1(e1907)* adults to lay eggs for 1 hour on seeded plates. After 9.5 hr (20° C), ~5% of the N2 eggs had hatched and most N2 and *hch-1* eggs had reached the pretzel stage. We washed these eggs off the plate with egg salt solution, treated them with 0.4% bleach for 1 min, rinsed with egg salts, added 20 mg/ml chitinase + 20 mg/ml chymotrypsin for 3 min, and then rinsed 3 times with egg salts (a slight modification of Lois Edgar's technique). These liberated hatchlings were allowed to mature overnight on seeded plates. The histograms show the distribution of the final positions of the Q descendants (Q.pax). 51% of the QL descendants incorrectly migrate anteriorly in control *hch-1(-)* animals (n=54), but only 8% of QL descendants migrate anteriorly when *hch-1(-)* animals are artificially hatched (n=53). Thus it seems likely that the Q phenotype seen in *hch-1* mutants is a secondary defect resulting from their delay in hatching.

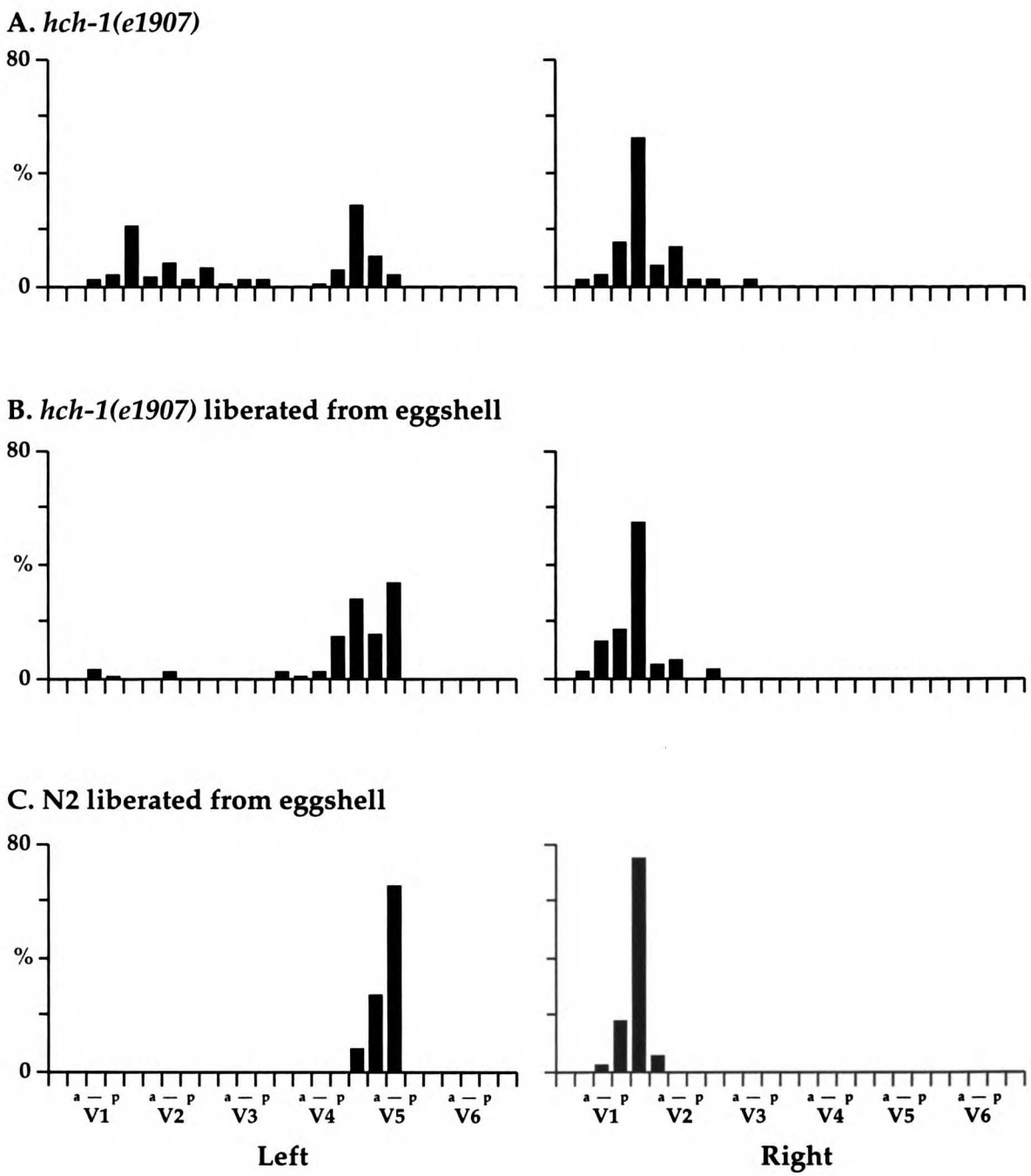
A. hch-1(e1907)
80
%
0
B. hch-1(e1907) liberated from eggshell
80
%
0
C. N2 liberated from eggshell
80
%
0
a — p
V1
V2
V3
V4
V5
V6
Left
Right

Figure A.2

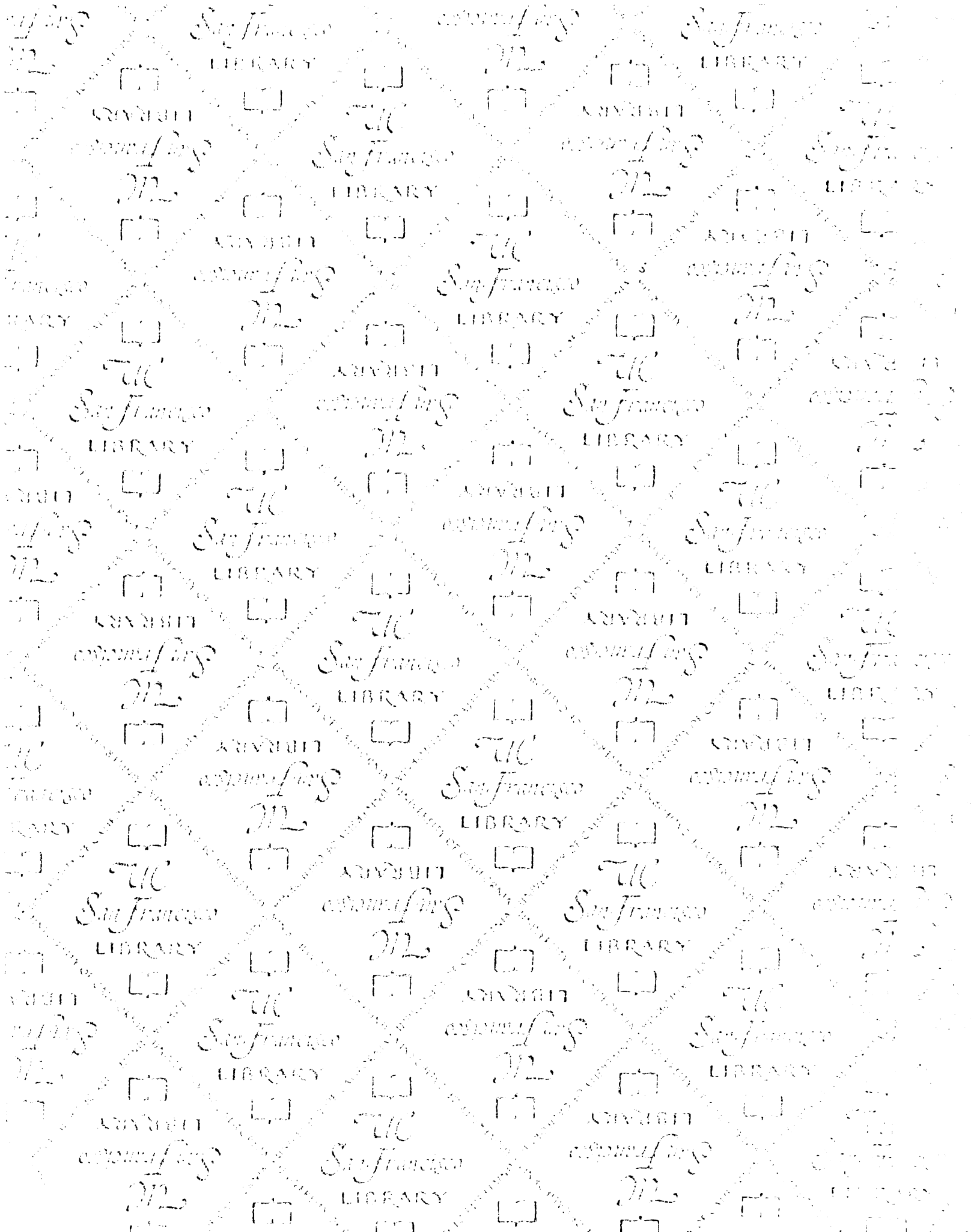
San Francisco
LIBRARY

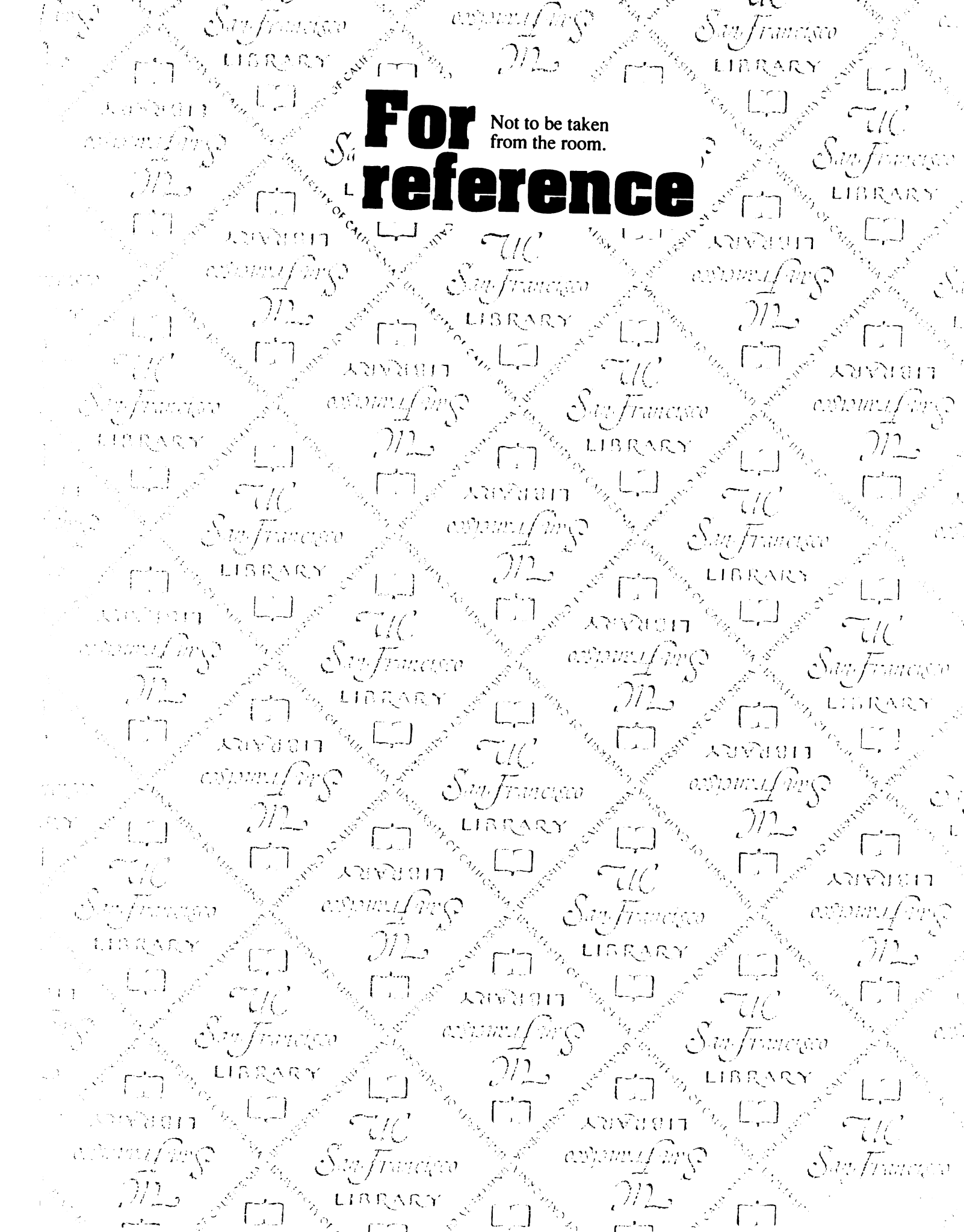
For reference
Not to be taken from the room.
UC San Francisco LIBRARY